Kinetic modeling of biomass-derived product

Phanuphong Nonwiangkae

A Report Submitted in Partial Fulfillment of the Requirements
for the Degree of Bachelor of Engineering (Petrochemical Engineering)
Department of Chemical Engineering, Faculty of Engineering,
King Mongkut's Institute of Technology Ladkrabang
Academic Year 2016

This material is reserved for educational use only, not allowed for commercial use.
Forbidden to modify the content, and cite the document when use

การสร้างแบบจำลองทางจลศาสตร์ของผลิตภัณฑ์จากชีวมวล

นาย ภานุพงค์ โนนเวียงแก



ปริญญานิพนธ์นี้เป็นส่วนหนึ่งของการศึกษาตามหลักสูตร

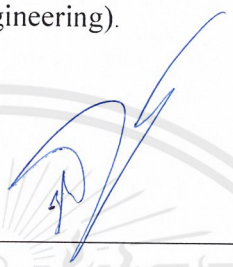
วิศวกรรมศาสตรบัณฑิต สาขาวิชาวิศวกรรมปิโตรเคมี

This material is reserved for educational use only, not allowed for commercial use.
Forbidden to modify the content, and cite the document when use

Title	Kinetic modeling of biomass-derived product
By	Mr. Phanuphong Nonwiangkae
Field of Study	Petrochemical Engineering
Advisor	Dr. Nuttapol Lerkkasemsan

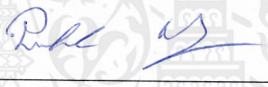
Accepted by the Faculty of Engineering, King Mongkut' s Institute of Technology Ladkrabang in Partial Fulfillment of the Requirements for the Degree of Bachelor of Engineering (Petrochemical Engineering).

Thesis Committee



_____ Chairman

(Dr. Nuttapol Lerkkasemsan)



_____ Committee

(Assoc. Prof. Prakob Kitchaiya)



_____ Committee

(Dr. Amata Anantpinijwatna)

This material is reserved for educational use only, not allowed for commercial use.
Forbidden to modify the content, and cite the document when use

Title	Kinetic modeling of biomass-derived product
By	Mr. Phanuphong Nonwiangkae
Advisor	Dr. Nuttapol Lerkkasemsan
Field of Study	Petrochemical Engineering
Affiliation	Phanuphong.N@hotmail.com

Abstract

This study investigates biomass process including the CO_2 gasification reaction of rice husk char (RH) and Ethanol fermentation using multiple kinetic models in order to searching for the suitable model and kinetic parameters. For gasification reaction of rice husk char (RH) , six representative gas-solid kinetic models including the volumetric model (VM) , the grain model (GM) , the Chronet model (CM) , the random pore model (RPM) , the modified random pore model (mRPM) and the shift-extended random pore model (sRPM) are used to model the experimental data of rice husk char gasification. From the results, volumetric model (VM) is the most robust model among the six kinetic models adopted in this study. For ethanol fermentation, three alternative modeling frameworks, namely Monod model, Modified Monod model and Extended-modified Monod model are used to model the experimental data of ethanol fermentation. We found that the prediction using Extended-modified Monod model is better than others two models. Finally, kinetic parameters are reported from these studies including activation energy (E) and Pre-exponential factor (k_o) , the maximum specific growth rate (μ_{MAX}) , Monod constant (K_S) and substrate inhibition constant for char gasification and ethanol formation which provide a basis parameter for design and operation rice husk char gasification process.

Keywords: gasification; model, rice husk, kinetic, volumetric model, ethanol fermentation, Monod, specific growth rate

This material is reserved for educational use only, not allowed for commercial use.
Forbidden to modify the content, and cite the document when use

เรื่อง	การสร้างแบบจำลองทางจลศาสตร์ของผลิตภัณฑ์จากชีวมวล
โดย	นาย ภานุพงค์ โนนวียงแก
อาจารย์ที่ปรึกษา	ดร. ณัฐพล ฤกษ์เกษมสันต์
สาขาวิชา	วิศวกรรมเคมี หลักสูตรวิศวกรรมปิโตรเคมี
สังกัด	สถาบันเทคโนโลยีพระจอมเกล้าเจ้าคุณทหารลาดกระบัง

บทคัดย่อ

งานวิจัยฉบับนี้ทำการศึกษาเกี่ยวกับปฏิกิริยาการแปรสภาพแปรสภาพเป็นแก๊สของถ่านที่ได้จากฟางข้าวด้วยแก๊สคาร์บอนไดออกไซด์และการหมักเอททานอลโดยใช้แบบจำลองทางจนลพลศาสตร์เพื่อค้นหาแบบจำลองและพารามิเตอร์ทางจลนพลศาสตร์ที่เหมาะสมในการใช้อธิบายปฏิกิริยา สำหรับงานวิจัยนี้แบบจำลองการแปรสภาพแปรสภาพเป็นแก๊สระหว่างของแข็ง-แก๊ส 6 แบบจำลอง ได้แก่ แบบจำลอง volumetric (VM) แบบจำลอง grain (GM) แบบจำลอง Chronet (CM) แบบจำลอง random pore (RPM) แบบจำลอง shift-extended random pore (sRPM) และแบบจำลอง modify random pore (mRPM) ถูกนำมาใช้เพื่อจำลองปฏิกิริยาการแปรสภาพแปรสภาพเป็นแก๊สของถ่านจากฟางข้าวด้วยแก๊สคาร์บอนไดออกไซด์ ผลการศึกษาพบว่าแบบจำลอง volumetric (VM) เป็นแบบจำลองที่สามารถใช้ในการทำนายผลการทดลองได้ดีกว่าแบบจำลองอื่นในการศึกษานี้ สำหรับการหมักเอททานอล 3 โมลเดลที่ใช้ในการศึกษานี้คือ Monod model Modified Monod model และ Extended-modified Monod model ถูกนำมาใช้เพื่อจำลองการหมักของแอทนอล จากการศึกษาเราพบว่า Extended-modified Monod model ให้ผลท่ดีกว่าอีกสองโมเดลในการจำลอง จากการศึกษาครั้งนี้ค่าที่ได้ได้จากการศึกษาครั้งนี้ เช่น พลังงานกระตุ้น (E) พรีเอกซ โพเนนเชียล (k_o) อัตราการเติบโตจำเพาะสูงสุดของเซลล์ (μ_{MAX}) ค่าคงที่โมนอด (K_S) ค่าคงที่การยับยั้งของสารตั้งต้น (K_P) ซึ่งสามารถใช้เป็นพื้นฐานในการออกแบบระบบที่มีการใช้ปฏิกิริยาการแปรสภาพแปรสภาพเป็นแก๊สเพื่อผลิตถ่านจากฟางข้าวได้

คำสำคัญ: การแปรสภาพแปรสภาพเป็นแก๊ส, แบบจำลอง, แกลบข้าว, การหมักเอททานอล, โมนอด, อัตราการเจริญจำเพาะ

This material is reserved for educational use only, not allowed for commercial use.
Forbidden to modify the content, and cite the document when use

Acknowledgements

First of all, I would like to thank my supervisor Dr. Nuttapol Lerkkasemsan who believed in me and was continuously supporting me in every problem that occurred during the writing of this report. I especially thank him for his encouragement and his accurate comments which were of critical importance, during this work

Special thanks go to my friends for their advice, their continuous support and their tolerance during the writing of this report, without your moral support and love I could not have made it until the end.

I would like to thankful my beloved parents and my sister who always believed in me, always were there and will always be whenever I need them.

This material is reserved for educational use only, not allowed for commercial use.
Forbidden to modify the content, and cite the document when use

Table of Contents

	Page
Abstract	A
Acknowledgements	C
Table of Contents	D
List of Figures	F
List of Tables	I
CHARPTER 1 Kinetic modeling of rice husk char gasification	1
1.1 Introduction	1
1.1.1 Background	1
1.1.2 Objective	2
1.1.3 Scopes of Work	3
1.1.4 Expected Outputs	3
1.2 Literature Review and Theory	4
1.2.1 Literature Review	4
1.2.2 Theory	4
1..3. Research Methodology	18
1.3.1 Methodology	18
1.3.2 Calculation	18
1.4 Results and Discussion	22
1.4.1 Modeling	22
1.4.2 Validation	26
1.5 Conclusion	34
References	35
Appendix 1	38
Appendix 1-A	38
Appendix 1-B	40
Appendix 1-C	47
CHARPTER 2 Kinetic modeling of ethanol fermentation in a two-tank system with cell recycling by using sucrose as substrate	51
2.1 Introduction	51
2.1.1 Background	51

This material is reserved for educational use only, not allowed for commercial use.
Forbidden to modify the content, and cite the document when use

Table of Contents (Cont.)

	Page
2.1.2 Objective	52
2.1.3 Scopes of Work	52
2.1.4 Expected Outputs	53
2.2 Literature Review and Theory	54
2.2.1 Literature	54
2.2.2 Theory	54
2.3 Research Methodology	63
2.3.1 Researching procedure	63
2.3.2 Calculation Tool	63
2.3.3 Tool	63
2.4 Results and Discussion	64
2.4.1 Monod model and Modified Monod model	64
2.4.2 Extended-Modified Monod model	66
2.5 Conclusion	74
2.6 Nomenclature	75
References	76
Appendix 2	78
Appendix 2-A	78
Appendix 2-B	79
Appendix 2-C	81

This material is reserved for educational use only, not allowed for commercial use.
Forbidden to modify the content, and cite the document when use

List of Figures

Page

Figure 1.2.1 The reaction mechanism of volumetric model 6

Figure 1.2.2 The model for sphere particle of unchanging size 7

Figure 1.2.3 a reacting particle when diffusion through the ash layer is the controlling resistance 8

Figure 1.2.4 A reacting particle when chemical reaction is the controlling resistance 10

Figure 1.2.5 Overlapping of cylindrical surfaces. 12

Figure 1.3.1 Method flowchart 19

Figure 1.4.1 Comparison between experimental data and predicted values by the VM 24

Figure 1.4.2 Comparison between experimental data and predicted values by the GM 24

Figure 1.4.3 Comparison between experimental data and predicted values by the CM 25

Figure 1.4.4 Comparison between experimental data and predicted values by the RPM 25

Figure 1.4.5 Comparison between experimental data and predicted values by the mRPM 26

Figure 1.4.6 Comparison between experimental data and predicted values by the sRPM 26

Figure 1.4.7 Model validation with experimental data from Thilakavathi M. (VM) 27

Figure 1.4.8 Model validation with experimental data from Thilakavathi M. (RPM) 28

Figure 1.4.9 Model validation with experimental data from Thilakavathi M. (GM) 29

Figure 1.4.10 Model validation with experimental data from Thilakavathi M. (sRPM) 29

Figure 1.4.11 Model validation with experimental data from Thilakavathi M. (CM) 30

Figure 1.4.12 Model validation with experimental data from Thilakavathi M. (mRPM) 30

This material is reserved for educational use only, not allowed for commercial use.
Forbidden to modify the content, and cite the document when use

List of Figures (Cont.)

Page

Figure 1.4.13 Model validation with experimental data from Ashish B.. (VM) 31

Figure 1.4.11 Model validation with experimental data from Ashish B.. (GM) 31

Figure 1.4.15 Model validation with experimental data from Ashish B.. (CM) 32

Figure 1.4.16 Model validation with experimental data from Ashish B. (RPM) 32

Figure 1.4.17 Model validation with experimental data from Ashish B. (sRPM). 33

Figure 1.4.18 Model validation with experimental data from Ashish B.. (mRPM) 33

Figure 1-B-1 VM linearized models for different temperature 41

Figure 1-B-2 GM linearized models for different temperature 41

Figure 1-B-3 CM linearized models for different temperature 42

Figure 1-B-4 RPM linearized models for different temperature 42

Figure 1-B-5 Curve fiiting for mRPM A:1123K, B:1148K, C:1173K, D:1198K and E:1223K 43

Figure 1-B-6 Curve fiiting for sRPM A:1123K, B:1148K, C:1173K, D:1198K and E:1223K 44

Figure 1-B-7 Arrhenius Plot for each models 46

Figure 1-C-1 Simulation code of VM model 48

Figure 1-C-2 Simulation code of CM model 49

Figure 1-C-3 Simulation code of GM model 49

Figure 1-C-4 Simulation code of mRPM model 50

Figure 1-C-5 Simulation code of RPM model 50

Figure 1-C-6 Simulation code of sRPM model 51

Figure 2.2.1 Illustration of a two-tank continuous fermentation system with cell recycles. 55

Figure 2.2.2 A simplified scheme of this approach for the ethanol fermentation process by yeasts and bacteria. 55

Figure 2.2.3 Schematic representation of sugar metabolism in Saccharomyces yeast. 56

Figure 2.2.4 Schematic representation of pathway of sucrose hydrolyed to glucose and fructose by Saccharomyces yeast 58

Figure 2.2.5 Schematic represent pathway of sucrose fermentation to ethanol by Saccharomyces yeast 60

This material is reserved for educational use only, not allowed for commercial use.
Forbidden to modify the content, and cite the document when use

List of Figures (Cont.)

Page

Figure 2.3.1 Calculation flow chart 63

Figure 2.4.1 Experimental data and Monod model results of ethanol production (Total sugar, Solid line: Model) 65

Figure 2.4.2 Experimental data and Modified Monod model results of ethanol production (Solid line: Model) 66

Figure 2.4.3 Experimental data and Extended-modified model results of ethanol production (Solid line: Model) 68

Figure 2.4.4 Comparison of total sugar prediction for each model 69

Figure 2.4.5 Comparison of ethanol prediction for each model 69

Figure 2.4.6 Comparison of biomass prediction for each model 70

Figure 2.4.7 Comparison of biomass prediction for each model (with continuous phase) 71

Figure 2.4.8 Comparison of sucrose prediction for each model (with continuous phase) 72

Figure 2.4.9 Comparison of glucose prediction for each model (with continuous phase) 72

Figure 2.4.10 Comparison of fructose prediction for each model (with continuous phase) 73

Figure 2.4.11 Comparison of ethanol prediction for each model (with continuous phase) 73

Figure 2-B-1 Lineweaver–Burk plots 80

Figure 2-C-1 Simulation code of Monod model for ethanol fermentation 81

Figure 2-C-2 Simulation code of Modified monod model for ethanol fermentation 82

Figure 2-C-3 Simulation of ethanol fermetation by Extended-modified monod model 82

This material is reserved for educational use only, not allowed for commercial use.
Forbidden to modify the content, and cite the document when use

List of Tables

	Page
Table 1.4.1 Comparisons of the kinetic parameters for each models	23
Table 1.4.2 Comparisons of correlation coefficient	27
Table 1.4.3 Comparison of correlation coefficient value (R^2) for each model	34
Table 1-A-1 Raw data of rice husk char gasification	38
Table 1-A- 2 Raw data of rice husk char gasification of Thilakavathi M. [7] for each temperature	40
Table 1-A- 3 Raw data of rice husk char gasification of Ashish B. [4] for each temperature	40
Table 2.1 Kinetic parameters	67
Table 2.2 The correlation coefficient (R^2) for each model (Batch mode)	71
Table 2.3 The correlation coefficient (R^2) for Modified Monod model and Extended-modified Monod model (With continuous mode)	74
Table 1-B-1 k value for each model	43
Table 1-B-2 Example of curve fitting for mRPM model at 1123 by using Polymath software	44
Table 1-B-3 Example of calculation of kinetic paramer for RPM model by using Polymath software	46
Table 2.4.1 Kinetic parameters	66
Table 2.4.2 The correlation coefficient (R^2) for each model	70
Table 2.4.3 The correlation coefficient ($R2$) for Modified Monod model and Extended-modified Monod model (With continuous mode)	73
Table 2-A- 1 Raw data of ethanol fermetation at any time	79
Table 2-A- 2 Concentration of total sugar in tank 1 and 2	79
Table 2-B-1 Calculation of rate of cell growth by polymath software	79
Table 2-B-2 Table show relation ship between 1/μ and 1/S	80

This material is reserved for educational use only, not allowed for commercial use.
Forbidden to modify the content, and cite the document when use

CHAPTER I
KINETIC MODELING OF RICE HUSK CHAR GASIFICATION

1.1 INTRODUCTION

1.1.1 Background

Activated carbons have always become a research interest due to their usefulness in many areas because it' s several applications such as gas purification, water purification, sewage treatment, air filter and decaffeination. In industry application, it is a one major material for purification of solution. For example, it is a main purification technique for removing organic compound form water before released to environment. In addition, activated carbon is used as the treat poisoning and overdose following oral ingestion in medical. Currently, the application of activated carbon has been developed to further useful application. For example, Mok-Hwa K.[1] uses the activated carbon as ultra-capacitor by design hierarchically structure of activated carbon.

These materials have been synthesized from many types of carbonaceous precursors. Formerly, coal was the major precursor for activated carbon production. Nowadays, since coal is more useful as energy source, people start to use other types of carbon source which is biomass such as woods, plant' s shells, rice husk, straw, hulls and sawdust as the precursors. Moreover, the utilization of several types of biomass for activated carbon production has a positive impact in reducing organic solid wastes.

Thailand is an agricultural country and the world's second rice exporter and exported 9.79 million tons of rice in the year 2015 [2]. Normally, rice husk is treated as waste and leads to a serious environmental problem because farmer usually burn rice husk in order to prepare the field for next rice farming season. Therefore, it is necessary to reduce the amount of rice husk waste. Rice husk consists of more than 37% of carbon element by weight, thus making it a promising raw material to produce activated carbon. Recently, rice husk is used as precursors to produce activated carbon[3]–[8]. To produce the activated carbon from biochar, we consider the gasification reaction of char as a major reaction [9] since the gasification reaction can eliminated contaminant in the pore.

This material is reserved for educational use only, not allowed for commercial use.
Forbidden to modify the content, and cite the document when use

Generally, char gasification reaction is very complex and include water evaporation, volatile gasification, volatile pyrolysis and solid residual (char). So, it is difficult to find the mathematic model to describe the gasification reaction. But there have been numerous researches on char gasification using various kinetics models. Guangwei Wang et al. [10] studied gasification properties and kinetics of biomass chars with CO_2 through the TGA method and various kinetic models such as the volume reaction model (VM), the grain model (GM), the random pore model (RPM), and the modified random pore model (mRPM). Hu Wu et al. [20] studies CO_2 gasification characteristics of three chars derived from medium temperature pyrolysis various kinetic models such as the shift extended random pore model (sRPM) and the modified random pore model (mRPM). A. Gómez-Barea et al. [11] studies the solution of single isothermal gas–solid non-catalytic reactions by various kinetic models such as the chornet model (CM). The kinetic models were used to investigate of how different experimental conditions can influence the speed of a reaction and yield information about the mechanism of reaction and transition states and describe the characteristics of a reaction. Therefore, kinetic models are necessary for designing and operating gasification processes.

The aim of this work is to investigate CO_2 gasification behaviors and kinetic model on biomass char gasification in CO_2 condition. The work will attempt to ascertain: (1) The difference of gasification behaviors among different kinetic models. (2) Determine the suitable kinetic model, apparent activation energy and Pre-exponential factor of gasification reaction of rice husk chars in CO_2 condition. (3) Verify models by using parameters obtained in (2) with other experimental data sets in order to determine the robustness of each model on predicting the conversion of gasification of rice husk.

1.1.2 Objective(s)

1.) To ascertain the difference of gasification behaviors among different kinetic models

2.) To determine the suitable kinetic model, apparent activation energy and Pre-exponential factor of gasification reaction of rice husk chars in CO2 condition.

This material is reserved for educational use only, not allowed for commercial use.
Forbidden to modify the content, and cite the document when use

3.) To verify models by using parameters obtained in (1.2.2) with other experimental data sets in order to determine the robustness of each model on predicting the conversion of gasification of rice husk.

1.1.3 Scopes of Work

1.) Bio-char that used for this study is rice husk.

2.) Kinetics model that used for this study including Volumetric model, Grain model, Chornet model, Random pore model, Modified random pore model and Shift random pore model.

3.) The gasification reaction is operated on isothermal condition

1.1.4 Expected Outputs

1.) The suitable kinetic model that can used to predict reaction of activation of bio-char.

This material is reserved for educational use only, not allowed for commercial use.
Forbidden to modify the content, and cite the document when use

1.2 LITERATURE REVIEW AND THEORY

1.2.1 Literature Review

The gasification reaction behaviors of biomass char have been widely investigate in past [17][21]. From the research, we found that it difficult to describe the reaction of gasification, but it has many literatures that can describe the reaction of gasification. For example, Wang et al[1 0] describe the gasification behavior of biomass char, four model are applied to described including the volumetic model (VM) , the grain model (GM) , the random pore model (RPM) and the modified random pore model (mRPM). It is found that RPM and mRPM are better than other model for describe the gasification reaction of biomass.

However, it also has many models to describe the gasification of biomass such as the chronet model[11] and the shift extended random pore model (s-eRPM)[22]. The s-eRPM is propose by Wu[2 2] , it has parameter c and p which added from RPM model. These parameters are used to improve the predict value to fit with experimental data. From this research, we found that the s-eRPM is suitable for char that have the maximum rate of reaction less than 0.2.

1.2.2 Theory

1.) Gasification reaction

Char gasification is two step including pyrolysis and gasification. The pyrolysis involved the evolution of compound of low molecular weight at temperatures between 300 – 500 ˚C. These compounds are mainly tars and non-condensable gases. Normally, the pyrolysis residue remains about 70% of original coal. Usually, the gasification reaction is slower than pyrolysis reaction. So, only those elements affecting char gasification reaction are consider for this study. The main reaction for gasification reactions are shown following.

$$C + CO_2 \rightarrow 2CO \qquad \Delta H = +159.7kJ/mol \qquad (1)$$

$$C + H_2O \rightarrow CO + H_2 \qquad \Delta H = +118.9kJ/mol \qquad (2)$$

$$C + O_2 \rightarrow CO_2 \qquad \Delta H = -405.9kJ/mol \qquad (3)$$

$$CO + H_2O \rightarrow CO_2 + H_2 \qquad \Delta H = -40.9kJ/mol \qquad (4)$$

This material is reserved for educational use only, not allowed for commercial use.
Forbidden to modify the content, and cite the document when use

$$C + 2H_2 \rightarrow CH_4 \qquad \Delta H = -87.4kJ/mol \qquad (5)$$

From the reaction, reaction (1) and (2) are endothermic reaction and they are considered as the important reaction for gasification reaction. The reaction (3) is exothermic reaction which provided energy for reaction (1) and (2). The shift reaction (4) occur during high steam concentration and reaction (5) more effect at high pressure. For this study, we investigate in CO_2 gasification. So, Equation (1) is considered for this study.

When gasification proceeds, the mass of char is used to determine the gasification rate.

$$r' = \frac{-1}{W_0}\frac{dW}{dt} = \frac{dX}{dt} \qquad (6)$$

And

$$X = \frac{W_0 - W}{W_0} \qquad (7)$$

Where r is normalized gasification rate

t is time

W is the char mass at time t

X is char conversion

W_0 is Initial mass of char

The rate of conversion of (reactivity or reaction rate) char gasification can expresses by:

$$\frac{dX}{dt} = k(T)f(X) \qquad (8)$$

Where $f(X)$ is the changes in the physical or chemical properties of the sample as the gasification proceeds and corresponds to chosen n^{th} order expressions

In this work, six nth-order models were applied in order to describe the reactivity of the chars studied: the volumetric model, the grain model, the random pore model, the Chornet model, the shift extended random pore model and the modified random pore model.

2.) Volumetric model

The volumetric model is developed by Kimura,Nakagaw and Ton [2 3], it is model that does not consider the structure changes of the sample during reaction, but

This material is reserved for educational use only, not allowed for commercial use.
Forbidden to modify the content, and cite the document when use

assumes that the gasifying agents react with the particles of char at all active sites (inside and out of particle). For the volumetric model, we assume that:

1. The structure change of solid due to reaction is negligible.
2. The system for this reaction is isothermal reaction.
3. Pseudo-steady state approximation is valid.
4. Gas film resistance is negligible.

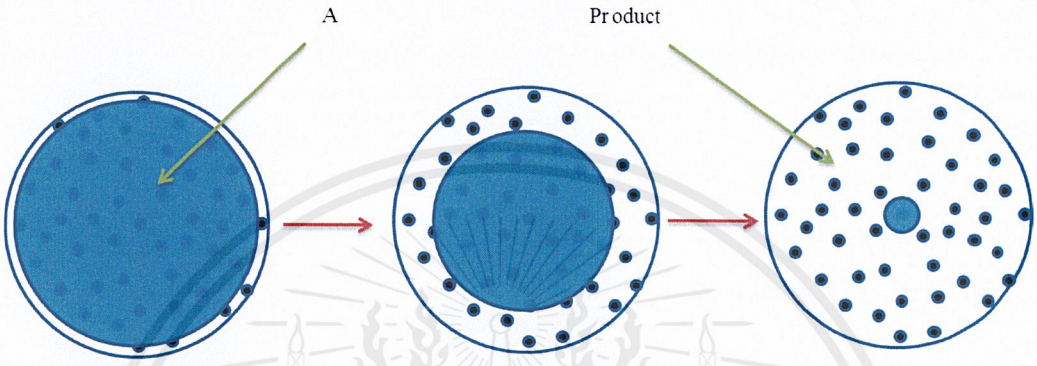


Figure 1.2.1 The reaction mechanism of volumetric model

From the Figure 1.2.1, the reaction is:

$$A_s \rightarrow Products \tag{9}$$

Suppose that N_{A0} is the initial amount of A in the reaction at time t = 0, and that N_A is the amount present at time t. Then the conversion of A in the constant volume system is given by:

$$X_A = \frac{N_{A0} - N_A}{N_{A0}} = 1 - \frac{N_A / V}{N_{A0} / V} = 1 - \frac{C_A}{C_{A0}} \tag{10}$$

Where X_A is the conversion of A

V is the volume of particle

C_A is the concentration of A at any time

C_{A0} is the concentration of A at t = 0

From (1), we assume that the reaction is first-order.

$$-r_A = \frac{-dC_A}{dt} = k_{VM} C_A \tag{11}$$

Where r is rate of reaction.

k_{VM} is rate constant.

When we separate and integrate equation (11), we obtain:

This material is reserved for educational use only, not allowed for commercial use.
Forbidden to modify the content, and cite the document when use

$$-\int_{C_{A0}}^{C_A} \frac{dC_A}{C_A} = k_{VM} \int_0^t dt \tag{12}$$

$$-ln\frac{C_A}{C_{A0}} = k_{VM} t \tag{13}$$

To obtain term of conversion, substitute $\frac{C_A}{C_{A0}}$ from (10) into (13):

$$-ln(1 - X_A) = k_{VM} t \tag{14}$$

3.) Grain model

Grain model is developed by Sohn andSzekely [2 4], its reaction involves heterogeneous gas-solid reaction with moving the boundary. For the grain model, the solid phases consist of unreacted core surrounded by the reacted shell. When the reactions are proceeded, the reacted zone will be expanded and the diffusion of reactant or product through this region may be one of rate limiting step.

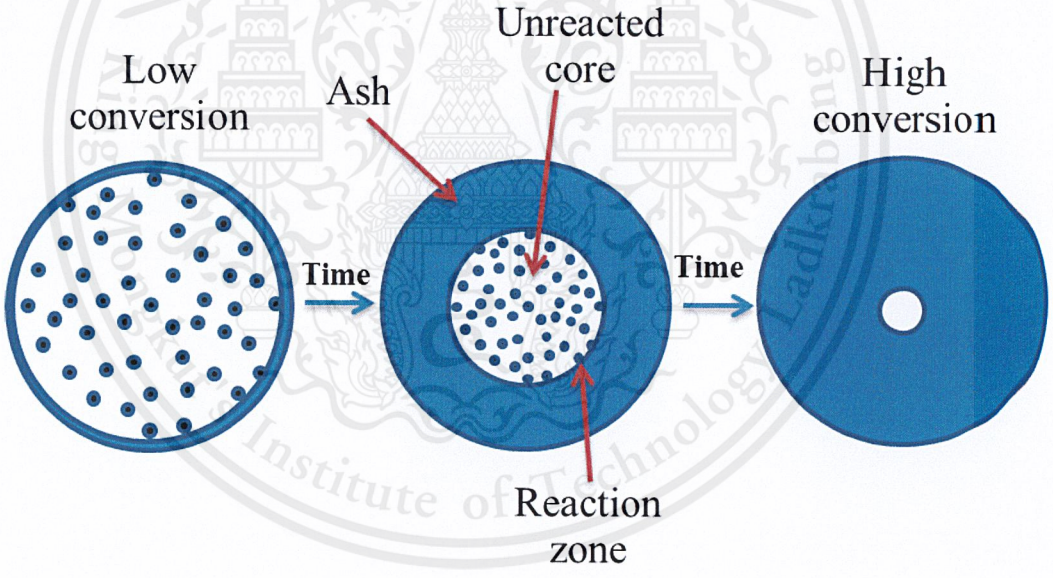


Figure 1.2.2 The model for sphere particle of unchanging size

From the Figure 1.2.2, the reaction for a particle of unchanging size is:

$$A_{(g)} + bB_{(S)} \rightarrow solid\ product \tag{15}$$

Where A is gasified agent

B is solid particle

For this reaction, it has five steps occurring in succession during reaction.

This material is reserved for educational use only, not allowed for commercial use.
Forbidden to modify the content, and cite the document when use

1. Diffusion of gaseous reactant A through the film surrounding the particle to the surface of the solid.
2. Penetration and diffusion of A through the blanket of ash to the surface of the unreacted core.
3. Reaction of gaseous A with solid at this reaction surface.
4. Diffusion of gaseous products through the ash back to the exterior surface of the solid.
5. Diffusion of gaseous products through the gas film back into the main body of fluid.

In some situations, some of these steps do not exist. For example, if no gaseous products are formed, steps 4 and 5 do not contribute directly to the resistance to reaction. Also, the resistances of the different steps usually vary greatly one from the other. In such cases we may consider that step with the highest resistance to be rate-controlling.

In this treatment, we develop the conversion equations for spherical particles in which steps 1, 2, and 3, in turn, are rate-controlling. We then extend the analysis to non-spherical particles and to situations where the combined effect of these three resistances must be considered.

Diffusion Through Gas Film Controls

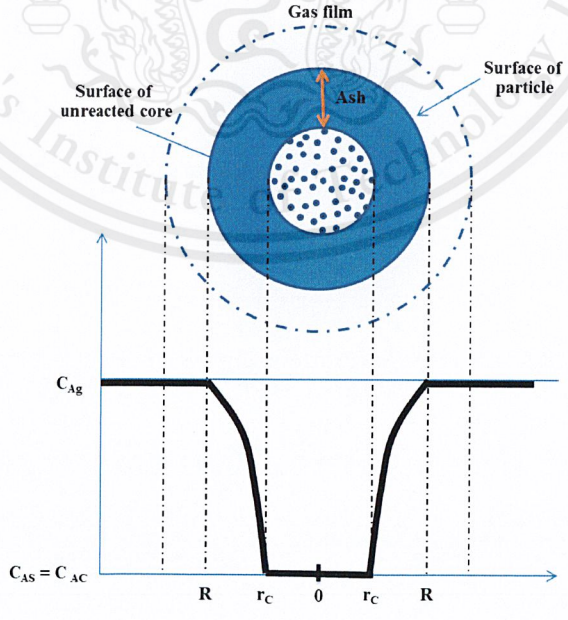


Figure 1.2.3 a reacting particle when diffusion through the ash layer is the controlling resistance

This material is reserved for educational use only, not allowed for commercial use.
Forbidden to modify the content, and cite the document when use

From the Figure 1.2.3, if we let N_B be the molar density of B in the solid and V be the volume of a particle, the reacting particle when diffusion through the gas film is the controlling resistance and the amount of B present in a particle can expression by:

$$-\frac{1}{S_{ex}}\frac{dN_B}{dt}=-\frac{1}{4\pi R^2}\frac{dN_B}{dt}=-\frac{b}{4\pi R^2}\frac{dN_A}{dt}=bk_g(C_{Ag}-C_{As})=bk_gC_{Ag} \quad (16)$$

$$N_B=\rho_B V \quad (17)$$

Where k_g is the mass transfer coefficient between fluid and particle.

b is stoichiometry of B

R is radius of particle

The decrease in volume or radius of unreacted core accompanying the disappearance of dN_B moles of solid reactant is then given by:

$$-dN_B=-bdN_A=-\rho_B dV=-\rho_B d(\frac{4}{3}\pi r_C^3)=-4\pi\rho_B r_C^2 dr_C \quad (18)$$

Where r_C is the radius of unreacted core.

Substitute (18) in (16) gives the rate of reaction in terms of the shrinking radius of unreacted core.

$$-\frac{1}{S_{ex}}\frac{dN_B}{dt}=-\frac{\rho_B r_C^2}{R^2}\frac{dr_C}{dt}=bk_gC_{Ag} \quad (19)$$

Integrating (19), we obtained:

$$-\frac{\rho_B}{R^2}\int_R^{r_C} r_C^2 dr_c=bk_gC_{Ag}\int_0^t dt \quad (20)$$

And

$$t=\frac{\rho_B R}{3bk_gC_{Ag}}\left[1-\left(\frac{r_C}{R}\right)^3\right] \quad (21)$$

Let the time for complete conversion of a particle be τ

$$\tau=\frac{\rho_B R}{3bk_gC_{Ag}} \quad (22)$$

Chemical reaction is the controlling resistance

This material is reserved for educational use only, not allowed for commercial use.
Forbidden to modify the content, and cite the document when use

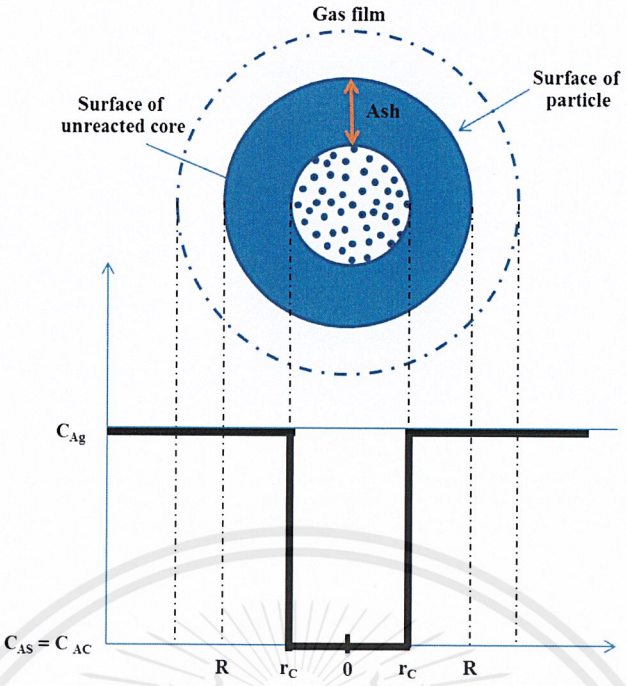


Figure 1.2.4 A reacting particle when chemical reaction is the controlling resistance

From the Figure 1.2.4, when the reaction is unaffected by the presence of any ash layer, the rate is proportional to the available surface of unreacted core. Thus, based on unit surface of unreacted core, the rate of reaction of reaction can express by:

$$-\frac{1}{4\pi r_C^2}\rho_B 4\pi r_C^2 \frac{dr_c}{dt} = \rho_B \frac{dr_c}{dt} = bk_g C_{Ag} \tag{23}$$

Integrate (23) become

$$-\rho_B \int_R^{r_C} dr_C = bk_g C_{Ag} \int_0^t dt \tag{24}$$

$$t = \frac{\rho_B}{bk_g C_{Ag}}(R - r_C) \tag{25}$$

Let (25) multiply by (14)

$$\frac{t}{\tau} = 3(R - r_C) \tag{26}$$

This can be written in terms of fractional conversion by noting that:

This material is reserved for educational use only, not allowed for commercial use.
Forbidden to modify the content, and cite the document when use

$$1 - X_B = \left(\frac{Volume\,of\,unreacted\,core}{Total\,volume\,of\,particle} \right) = \frac{\frac{4}{3}\pi r_C^3}{\frac{4}{3}\pi R^3} = \left(\frac{r_C}{R} \right)^3 \tag{27}$$

So,

$$\frac{t}{\tau} = kt = 3\left(1 - \left(1 - X_B\right)^{1/3}\right) \tag{28}$$

The derivative form:

$$\frac{dX}{dt} = k_{GM}(1 - X)^{2/3} \tag{29}$$

Where k is rate constant of reaction

4.) Chotnet model

Chornet model is propose by E. Chornet [25], it is developed from the semi-empirical models of Gardner and Johnson shown in equation (30) and equation (31) to fit with experimental data.

$$\frac{dX}{d\tau} = k_1\, exp(-aX)(1 - X) \tag{30}$$

$$\frac{dX}{d\tau} = k_2\, exp(-bX^2)(1 - X)^{2/3} \tag{31}$$

Where X is conversion

k_1, k_2 are kinetic constant

a, b are characteristic parameters

t is dimensionless time

To improve the kinetic model, E. Chornet consider that system of reaction undergoes three distinct although sequential phases:

1. At the beginning point, the reaction the total number of 'active sites' is rather limited and consequently the reaction proceeds slowly.
2. During the reaction, the rate of reaction up to maximum. It indicates that destruction and creation of active site affect to rate of reaction.
3. Beyond the maximum point the availability of 'active sites' decreases regularly. A decrease in the rate is also observed.

From the above reasonable, we can be applied the general model for gas-char reaction

$$\frac{dX}{d\tau} = k_{CM} X^C (1 - X)^d \tag{32}$$

This material is reserved for educational use only, not allowed for commercial use.
Forbidden to modify the content, and cite the document when use

Where k_3 is kinetic constant

c, d are adjustable characteristic parameters.

Using the method of Gorbachev for the determination of kinetic parameters in gas-char reactions:

$$c = 0.5 \text{ and } d = 1$$

5.) Random pore model

It propose by Bhatia and Perlmutter[26], it is common to consider the reaction as occurring on internal surfaces of the solid. The models can be classified into two categories: those that consider the reaction on the surfaces of nonporous grains and those that emphasize instead the reaction initiated on pore surfaces within the solid. The reaction for gas-solid can express by:

$$aA_g + bB_S \rightarrow pP_g + qQ_S \quad (33)$$

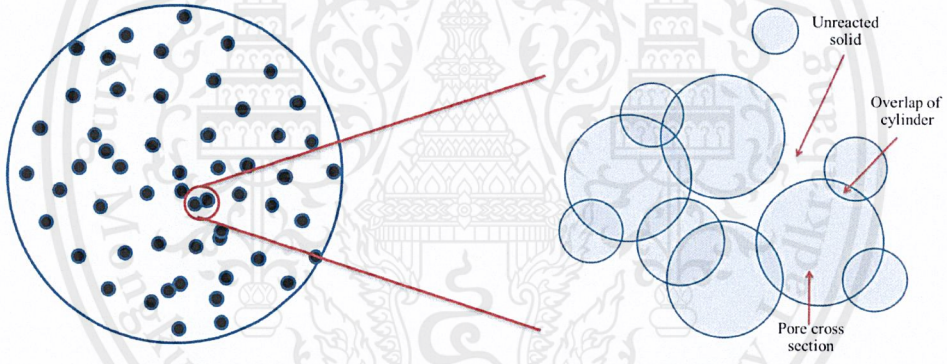


Figure 1.2.5 Overlapping of cylindrical surfaces.

From the reaction (33), consider the isothermal chemical reaction of particles of the solid B with a gas A according to the stoichiometry of Equation (33). The reaction is initiated on the surfaces of pores in the solid B. As further reaction occurs, a layer of product Q is formed around each pore which separates the growing reaction surface of the solid B from the fluid reactant A within the pores. Reactant A diffuses through the product layer to the reaction surface where chemical change occurs. If all diffusional resistances are assumed negligible, no distinction need be made between macro and micro-pores. It is assumed that the reactant B has no significant closed pore volume.

As reaction progresses, each pore of the particle has associated with it a growing reaction surface which initially corresponds to the inner surface of the pore.

This material is reserved for educational use only, not allowed for commercial use.
Forbidden to modify the content, and cite the document when use

As the various reaction surfaces in the particle grow, it is inevitable that neighboring surfaces will intersect one another as the solid B separating them is consumed and replaced by the product Q. Consider the actual reaction surface of the solid B at any time to be the result of the random overlapping of a set of cylindrical surfaces of size distribution $f(r)$, where $f(r)dr$ is the total length of the cylindrical surfaces per unit volume of space having radius between r and $r + dr$. Define as :

$$L_E = \int_0^\infty f(r)dr \tag{34}$$

$$S_E = 2\pi \int_0^\infty r \cdot f(r)dr \tag{35}$$

And

$$V_E = \pi \int_0^\infty r^2 \cdot f(r)dr \tag{36}$$

Where L_E is total length of non-overlapped system

S_E is surface area of cylindrical system, per unit volume

V_E is volume enclosed by cylindrical system, per unit volume of space

$f(r)$ is size distribution of non-overlapped system at any time

r is radius of cylindrical surface

As the total length, total surface area and total enclosed volume of the non-overlapped cylindrical system. A balance over the size distribution of the growing cylinders yields.

$$\frac{\partial f}{\partial t} + \frac{\partial}{\partial r}\left(f\frac{dr}{dt}\right) = 0 \tag{37}$$

Where it is assumed that no cylinders are created or destroyed.

If the rate of reaction on the actual surface is proportional to the total surface area, it can express by following equation:

$$\frac{dr}{dt} = k_s C^n \tag{38}$$

Where k_s is rate constant for surface reaction

C is concentration of gaseous reactant A

n is reaction order with respect to gas A

Combining Equations (37) and (38)

This material is reserved for educational use only, not allowed for commercial use.
Forbidden to modify the content, and cite the document when use

$$\frac{\partial f}{\partial t} = k_s C^n \frac{\partial f}{\partial r} \tag{39}$$

Integrating Equation (39) with respect to r, and using Equation (34) together with the conditions $f(0) = f(\infty) = 0$

$$\frac{dL_E}{dt} = 0 \tag{40}$$

Multiplying equation (29) by $2\pi r$, integrating with respect to r and inserting definitions (34) and (35).

$$\frac{dS_E}{dt} = 2\pi k_s C^n L_E \tag{41}$$

If we multiply equation (39) by πr^2, integrate with respect to r and substitute equation (23), an equation for the total volume is:

$$\frac{dV_E}{dt} = k_s C^n S_E \tag{42}$$

Equations (40), (41) and (42) can be solved to yield

$$S_E = \sqrt{S_{E0}^2 + 4\pi L_{E0}(V_E - V_{E0})} \tag{43}$$

And

$$V_E = V_{E0} + S_{E0}(k_g C^n t) + \pi L_{E0}(k_s C^n t)^2 \tag{44}$$

Where S_{E0} is S_E at $t = 0$

V_{E0} is V_E at $t = 0$

L_{E0} is L_E at $t = 0$

The fractional volume of space occupied by the unreacted solid B is:

$$dV = (1 - V)dV_E \tag{45}$$

With the observation that $V \to 0$ as $V_E \to 0$, Equation (45) can be integrated to:

$$V = 1 - exp(-V_E) \tag{46}$$

To obtain a relationship between the surface areas of the overlapped and non-overlapped systems, consider the increase in volume of the overlapped system by an amount dV in time dt.

Since the rate of reaction is assumed proportional to surface area

$$dV_E = S_E k_s C^n dt \tag{47}$$

This material is reserved for educational use only, not allowed for commercial use.
Forbidden to modify the content, and cite the document when use

And

$$dV = Sk_s C^n dt \tag{48}$$

Combining equations (45), (47) and (48), we get

$$S = S_E(1-V) \tag{49}$$

As the overlapped system increases in volume by an amount mi, the change in the total length of the system due to additional intersections may be written as

$$dL = -\frac{L}{(1-V)}dV \tag{50}$$

Since no overlapping is possible at $V = 0$

$$\lim_{V \to 0} L = L_E \tag{51}$$

Integrating Equation (50) with boundary condition (51) we can obtain

$$L = L_E(1-V) \tag{52}$$

Combining Equations (46), (49) and (52) with Equations (43) and (44), we get

$$\frac{S}{S_0} = \left(\frac{1-V}{1-V_0}\right)\sqrt{1 - \frac{4\pi L_0(1-V_0)}{S_0^2} ln\left(\frac{1-V}{1-V_0}\right)} \tag{53}$$

$$V = 1-(1-V_0)exp\left[-\frac{k_s C^n t}{1-V_0}\left(S_0 + \pi L_0 k_s C^n t\right)\right] \tag{54}$$

Where S_0 is S at $t = 0$

V_0 is V at $t = 0$

For a spherical particle in the regime of reaction control

$$1-X = \left(\frac{1-V}{1-V_0}\right)\left(1-\frac{k_S C^n t}{R_0}\right)^3 \tag{55}$$

In dimensionless form, Equations (53) and (54), upon combining with Equation (45) and the initial condition

$$V_0 = \varepsilon_0 \tag{56}$$

Become

This material is reserved for educational use only, not allowed for commercial use.
Forbidden to modify the content, and cite the document when use

$$\frac{S}{S_0} = \frac{(1-X)}{\left(1-\frac{\tau}{\sigma}\right)^3}\sqrt{\left[1-\psi\, ln\left(\frac{1-X}{\left(1-\frac{\tau}{\sigma}\right)^3}\right)\right]} \tag{57}$$

$$X = 1-\left(1-\frac{\tau}{\sigma}\right)^3 exp\left[-\tau\left(1+\frac{\pi\tau}{4}\right)\right] \tag{58}$$

Where σ is the particle size parameter

X is conversion

Differentiate Equation (58) as $\sigma \to \infty$ to give

$$\frac{dX}{d\tau} = (1-X)\sqrt{[1-\psi\, ln(1-X)]} \tag{59}$$

Where

$$\tau = \frac{k_s t S_0 C^n}{1-\varepsilon_0} \tag{60}$$

Substitute equation (60) in to (59)

$$\frac{dX}{dt} = k_{RPM}(1-X)\sqrt{[1-\psi\, ln(1-X)]} \tag{61}$$

And

$$\psi = \frac{4\pi L_0(1-\varepsilon_0)}{S_0^2} \tag{62}$$

$$k_{RPM} = \frac{K_s \tau C^n S_0}{1-\varepsilon_0} \tag{63}$$

Where k is rate constant of reaction

ψ is a structural parameter.

ε_0 is char porosity at $t = 0$

6.) Shift extended random pore model

The random pore model has been successfully used for modeling the gasification of char. However, it fails to describe and predict for some biomass char. So, the random pore model is modified to shift extended random pore model by add term of conversion [2 2] $(1+(cX)^p)$. The random pore model is multiplied by additional term, the empirical parameter c and p to better fit the experimental data

This material is reserved for educational use only, not allowed for commercial use.
Forbidden to modify the content, and cite the document when use

obtain from gasification of biomass. The shift extended random pore model (s-ePRM) is expressed in equation:

$$\frac{dX}{dt} = \frac{k_{sRPM}(1-X)\sqrt{[1-\psi\, ln(1-X)]}}{1+(cX)^P} \tag{64}$$

7.) Modified random pore model

The modified random pore model is propose by Zhang, Wang,Shao and Zuo[10],[27], it is developed from random pore model, it different from the random pore model by added the conversion term to random pore model. It can be written as:

$$\frac{dX}{dt} = k_{mRPM}(1-X)^n\sqrt{[1-\psi\, ln(1-X)]} \tag{65}$$

Where n is the dimension less power raw

This material is reserved for educational use only, not allowed for commercial use.
Forbidden to modify the content, and cite the document when use

1.3 RESEARCH METHODOLOGY

1.3.1 Researching Procedure

1. Research Question

This step, the project is to determine what important objective for this study. For this project, we investigate in gasification reaction of rice husk char to find the suitable kinetic model and to describe the gasification reaction of rice husk char. Moreover, we investigate in kinetic parameter of this reaction and indicate that what effect of this parameter to reaction of rice husk char gasification

2. Data Collection

For this step, theory of char gasification reaction, properties of rice husk as well as the gas-solid reaction are investigated and studied. To understand in this project, we study theory of gasification in part of gasification of biomass. The properties of rice husk char are investigated by several of research. Moreover, kinetic theory is adept tin to mathematics model by using mathematic method.

3. Research Method

The kinetic model and experimental data from previous step is used to find the kinetic parameters. The kinetic parameters are determined by Levenberge-Marquart method and linearization. The kinetic parameter that obtain from previous step is used to predict the experimental data result.

4. Analysis result from model and conclude result

the result form previous step is analysis by compare with the experimental data, the best model for describe the reaction of rice husk char gasification are indicated by using correlation coefficient. After obtaining the suitable kinetic model, the reaction is described base on assumption of this model and the reaction behavior of this reaction are described and concluded.

1.3.2 Calculation Tool

1. Polymath Fogler 6.10 Professional
2. Microsoft Excel 2016

This material is reserved for educational use only, not allowed for commercial use.
Forbidden to modify the content, and cite the document when use

1.3.3 Calculation

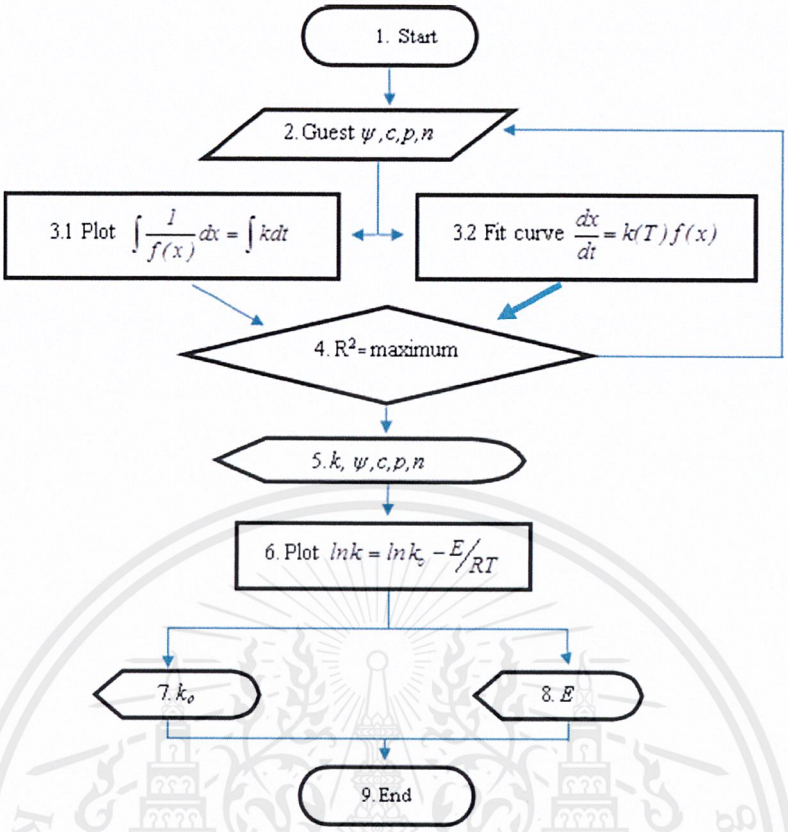


Figure 1.3.1 Method flowchart

From Figure 1.3.1, we can be described by step following:

1.) Select the kind of char to calculate the kinetics parameter for each model.

2.) Select the model to predict conversion time of char.

3.) Calculate the kinetic parameter of char, for each model that different method to calculate which show following.

- Volumetric model

-Use the experimental data from research paper plot graph relationship between $-ln(1-X)$ and t . From the equation

$$-ln(1-X) = k_{VM} t$$

k_{VM} can find from the slop of graph

- Use the k_{VM} value from step 1 plot graph relationship between lnk_{VM} and $1/T$ (Arrhenius plot). From Arrhenius plot

$$ln\, k_{VM} = ln\, k_0 - \frac{E}{RT}$$

This material is reserved for educational use only, not allowed for commercial use.
Forbidden to modify the content, and cite the document when use

From graph, pre-exponential factor (k_0) and activation energy (E) can find from intersection point at Y-axis and slop of graph respectively.

- Grain model

-Use the experimental data from research paper plot graph relationship between $3(1-(1-X)^{1/3})$ and t . From the equation

$$3\left(1-(1-X)^{1/3}\right)=k_{GM}t$$

k_{GM} can find from the slop of graph

-Use the k_{GM} value from step 1 plot graph relationship between lnk_{GM} and $1/T$ (Arrhenius plot). From Arrhenius plot

$$ln\,k_{GM}=ln\,k_0-\frac{E}{RT}$$

From graph, pre-exponential factor (k_0) and activation energy (E) can find from intersection point at Y-axis and slop of graph respectively.

- Chornet model

-Use the experimental data from research paper plot graph relationship between $2arctanh(X^{1/2})$ and t . From the equation

$$2\,arctanh\left(\sqrt{X}\right)=k_{CM}t$$

k_{CM} can find from the slop of graph

-Use the k_{CM} value from step 1 plot graph relationship between lnk_{CM} and $1/T$ (Arrhenius plot). From Arrhenius plot

$$ln\,k_{CM}=ln\,k_0-\frac{E}{RT}$$

From graph, pre-exponential factor (k_0) and activation energy (E) can find from intersection point at Y-axis and slop of graph respectively.

- Random pore model

-Determine rate of reaction of experimental data by using polymath program.

-After that, fitted graph with experimental data using equation below.

$$\frac{dX}{dt}=k_{RPM}(1-X)\sqrt{[1-\psi\,ln(1-X)]}$$

- Guest initial value of parameter, k_{RPM} = 0.0001 and ψ = 1

-Used the value of ψ from step 3 plot graph relationship between $(2/\Psi)[(1-\Psi ln(1-X)^{1/2}-1)]$ and t. from the equation below

$$(2/\psi)(1-\psi_0\,ln(1-X))^{1/2}=k_{RPM}t$$

This material is reserved for educational use only, not allowed for commercial use.
Forbidden to modify the content, and cite the document when use

k_{RPM} can find from the slop of graph

- Plot graph relationship between lnk_{RPM} and $1/T$ to find pre-exponential factor (k_0) and activation energy (E)

$$ln\,k_{RPM} = ln\,k_0 - \frac{E}{RT}$$

From the equation above, E and k_0 can find from intersection point at Y-axis and slop of graph respectively.

- Shift-Random pore model

-Step 1 same as random pore model

-After that, fitted graph with experimental data using equation below

$$\frac{dX}{dt} = \frac{k_{sRPM}(1-X)\sqrt{[1-\psi\,ln(1-X)]}}{1+(cX)^P}$$

- Guest initial value of parameter, $k_{sRPM} = 0.0001$, $\psi = 1$, $C = 1$ and $P = 1$

-If graph can have fitted with data, change the initial guest value until R-square more than 0.95

-Used the value of ψ, C and P that most fitted with graph from step 4 as the parameter and substitute them in equation in step 2 to find k value for each temperature.

- Plot graph relationship between lnk_{sRPM} and $1/T$ to find pre-exponential factor (k_0) and activation energy (E)

$$ln\,k_{sRPM} = ln\,k_0 - \frac{E}{RT}$$

From the equation above, E and k_0 can find from intersection point at Y-axis and slop of graph respectively.

- Modified random pore model

-Step 1 same as random pore model

-After that, fitted graph with experimental data using equation below.

$$\frac{dX}{dt} = k_{mRPM}(1-X)^n\sqrt{[1-\psi\,ln(1-X)]}$$

- Guest initial value of parameter, $k_{mRPM} = 0.0001$, $\psi = 1$ and $n = 1$
- If graph can fit with data, change the initial guest value until R^2 more than 0.95

This material is reserved for educational use only, not allowed for commercial use.
Forbidden to modify the content, and cite the document when use

-Used the value of ψ and n that most fitted with graph from step 4 as the parameter and substitute them in equation in step 2 to find k_{mRPM} value for each temperature.

- Plot graph relationship between lnk_{mRPM} and $1/T$ to find pre-exponential factor (k_0) and activation energy (E)

$$ln\, k_{mRPM} = ln\, k_0 - \frac{E}{RT}$$

From the equation above, E and k_0 can find from intersection point at Y-axis and slop of graph respectively.

This material is reserved for educational use only, not allowed for commercial use.
Forbidden to modify the content, and cite the document when use

1.4 RESULTS AND DISCUSSION

1.4.1 Modeling

The experimental data from Xiaoyan Gao et al. [3] is used to find the kinetic parameter for each model. The experimental data are fitted by various models. By plotting $-ln(1-X)$, $3[1-(1-X)^{1/3}]$, $2arctanh(X^{1/2})$ and $(2/\psi)(1-\psi ln(1-X))^{1/2}$ as the function of t, the slopes of curves at different reaction temperatures could be obtained to represent the reaction rate constants (k_{VM}, k_{GM}, k_{RPM}, k_{CM}) of the gasification process. In the RPM model, the values of ψ is estimate by guess value to obtain the optimum fitting of graph.

In the mRPM and sRPM model, the parameter of ψ, c, p and n are estimated by curve fitting. These parameters are obtained by optimum fitting and are constant under different temperatures because ψ and n are represented the original pore structure of the semi-char and reaction order. After that the Arrhenius plot (lnk vs $1/T$) is used to calculate the activation energy (E) and the pre - exponential factor (k_o).

Table 1.4.1 shows the kinetic parameters obtained by applications of different models. It can be seen in Table 1.1 that activation energies of rice husk for each model are distributed in the range of 210. 2-210. 7 kJ/ mol. However, the pre-exponential factor varied greatly, for example, the pre-exponential factors of the VM and mRPM are 2.60×10^6 s^{-1} and 9.74×10^5 s^{-1}, respectively.

Table 1.4.1 Comparisons of the kinetic parameters for each models

This study							
Char		CO_2 gasification (Model)					
		E (kJ/mole/K)	k_o (1/s)	ψ	n	c	p
Rice husk	VM	210.51	2.60×10^6				
	GM	209.26	1.80×10^6				
	CM	210.67	5.16×10^6				
	RPM	209.67	1.16×10^6	6.30			
	mRPM	205.52	9.74×10^6	1.30	0.76		
	sRPM	210.26	8.32×10^6	33.30		0.34	0.55
Other study	Xiaoyan Gao	232.28	2.38×10^5	6.00			
	Yafei Shen	169.2	2.78×10^6	2.58			

For each parameter is indicated to physical property of char. for example, ψ is porosity of char. it indicated that how many porous in particle of char. n is the

This material is reserved for educational use only, not allowed for commercial use.
Forbidden to modify the content, and cite the document when use

reaction order of rice husk char gasification. *C* and *P* in shift random pore model are two parameters take the effects of inherent minerals on the pore structure or pore structure changing with conversion into consideration

In order to compare the accuracy for each model, the experimental conversion is compared with the calculated values at the different temperatures. The results are shown in Figure 1.4.1 - 1.4.6. In order to quantify the errors produced by the kinetic models, the coefficient of correlation between the experimental and predicted values are obtained using R^2. The results obtain from the six models are summarized in Table 1.2. From Table 1.2, we found that, at temperature 1123K, 1148K and 1173K, the most accurate prediction model is mRPM. But at high temperature (1198-1223K), the most accurate prediction model is sRPM model

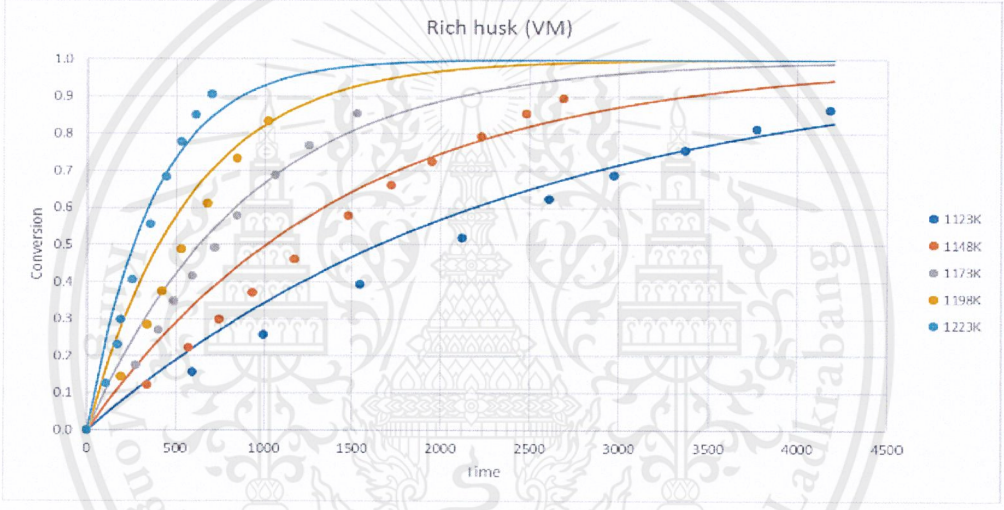


Figure 1.4.1 Comparison between experimental data and predicted values by the VM

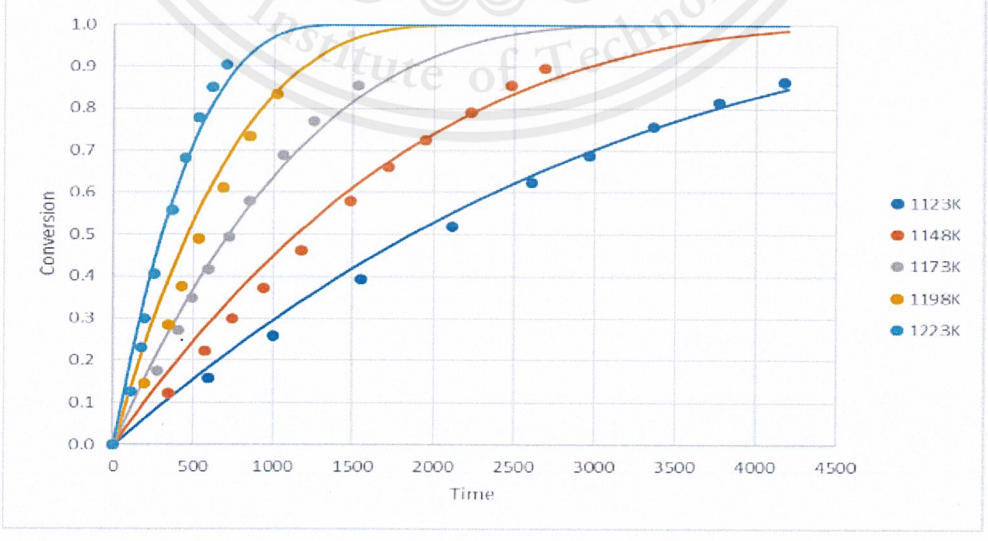


Figure 1.4.2 Comparison between experimental data and predicted values by the GM

This material is reserved for educational use only, not allowed for commercial use.
Forbidden to modify the content, and cite the document when use

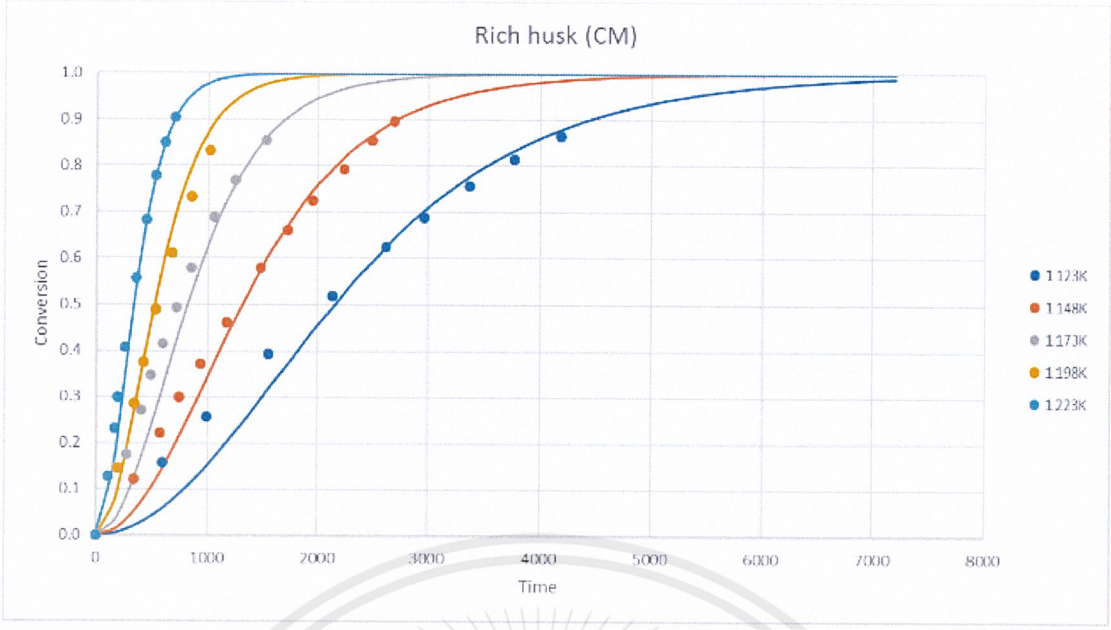


Figure 1.4.3 Comparison between experimental data and predicted values by the CM

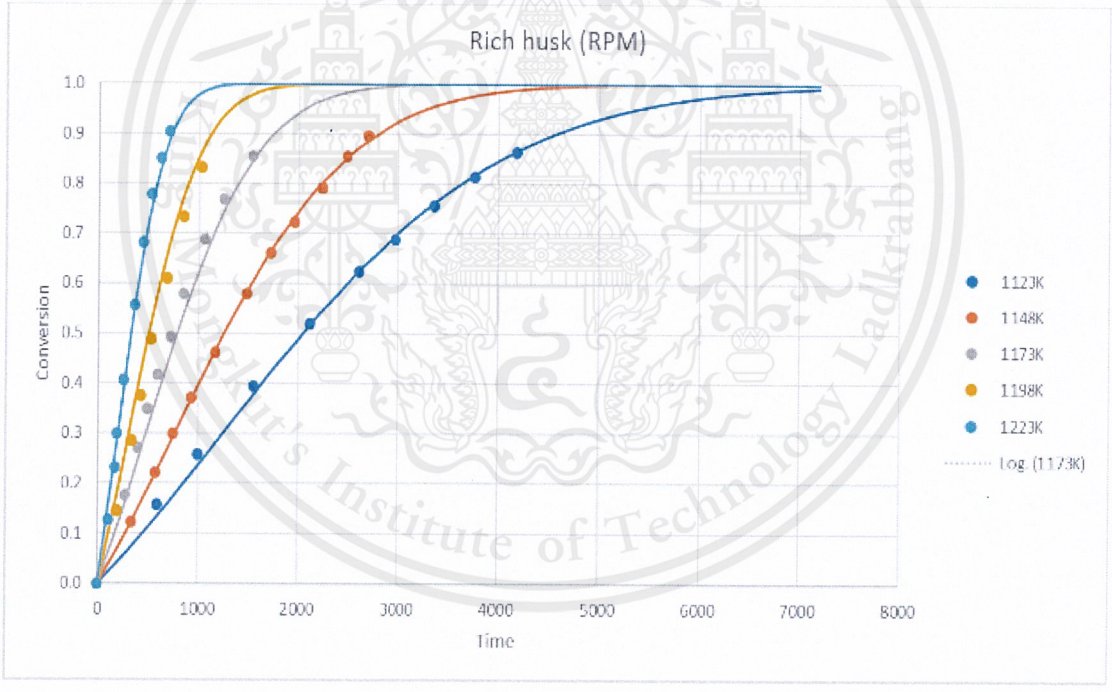


Figure 1.4.4 Comparison between experimental data and predicted values by the RPM

This material is reserved for educational use only, not allowed for commercial use.
Forbidden to modify the content, and cite the document when use

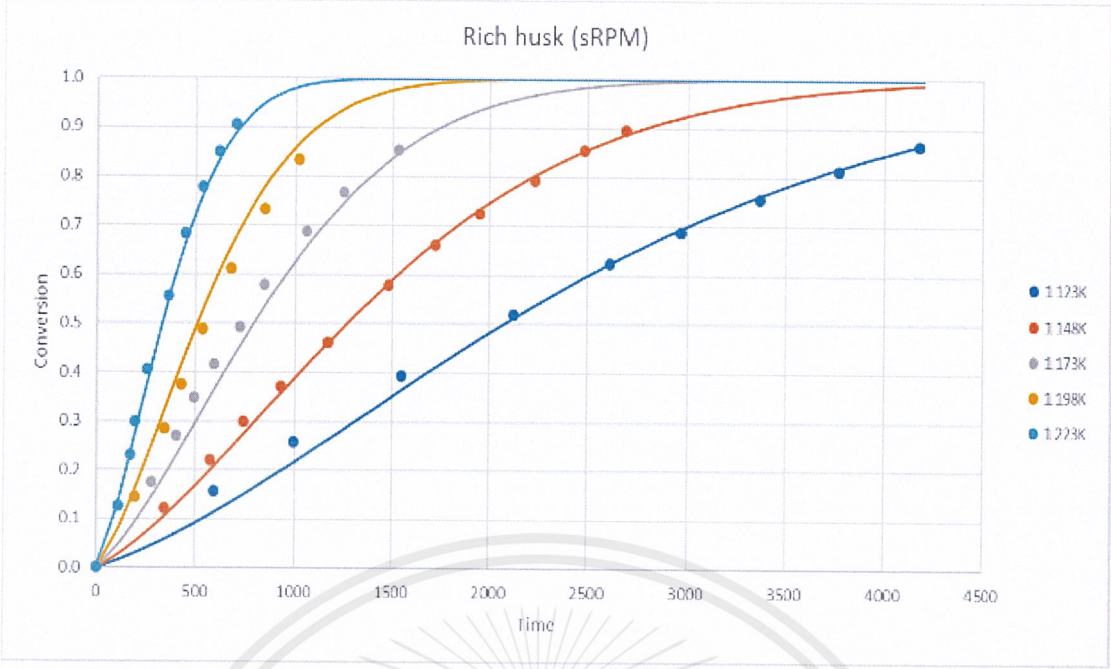


Figure 1.4.5 Comparison between experimental data and predicted values by the mRPM

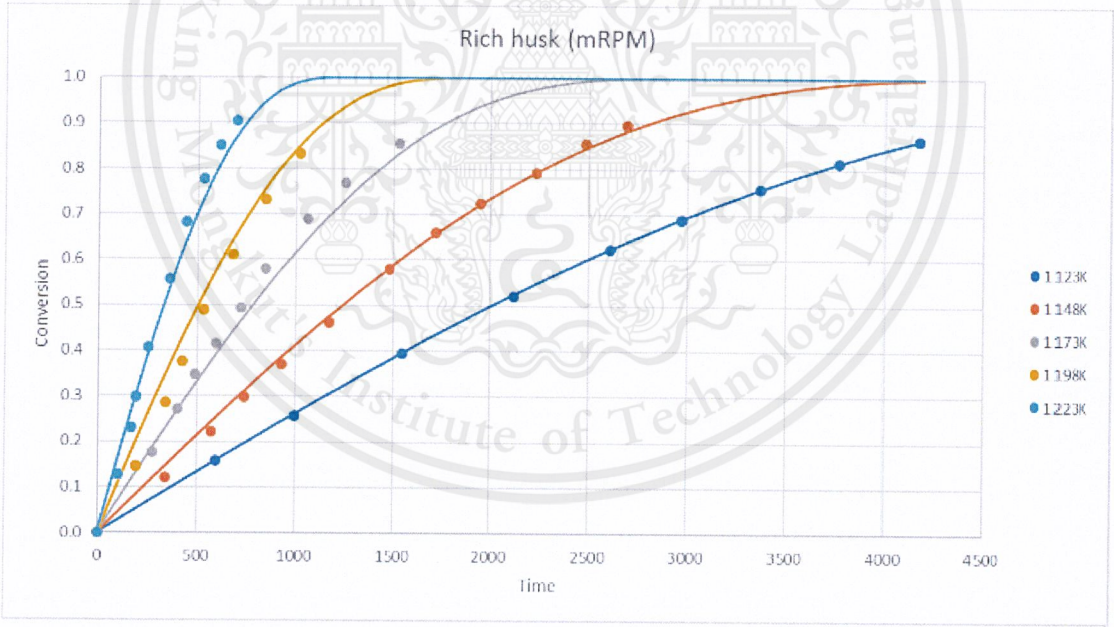


Figure 1.4.6 Comparison between experimental data and predicted values by the sRPM

This material is reserved for educational use only, not allowed for commercial use.
Forbidden to modify the content, and cite the document when use

Table 1.4.2 Comparisons of correlation coefficient

Char	CO_2 gasification (Model)						
	Temp(K)	VM	GM	CM	RPM	mRPM	sRPM
Rice husk	1123	0.96	0.99	0.96	0.99	0.99	0.99
	1148	0.94	0.98	0.97	0.99	0.99	0.99
	1173	0.95	0.99	0.91	0.98	0.98	0.97
	1198	0.85	0.93	0.98	0.97	0.97	0.98
	1223	0.93	0.97	0.97	0.99	0.98	0.99

From the result, Figure 1.4.1 - 1.4.6 shown graph comparison of prediction value and experimental data of rich husk char gasification. We found that the experimental data of rich husk agree with sRPM model, it indicate that the reaction of char gasification of this experiment as follow with assumption of sRPM model which assume that at initial the char particle consist of pore volume on surface and don' t have the overlapping of pore. When the reaction proceeds, the gasify agent react char at pore of surface and the reaction will expand to inside of particle.

1.4.2 Validation

The experimental data of Thilakavathi M [7] and Ashish B [4] are used to validate the kinetic models rice husk char gasification, six kinetic models from modeling step are used to predict the both experimental data. The variation of each model is indicated by correlation coefficient value (R^2) to find the most accurate prediction for char gasification reaction of rice husk.

1.) Kinetics validation with Thilakavathi M's experiment

The rich husk is pyrolyzed in tubular reactor under atmosphere pressure at a temperature of 500°C and heating rate 12°C/ min. After that, rich husk char is activated by gasification reaction under CO_2 as gasify agent with flow rate 50 ml/min at temperature about 750 - 900°C. Rice husk char is kept at gasifying temperature for 45 minutes to complete reaction.

This material is reserved for educational use only, not allowed for commercial use.
Forbidden to modify the content, and cite the document when use

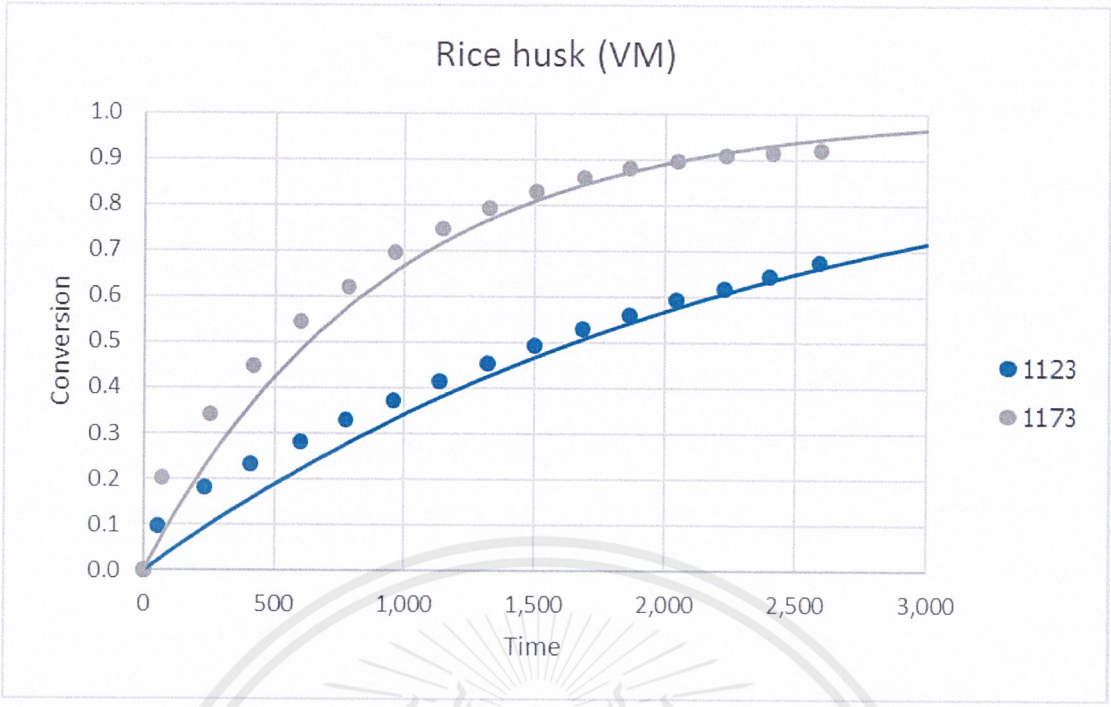


Figure 1.4.7 Model validation with experimental data from Thilakavathi M. (VM)

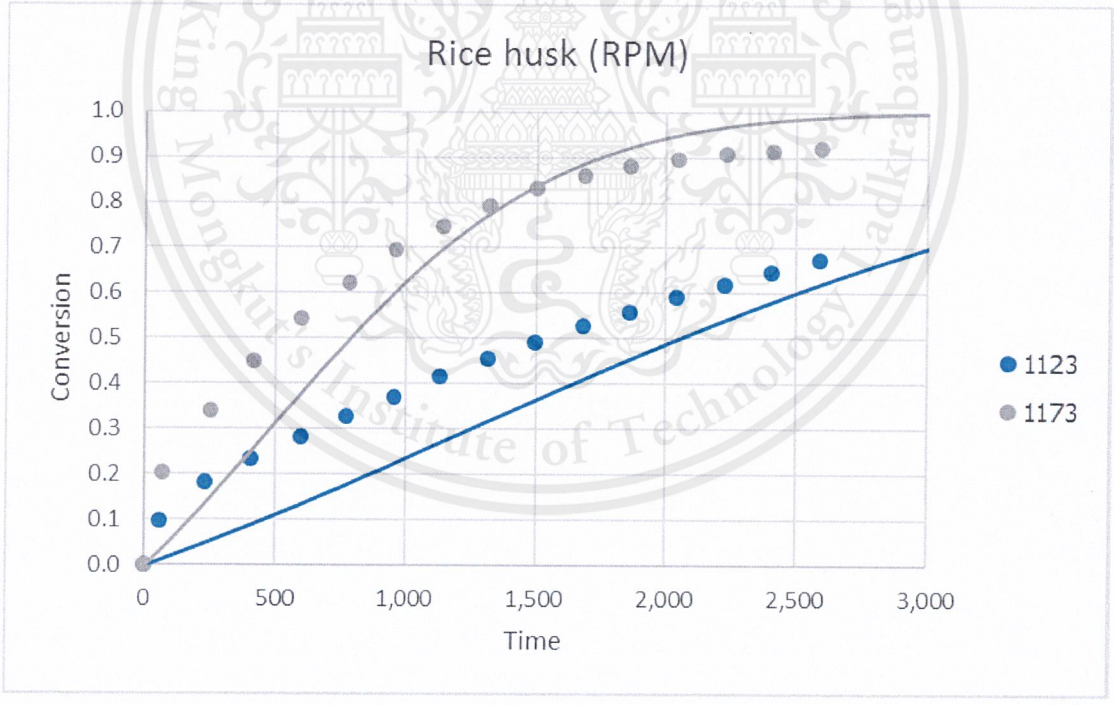


Figure 1.4.8 Model validation with experimental data from Thilakavathi M. (RPM)

This material is reserved for educational use only, not allowed for commercial use.
Forbidden to modify the content, and cite the document when use

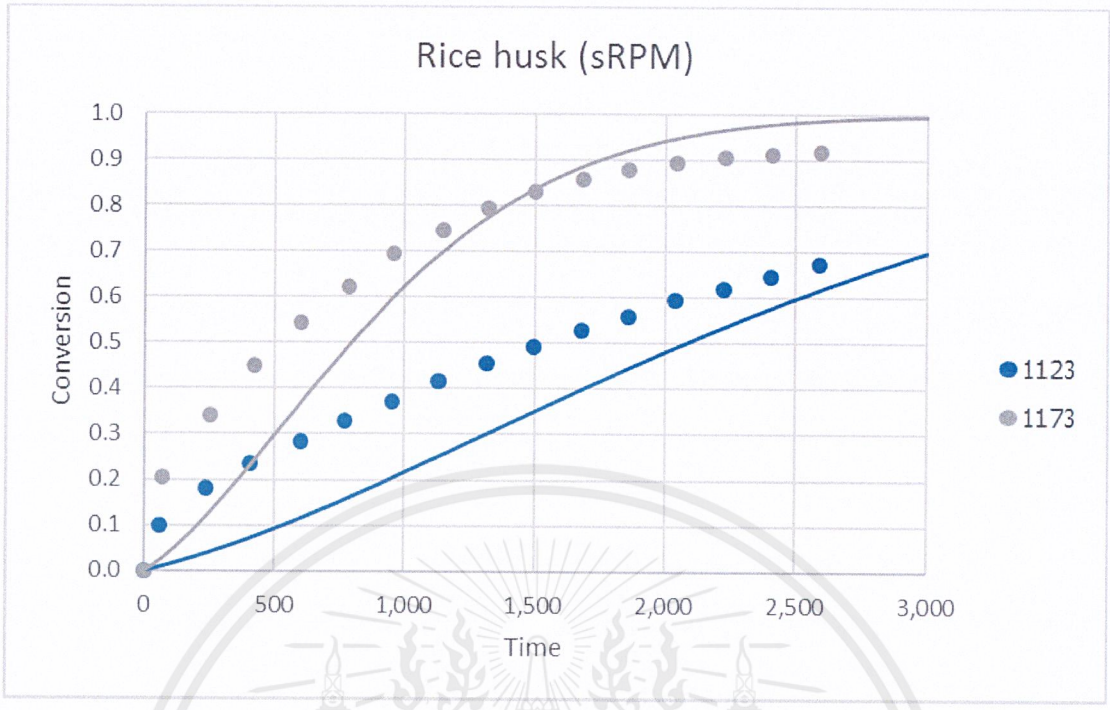


Figure 1.4.9 Model validation with experimental data from Thilakavathi M. (sRPM)

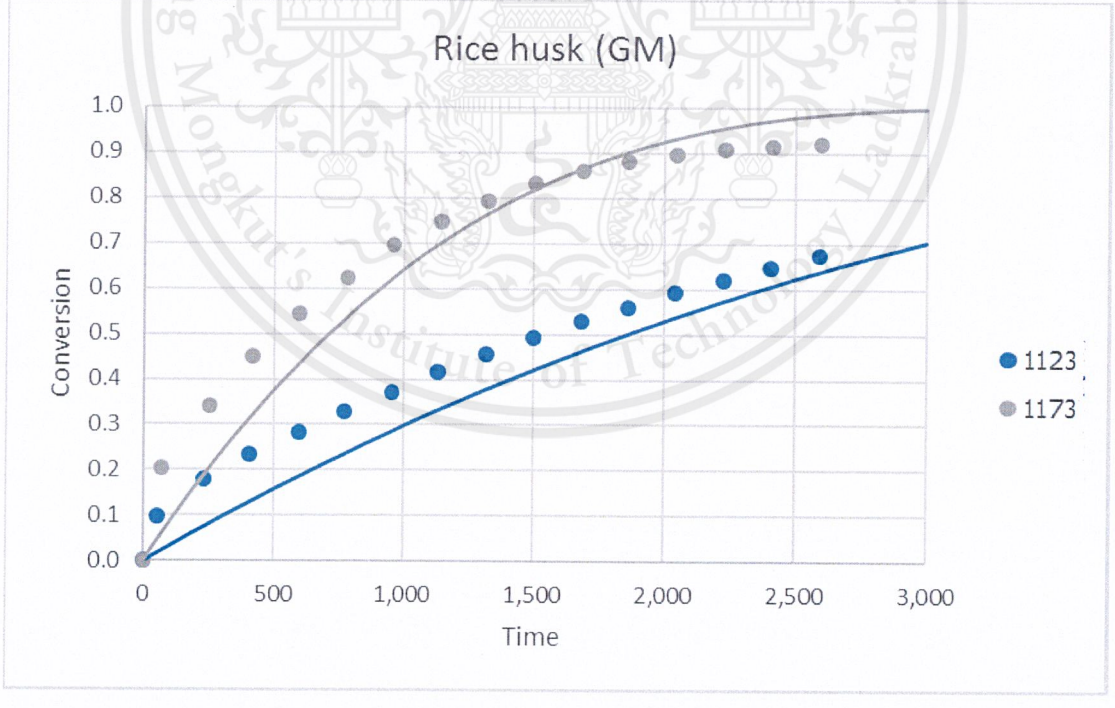


Figure 1.4.10 Model validation with experimental data from Thilakavathi M. (GM)

This material is reserved for educational use only, not allowed for commercial use.
Forbidden to modify the content, and cite the document when use

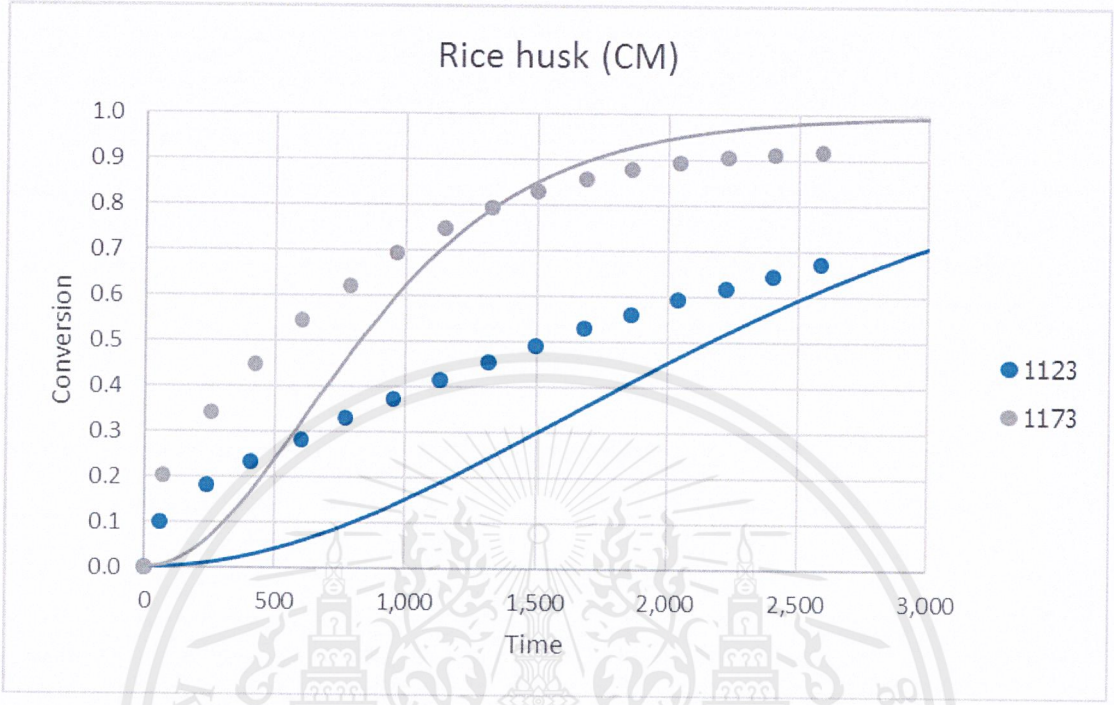


Figure 1.4.11 Model validation with experimental data from Thilakavathi M. (CM)

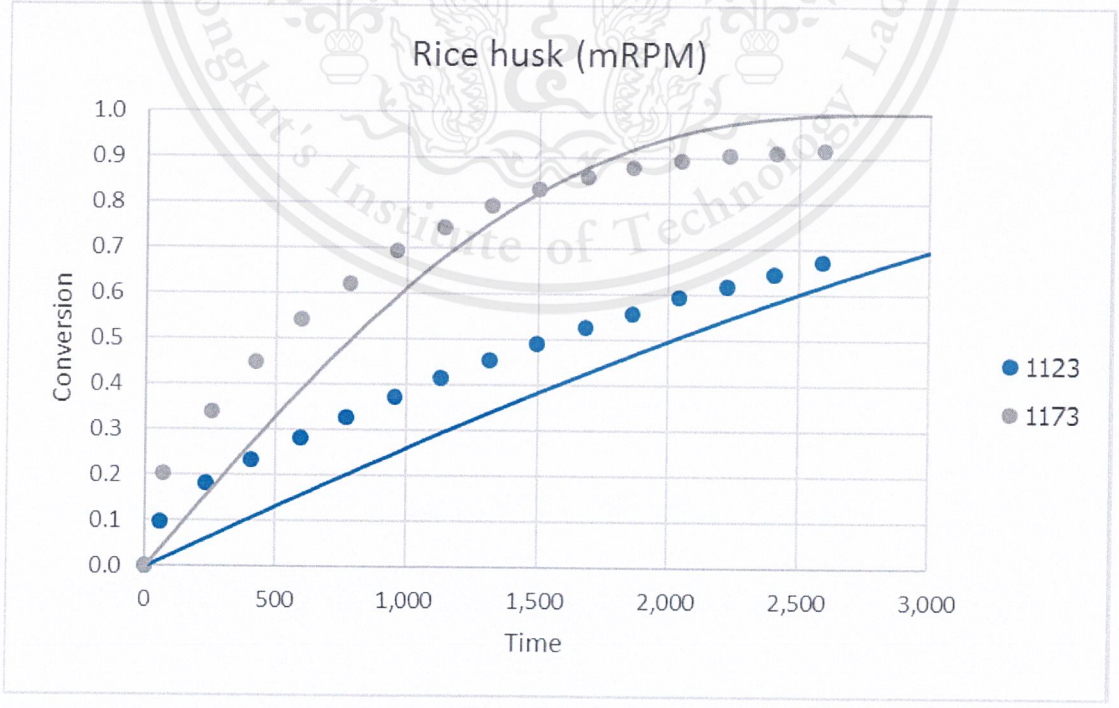


Figure 1.4.12 Model validation with experimental data from Thilakavathi M. (mRPM)

This material is reserved for educational use only, not allowed for commercial use.
Forbidden to modify the content, and cite the document when use

2.) Kinetics validation with Ashish B.'s experiment

Ashish B. ' s experiment, rich husk char is prepared in batch pyrolizer at atmosphere and temperature about 600-700 ˚C. The char is made by grinding and sieving the char grain. The average size of char about 10 μm. After that, 10 mg of char are carried out in TGA. The heating rate of 50 K/min and CO_2 as gasify agent.

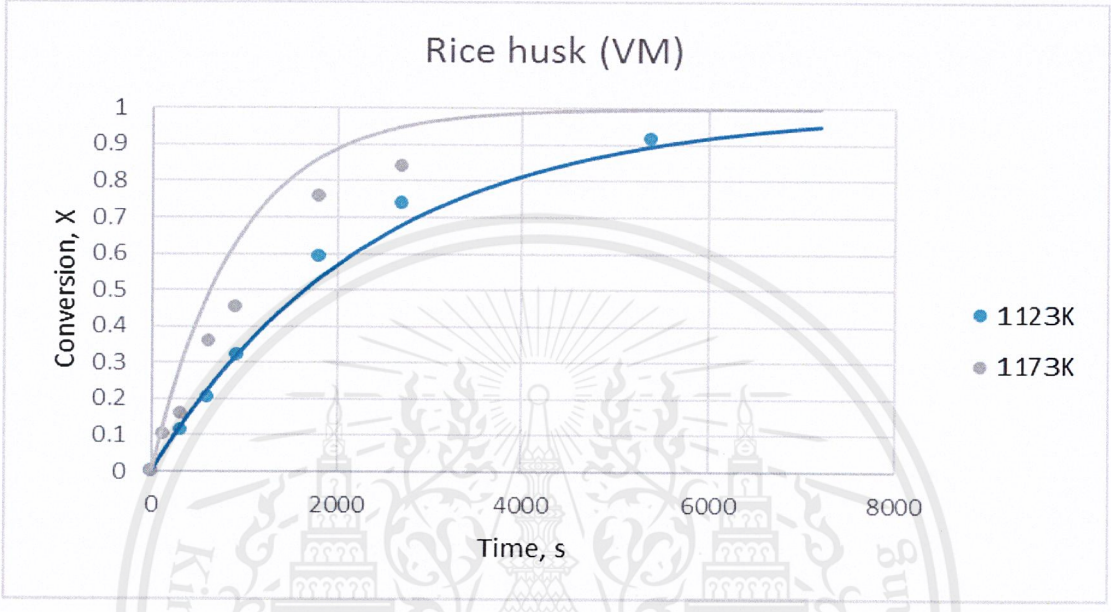


Figure 1.4.13 Model validation with experimental data from Ashish B.. (VM)

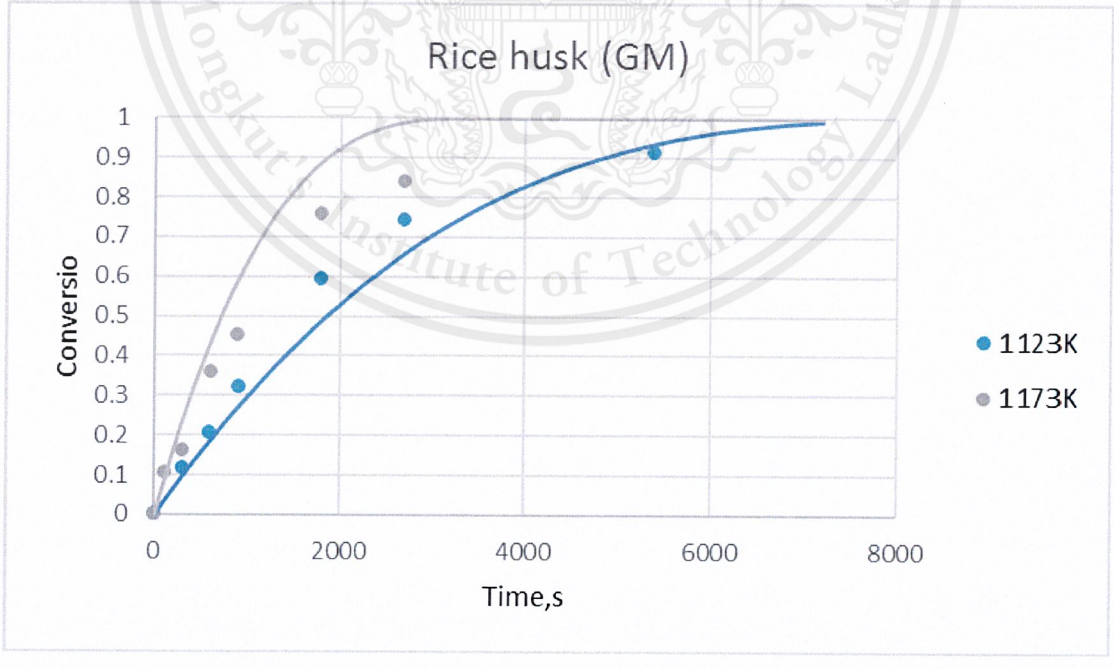


Figure 1.4.14 Model validation with experimental data from Ashish B.. (GM)

This material is reserved for educational use only, not allowed for commercial use.
Forbidden to modify the content, and cite the document when use

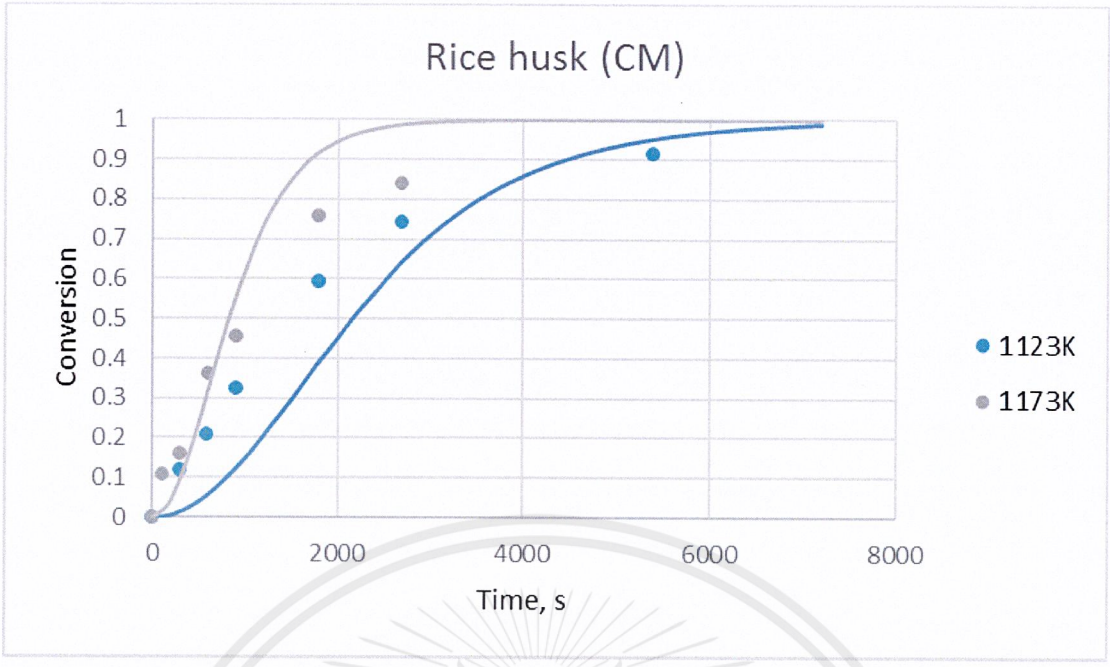


Figure 1.4.15 Model validation with experimental data from Ashish B.. (CM)

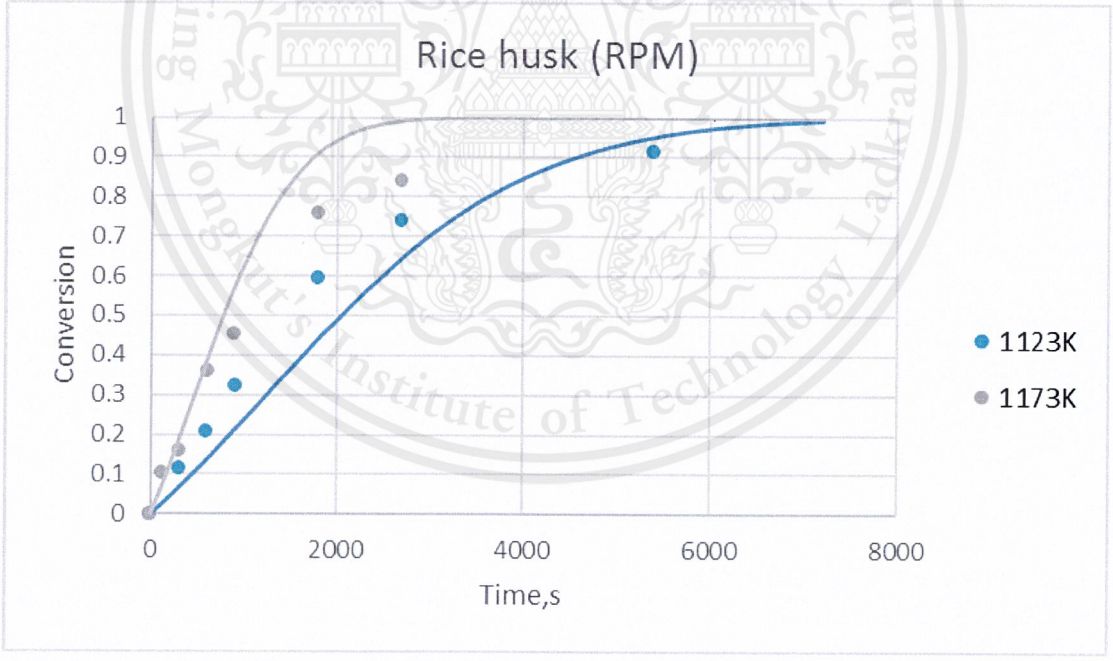


Figure 1.4.16 Model validation with experimental data from Ashish B. (RPM)

This material is reserved for educational use only, not allowed for commercial use.
Forbidden to modify the content, and cite the document when use

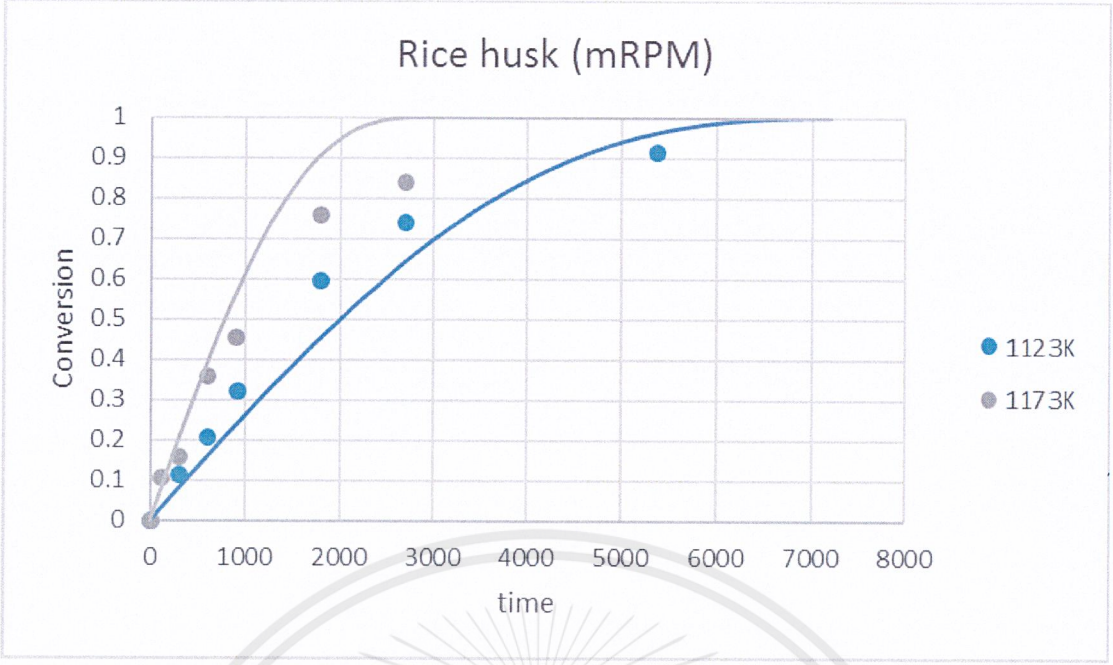


Figure 1.4.17 Model validation with experimental data from Ashish B.. (mRPM)

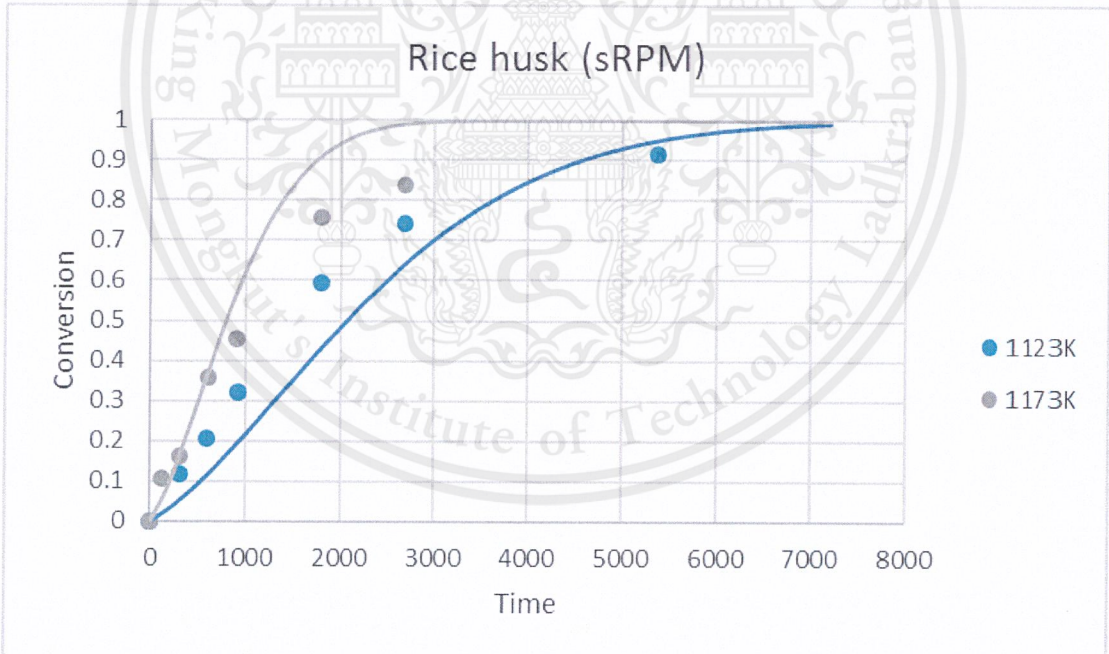


Figure 1.4.18 Model validation with experimental data from Ashish B. (sRPM).

This material is reserved for educational use only, not allowed for commercial use.
Forbidden to modify the content, and cite the document when use

Table 1.4.3 Comparison of correlation coefficient value (R^2) for each model

Char	CO_2 gasification (Verify)						
	Temp(K)	VM	GM	CM	RPM	mRPM	sRPM
Rice husk (Ashish B)	1123	0.99	0.97	0.83	0.92	0.94	0.90
	1173	0.86	0.88	0.89	0.90	0.90	0.90
Rice husk (Thilakavathi M)	1123	0.96	0.88	0.39	0.72	0.79	0.65
	1173	0.97	0.94	0.81	0.89	0.90	0.88

The experimental data from Ashish B.[4] and Thilakavathi M.[7] are used to validate kinetic model. In order to compare the validation of each model, the experimental conversion is compared with the calculated values at the different temperatures. The results are shown in Figure 1.4.7 – 1.4.18 and the error value in prediction is defined by correlation coefficient (R^2). The R-square for each model shows in Table 1.4.3. From the model validation, we found that the volumetric model (VM) is the most robust model to predict conversion time of gasification reaction of rice husk. It gives the most reasonable conversion when we use it to predict the conversion of rice husk char in compare with another model.

This material is reserved for educational use only, not allowed for commercial use.
Forbidden to modify the content, and cite the document when use

1.5 CONCLUSION

From the result, the suitable table kinetic model is indicated in modeling step. The kinetic parameters for each model are obtained by method form Figure 1.3.1. From the results, there is an effect of temperature on the mechanism of the reaction. At lower temperature, the mRPM, RPM, and GM show better result at 1123, 1148, 1173 °C, respectively. The sRPM describes the reaction better than others at the high temperature region from 1198 to 1223 °C. However, in validation step, six kinetic models are used to validate with experimental data from Ashish B and Thilakavathi M. The results show that the volumetric model is the most robust model which can describe the experimental data of Thilakavathi M. and Ashish B's experimental data better than others. Although the kinetic model will fit with the experimental data in modeling step, but it can' t conclude that it can most suitable model for other experiment prediction. Because many factors of experiment such as condition and particle size of char. So, we should use several experimental data to validate the kinetic model to achieved the suitable kinetic model for prediction. For this study, we can conclude that the volumetric model was the most suitable model for conversion time prediction for rice husk.

This material is reserved for educational use only, not allowed for commercial use.
Forbidden to modify the content, and cite the document when use

REFFERENCES

[1] Kim, M.-H.; Kim, K.-B.; Park, S.-M.; Roh, K. C. Hierarchically Structured Activated Carbon for Ultracapacitors. *Nat. Publ. Gr.* **2016**, No. February, 2–7.

[2] THE RICE TRADER. Thai rice exporters association.

[3] Gao, X.; Zhang, Y.; Li, B.; Zhao, Y.; Jiang, B. Determination of the Intrinsic Reactivities for Carbon Dioxide Gasification of Rice Husk Chars through Using Random Pore Model. *Bioresour. Technol.* **2016**, *218*, 1073–1081.

[4] Bhat, A.; Ram Bheemarasetti, J. V.; Rajeswara Rao, T. Kinetics of Rice Husk Char Gasification. *Energy Convers. Manag.* **2001**, *42* (18), 2061–2069.

[5] Cao, Q.; Xie, K. C.; Bao, W. R.; Shen, S. G. Pyrolytic Behavior of Waste Corn Cob. *Bioresour. Technol.* **2004**, *94* (1), 83–89.

[6] Alvarez, J.; Lopez, G.; Amutio, M.; Bilbao, J.; Olazar, M. Kinetic Study of Carbon Dioxide Gasi Fi Cation of Rice Husk Fast Pyrolysis Char. **2015**.

[7] Mani, T.; Mahinpey, N.; Murugan, P. Reaction Kinetics and Mass Transfer Studies of Biomass Char Gasification with CO 2. *Chem. Eng. Sci.* **2011**, *66* (1), 36–41.

[8] Fermoso, J.; Gil, M. V; Pevida, C.; Pis, J. J.; Rubiera, F. Kinetic Models Comparison for Non-Isothermal Steam Gasification of Coal – Biomass Blend Chars. *Chem. Eng. J.* **2010**, *161* (1–2), 276–284.

[9] Marsh, H.; Rodriguez-Reinoso, F. *Activated Carbon*; 2006.

[10] Wang, G.; Zhang, J.; Shao, J.; Liu, Z.; Wang, H.; Li, X.; Zhang, P.; Geng, W.; Zhang, G. Experimental and Modeling Studies on CO2 Gasification of Biomass Chars. *Energy* **2016**, *114*, 143–154.

[11] Gómez-Barea, A.; Ollero, P. An Approximate Method for Solving Gas-Solid Non-Catalytic Reactions. *Chem. Eng. Sci.* **2006**, *61* (11), 3725–3735.

[12] Zuo, H. bin; Geng, W. wei; Zhang, J. liang; Wang, G. wei. Comparison of Kinetic Models for Isothermal CO<inf>2</inf> Gasification of Coal Char-Biomass Char Blended Char. *Int. J. Miner. Metall. Mater.* **2015**, *22* (4), 363–370.

[13] Lundberg, L.; Tchoffor, P. A.; Johansson, R.; Pallarès, D. Determination of Kinetic Parameters for the Gasification of Biomass Char Using a Bubbling Fluidised Bed Reactor. 456–464.

[14] Jing, X.; Wang, Z.; Yu, Z.; Zhang, Q.; Li, C.; Fang, Y. Experimental and

This material is reserved for educational use only, not allowed for commercial use.

Forbidden to modify the content, and cite the document when use

Kinetic Investigations of CO 2 Gasi Fi Cation of Fine Chars Separated from a Pilot-Scale Fluidized-Bed Gasi Fi Er. **2013**.

[15] Guizani, C.; Louisnard, O.; Sanz, F. J. E.; Salvador, S. Gasification of Woody Biomass under High Heating Rate Conditions in Pure CO2: Experiments and Modelling. *Biomass and Bioenergy* **2015**, *83*, 169–182.

[16] Wang, Y.; Kinoshita, C. M. Kinetic Model of Biomass Gasification. *Sol. Energy* **1993**, *51* (1), 19–25.

[17] Di Blasi, C. Kinetic Modeling of Biomass Gasification and Combustion. *Therm. Net* **2010**.

[18] Xu, C.; Hu, S.; Xiang, J.; Yang, H.; Sun, L.; Su, S.; Wang, B.; Chen, Q.; He, L. Kinetic Models Comparison for Steam Gasification of Coal/biomass Blend Chars. *Bioresour. Technol.* **2014**, *171* (1), 253–259.

[19] Zhou, L.; Zhang, G.; Schurz, M.; Steffen, K.; Meyer, B. Kinetic Study on CO 2 Gasification of Brown Coal and Biomass Chars : Reaction Order. *FUEL* **2016**, *173*, 311–319.

[20] Wu, H.; An, Q.; Shen, Y.; Harada, N.; Chen, L.; Yoshikawa, K. The CO 2 Gasification Kinetic Study of WEEE Plastic Char Derived from Medium Temperature Pyrolysis. **2015**, *5* (1).

[21] Dupont, C.; Boissonnet, G.; Seiler, J. M.; Gauthier, P.; Schweich, D. Study about the Kinetic Processes of Biomass Steam Gasification. *Fuel* **2007**, *86* (1–2), 32–40.

[22] Wu, H. The CO2 Gasification Kinetic Study of WEEE Plastic Char Derived from Medium Temperature Pyrolysis. *Energy Environ. Res.* **2015**, *5* (1).

[23] Kimura, S.; Nakagaw, J.; Ton, S.; Otak, T. THE VOLUME REACTION MODEL BASED ON A SECOND ORDER RATE EQUATION AND ITS APPLICATION TO A GAS-SOLID REACTION. *Chem. Eng. JAPAN* **1981**, *14* (3), 190–195.

[24] Sohn, H. Y.; Szekely, J. A Structural Model for Gas-Solid Reactions with a Moving Boundary-IV. Langmuir-Hinshelwood Kinetics. *Chem. Eng. Sci.* **1973**, *28* (5), 1169–1177.

[25] Chornet, E.; Baldasano, J. M.; Tarki, H. T. Kinetic Expressions for Coal Char-Gas Reactions. *Fuel* **1992**, *15* (October), 1106–1107.

[26] Bhatia, S. K.; Perlmutter, D. D. A Rondom Pore Model for Fluid-Solid Reactions : 1 . Isothermal , Kinetic Control. *AIChE J.* **1980**, *26* (3), 379–386.

This material is reserved for educational use only, not allowed for commercial use.
Forbidden to modify the content, and cite the document when use

[27] Zhang, J.; Wang, G.; Shao, J.; Zuo, H. Com A Modified Random Pore Model for the Kinetics of Char Gasification. *Bioresources* **2014**, *9* (2), 3497–3507.

This material is reserved for educational use only, not allowed for commercial use.
Forbidden to modify the content, and cite the document when use

APPENDIX 1

Appendix 1-A Additional data

The experimental data that use to modeling in this project is show in Table A-1. It is the gasification of rice husk char under CO_2 condition. The result from the modeling is validate by using raw data of Ashish B. and Thilakavathi M. that show in Table 1-A-2 and 1-A-3

Table 1-A-1 Raw data of rice husk char gasification

Rice husk CO_2 gasification									
1123 K		1148 K		1173 K		1198 K		1223 K	
t (s)	X	t (s)	X	t (s)	X	t (s)	X	t (s)	X
0.00	0.00	0.00	0.00	0.00	0.00	0.00	0.00	0.00	0.00
594.00	0.16	339.00	0.12	276.00	0.18	191.00	0.15	106.00	0.13
996.00	0.26	572.00	0.22	403.00	0.27	339.00	0.29	170.00	0.23
1550.00	0.39	742.00	0.30	488.00	0.35	424.00	0.38	191.00	0.30
2120.00	0.52	933.00	0.37	594.00	0.42	530.00	0.49	254.00	0.41
2610.00	0.62	1170.00	0.46	721.00	0.49	678.00	0.61	360.00	0.56
2970.00	0.69	1480.00	0.58	848.00	0.58	848.00	0.73	445.00	0.68
3370.00	0.76	1720.00	0.66	1060.00	0.69	1020.00	0.83	530.00	0.78
3770.00	0.81	1950.00	0.72	1250.00	0.77			615.00	0.85
4180.00	0.86	2230.00	0.79	1530.00	0.86			700.00	0.91
		2480.00	0.86						
		2690.00	0.90						

This material is reserved for educational use only, not allowed for commercial use.
Forbidden to modify the content, and cite the document when use

Table 1-A-1 Raw data of rice husk char gasification of Thilakavathi M. [7] for each temperature

Rice husk CO_2 gasification			
1123K		1173K	
t (s)	x	t (s)	x
0.00	0.00	0.00	0.00
55.44	0.10	67.76	0.20
234.09	0.18	252.57	0.34
406.57	0.23	418.89	0.45
597.54	0.28	597.54	0.54
770.02	0.33	782.34	0.62
954.83	0.37	960.99	0.70
1133.47	0.42	1145.79	0.75
1318.28	0.46	1324.44	0.79
1496.92	0.49	1503.08	0.83
1681.72	0.53	1687.89	0.86
1860.37	0.56	1860.37	0.88
2039.01	0.59	2045.17	0.90
2223.82	0.62	2229.98	0.91
2402.46	0.65	2408.62	0.91
2587.27	0.67	2593.43	0.92

Table 1-A-2 Raw data of rice husk char gasification of Ashish B. [4] for each temperature

Rice husk char gasification			
1123K		1173K	
t (s)	X	t (s)	X
0.00	0.00	0.00	0.00
188.76	0.08	126.00	0.13
350.56	0.18	243.00	0.27
539.33	0.27	360.00	0.40
728.09	0.36	486.00	0.54
889.89	0.44	603.00	0.65
1078.65	0.52	720.00	0.75
1240.45	0.59	846.00	0.83
1429.21	0.65		
1617.98	0.70		
1806.74	0.76		
1968.54	0.80		
2157.30	0.85		
2346.07	0.89		

This material is reserved for educational use only, not allowed for commercial use.
Forbidden to modify the content, and cite the document when use

Appendix 1-B Example of calculation
Calculation of *k* value

The experimental data from Xiaoyan Gao et al. [3] is used to find the kinetic parameter for each model. The experimental data are fitted by various models. By plotting $-ln(1-X)$, $3[1-(1-X)^{1/3}]$, $2arctanh(X^{1/2})$ and $(2/\psi)(1-\psi ln(1-X))^{1/2}$ as the Function of t shown in Figure 1-B-1 to 1-B-3, the slopes of curves at different reaction temperatures could be obtained to represent the reaction rate constants (k_{VM}, k_{GM}, k_{RPM}, k_{CM}) of the gasification process. For RPM model, the values of ψ is estimate by guess value to obtain the optimum fitting of graph as shown in Figure 1-B-4.

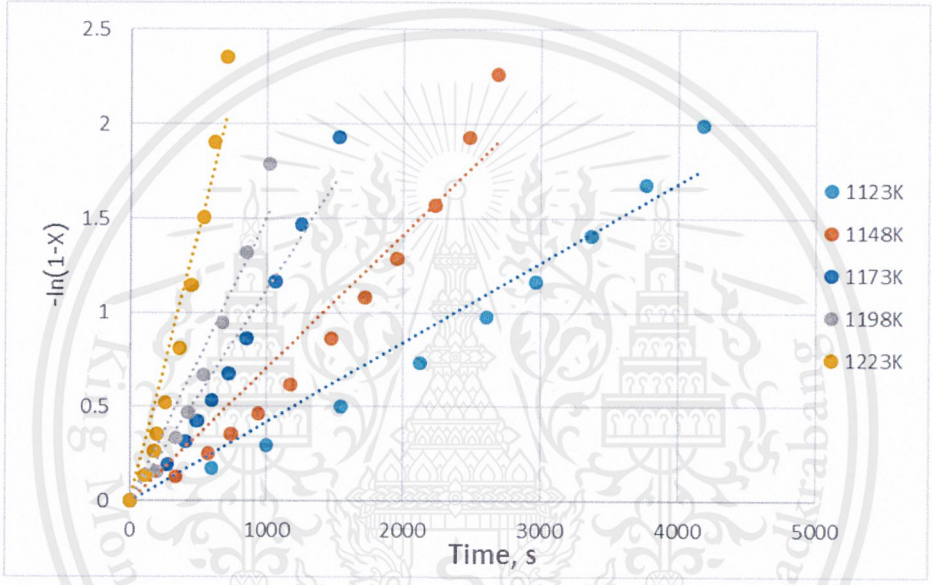


Figure 1-B-1 VM linearized models for different temperature

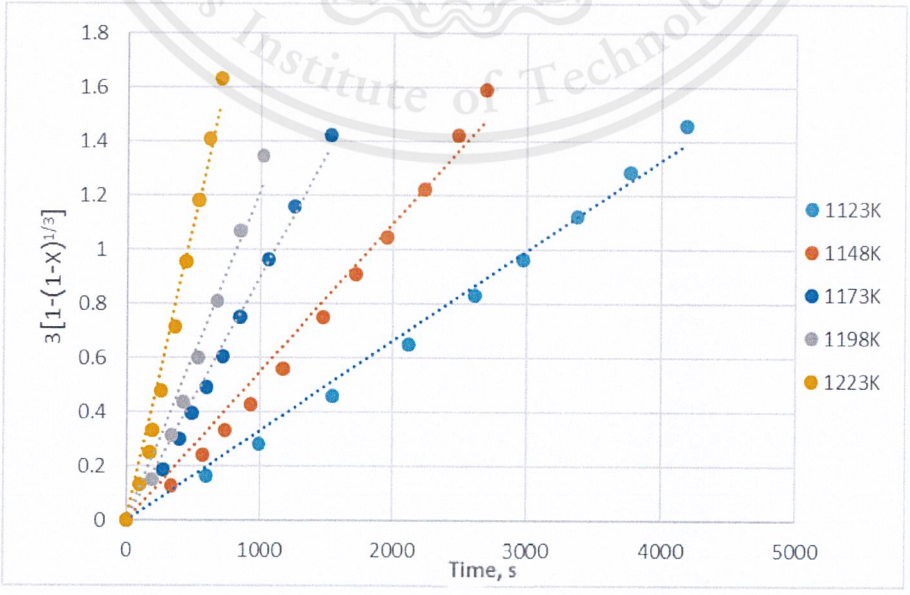


Figure 1-B-2 GM linearized models for different temperature

This material is reserved for educational use only, not allowed for commercial use.
Forbidden to modify the content, and cite the document when use

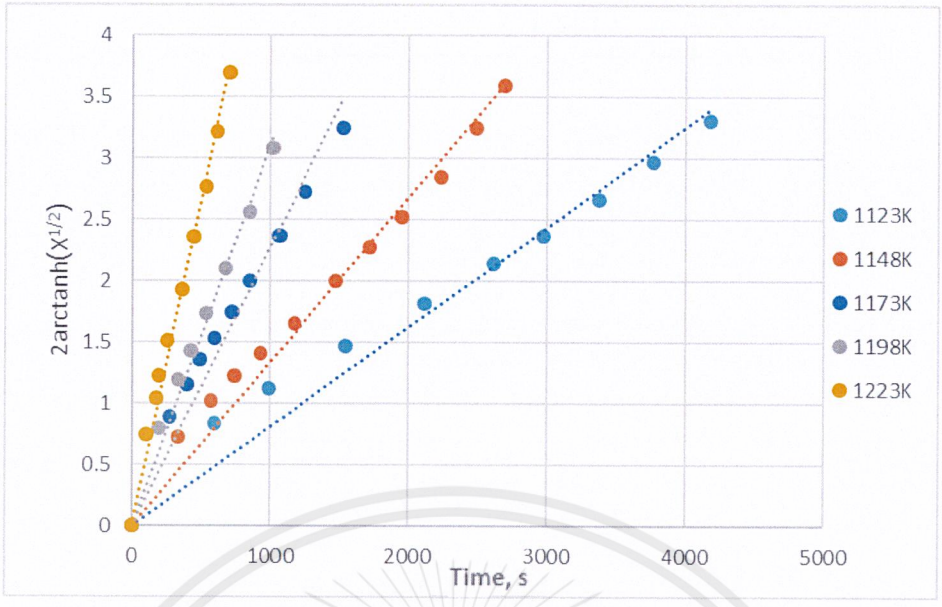


Figure 1-B-3 CM linearized models for different temperature

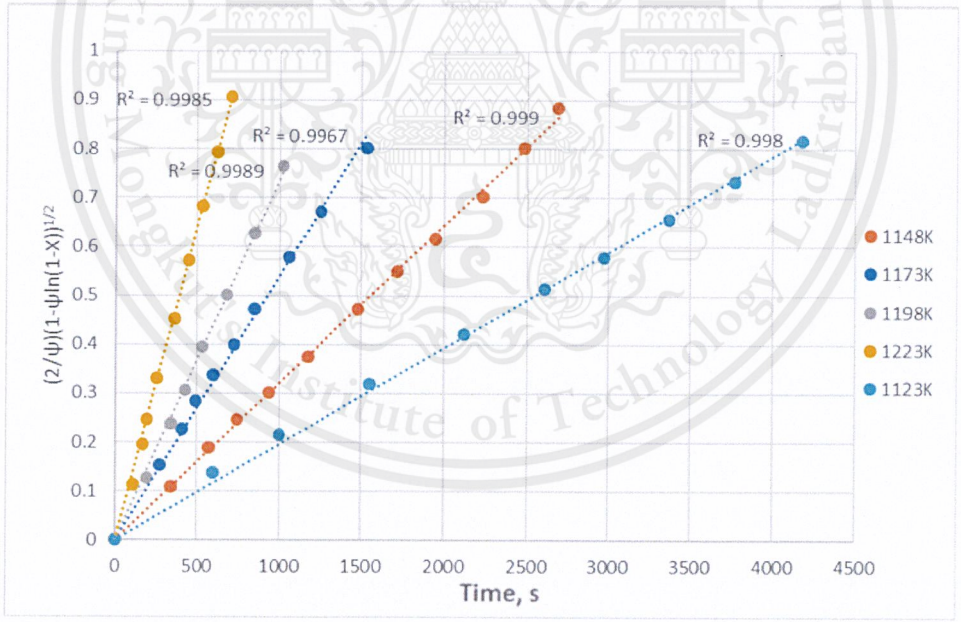


Figure 1-B-4 RPM linearized models for different temperature

This material is reserved for educational use only, not allowed for commercial use.
Forbidden to modify the content, and cite the document when use

The experimental data from Xiaoyan Gao et al. is fitted with mRPM and sRPM to find the kinetic parameter for mRPM and sRPM model. Polymath software is used to fit curve of experiment data and model, this program uses the Levenberg-Marquardt (LM) algorithm as the default for finding the rate constant values (k_{mRPM} and k_{sRPM}) and the result for curve fitting of mRPM and sRPM show in Figure 1-B-5 and 1-B-6. The LM technique is an iterative solution method that usually converges very rapidly. The objective of this function that is minimize the square of error value. The k value for each model are show in Table 1-B-1. The example of Curve fitting by Polymath are show in Table 1-B-2

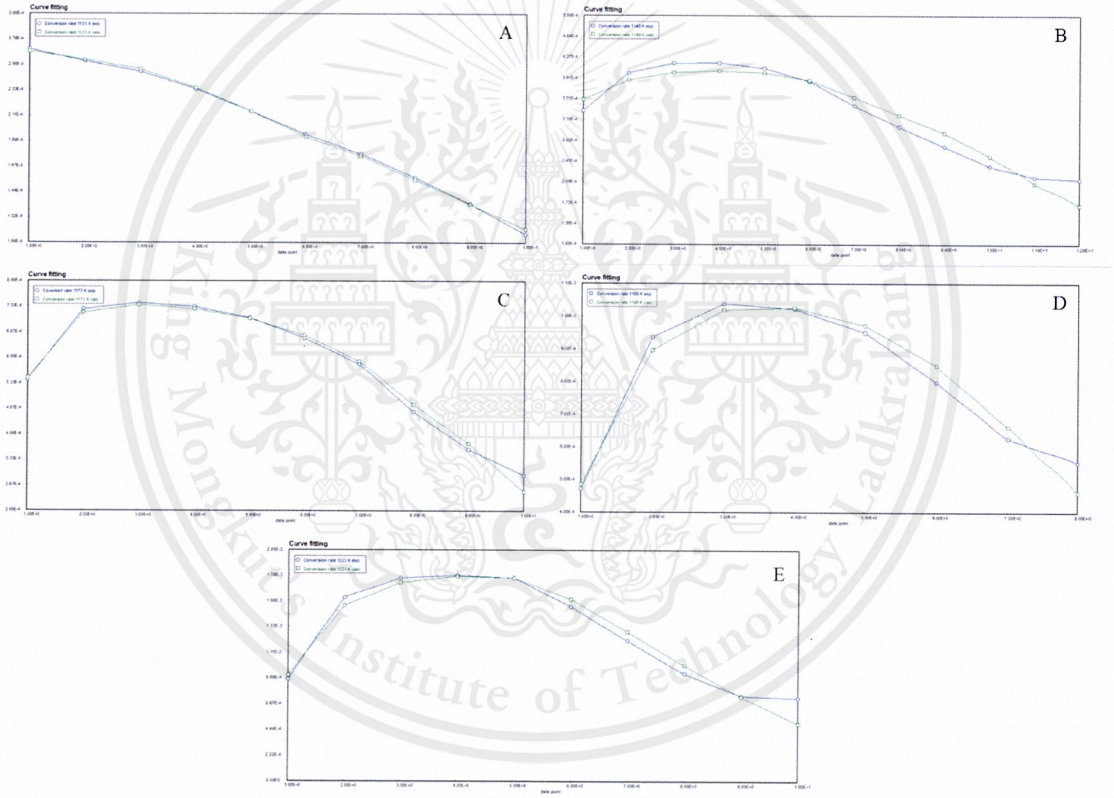


Figure 1-B-5 Curve fiiting for mRPM A:1123K, B:1148K, C:1173K, D:1198K and E:1223K

This material is reserved for educational use only, not allowed for commercial use.
Forbidden to modify the content, and cite the document when use

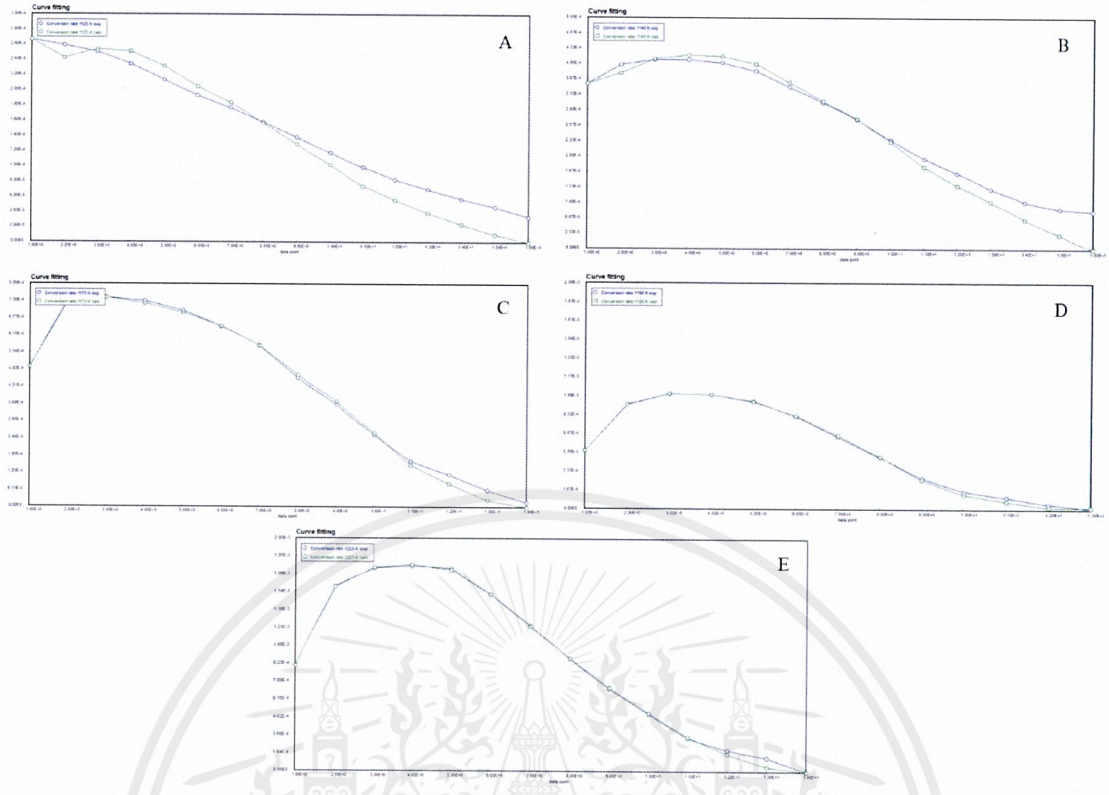


Figure 1-B- 6 Curve fiiting for sRPM A:1123K, B:1148K, C:1173K, D:1198K and E:1223K

Table 1-B-1 *k* value for each model

Temp (K)	k_{VM} (s^{-1})	k_{GM} (s^{-1})	k_{CM} (s^{-1})	k_{RPM} (s^{-1})	k_{mRPM} (s^{-1})	k_{sRPM} (s^{-1})
1123	0.0004211	0.0003327	0.0008129	0.0002038	0.0002673	0.0002665
1148	0.0007085	0.0005479	0.0013367	0.0003343	0.0004322	0.0003565
1173	0.0011209	0.0000009	0.0022709	0.0005611	0.0007347	0.0000502
1198	0.0015134	0.0012258	0.0031155	0.0007674	0.0009736	0.0005151
1223	0.0028928	0.0022004	0.0053423	0.0013356	0.0016889	0.0009044

This material is reserved for educational use only, not allowed for commercial use.
Forbidden to modify the content, and cite the document when use

Table 1-B-2 Example of curve fitting for mRPM model at 1123 by using Polymath software

POLYMATH Report No Title
Nonlinear Regression (L-M) 19-พ.ค.-2560

Model: DX1123 = K*((1-X1123)^N)*(1-W*ln(1-X1123))^(1/2)

Variable	Initial guess	Value	95% confidence
K	0.1	0.0002673	2.4E-07
N	1.	0.760576	0.0011242
W	1.	1.324338	0.0056359

Nonlinear regression settings
Max # iterations = 64

Precision

R^2	0.9984142
R^2adj	0.9979611
Rmsd	6.589E-07
Variance	6.202E-12

General

Sample size	10
Model vars	3
Indep vars	1
Iterations	8

Source data points and calculated data points

	X1123	DX1123	DX1123 calc	Delta DX1123
1	0	.0002692	0.0002673	1.885E-06
2	.158	.0002587	0.0002599	-1.18E-06
3	.258	.0002496	0.0002516	-2.036E-06
4	.394	.0002342	0.0002355	-1.341E-06
5	.52	.0002147	0.0002148	-1.024E-07
6	.624	.0001946	0.0001925	2.135E-06
7	.688	.0001778	0.0001758	2.039E-06
8	.756	.000157	0.0001548	2.16E-06
9	.814	.0001339	0.0001336	2.808E-07
10	.864	.0001075	0.0001119	-4.365E-06

Where W, N and K are ψ, n and k_{mRPM} parameters in mRPM model, respectively.

This material is reserved for educational use only, not allowed for commercial use.
Forbidden to modify the content, and cite the document when use

Kinetic parameter estimation (k_0 and E)

To obtain the pre-exponential factor (k_O) and activation energy (E) , the Arrhenius equation in equation (B-1) to obtain equation (B-2) to plot linearize. The rate constant (k) for each kinetic model are plot as the function of 1/T (Arrhenius Plot) show in Figure 1-B-7. The pre-exponential factor and activation energy can deter mind from intercept point on x-axis and slop of graph, respectively.

$$k = k_0 e^{-E/RT} \tag{B-1}$$

Take ln equation (B-1)

$$\ln k = \ln k_O - E/RT \tag{B-2}$$

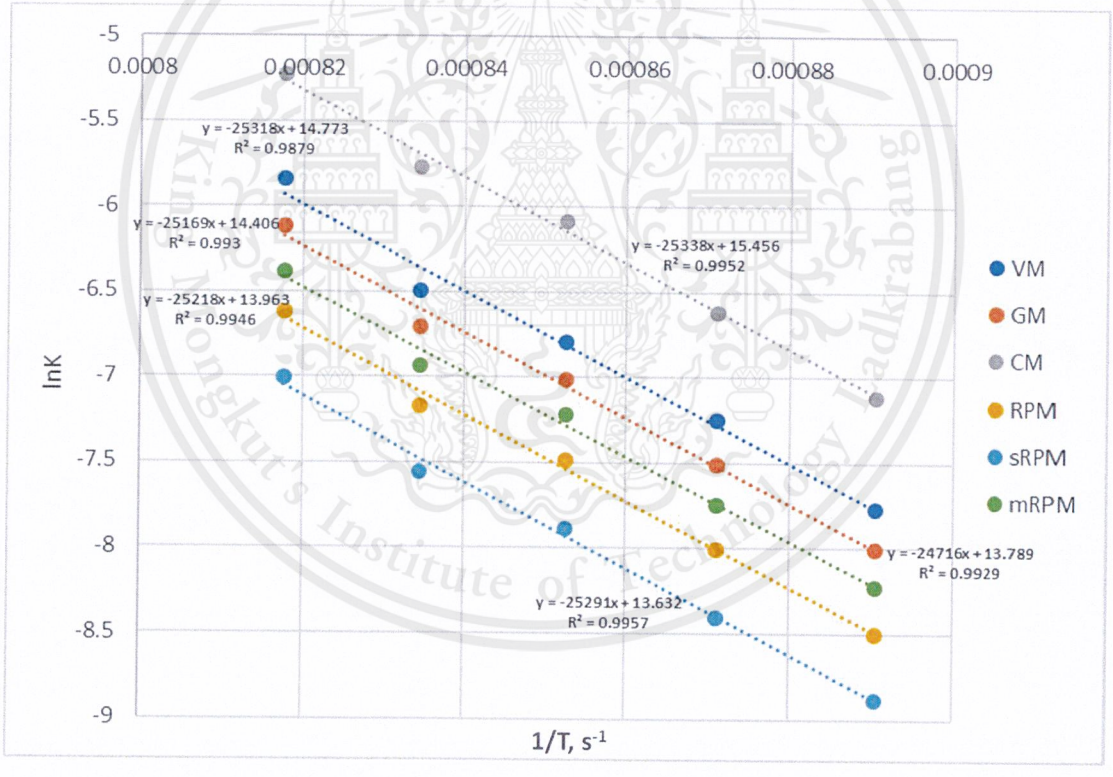


Figure 1-B- 7 Arrhenius Plot for each models

This material is reserved for educational use only, not allowed for commercial use.
Forbidden to modify the content, and cite the document when use

Table 1-B-3 Example of calculation of kinetic paramer for RPM model by using Polymath software

POLYMATH Report No Title
Linear Regression 19-พ.ค.-2560

Model: $lnk_{rpm} = a0 + a1*T1$

Variable	Value	95% confidence
a0	13.96322	2.914926
a1	-2.522E+04	3414.508

General
Regression including a free parameter
Number of observations = 5

Statistics

R^2	0.9945976
R^2adj	0.9927968
Rmsd	0.0214011
Variance	0.0038167

Source data points and calculated data points

	T1	lnKrpm	lnKrpm calc	Delta lnKrpm
1	.0008905	-8.498371	-8.493792	-0.0045791
2	.0008711	-8.003472	-8.004554	0.0010823
3	.0008525	-7.485611	-7.535491	0.0498805
4	.0008347	-7.172502	-7.086603	-0.0858987
5	.0008177	-6.618375	-6.65789	0.039515

Model $lnk = a0 + a1*T1$ is compare with equation $\ln k = \ln k_O - E/RT$. From the equation, the kinetic parameter can be determined from relationship.

$$Lnk_0 = a0 \text{ and } E/R = -a1$$

So,

$$k_0 = 1.16\times10^6\ s^{-1} \text{ and } E = 2.09\times10^6\ J/mol$$

This material is reserved for educational use only, not allowed for commercial use.
Forbidden to modify the content, and cite the document when use

Appendix 1-C Simulation program
Simulation program for each model

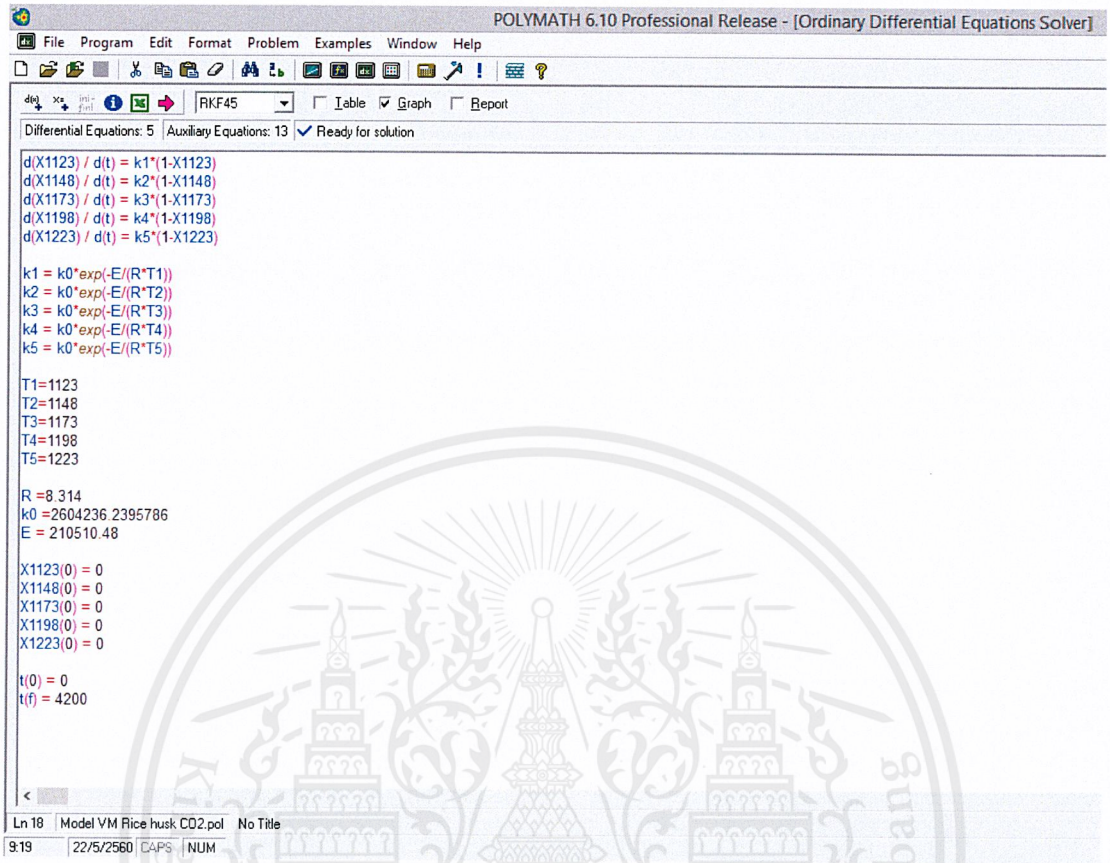


Figure 1-C- 1 Simulation code of VM model

This material is reserved for educational use only, not allowed for commercial use.
Forbidden to modify the content, and cite the document when use

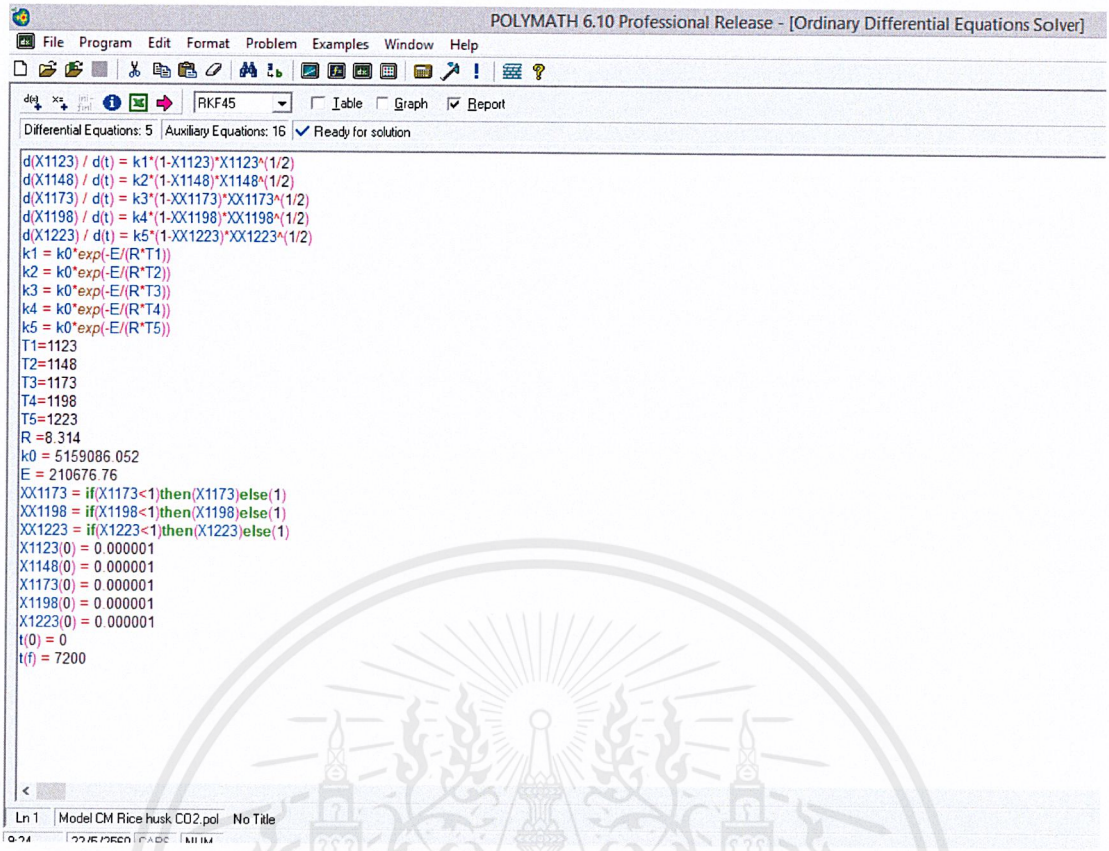


Figure 1-C- 2 Simulation code of CM model

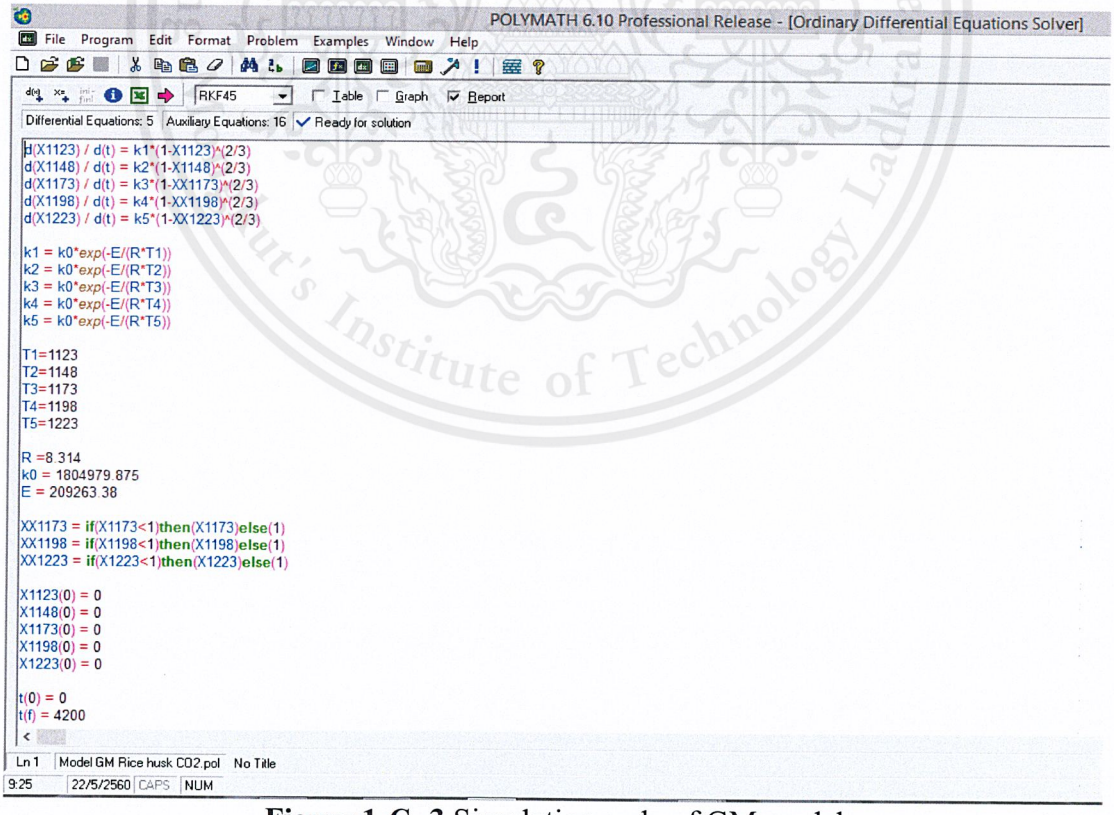


Figure 1-C- 3 Simulation code of GM model

This material is reserved for educational use only, not allowed for commercial use.
Forbidden to modify the content, and cite the document when use

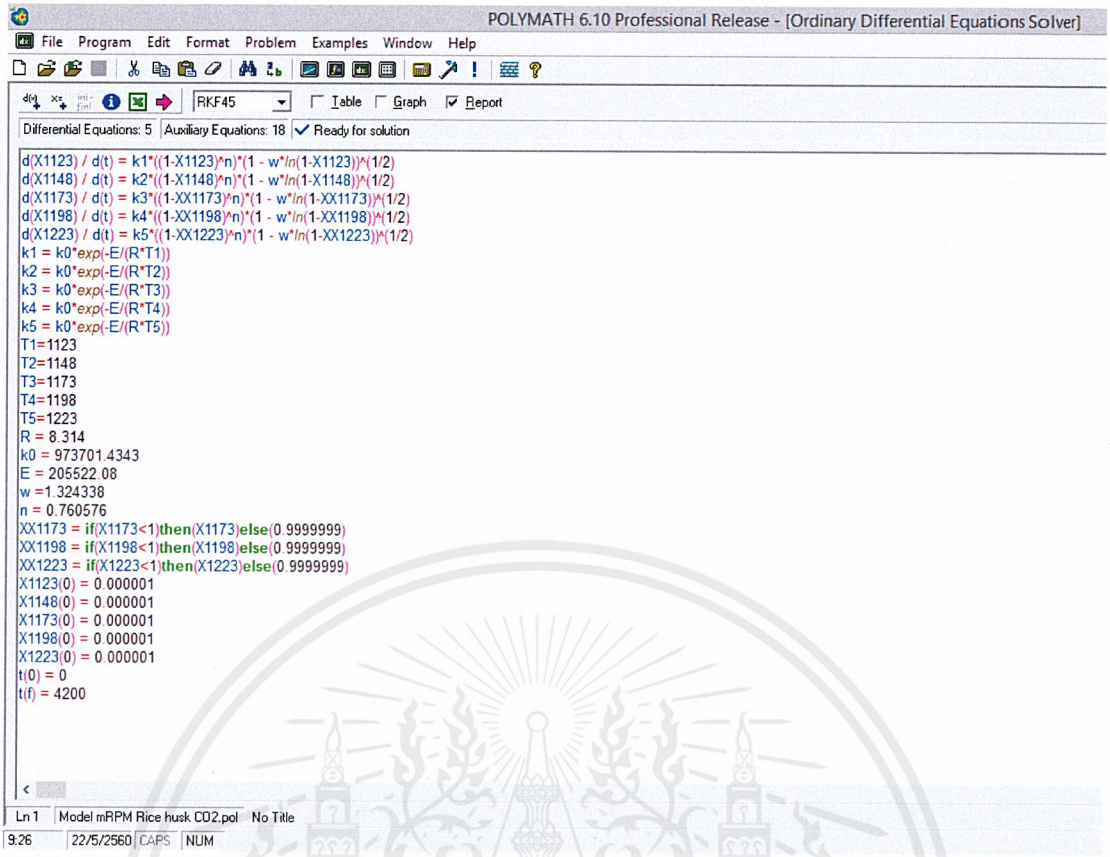


Figure 1-C- 4 Simulation code of mRPM model

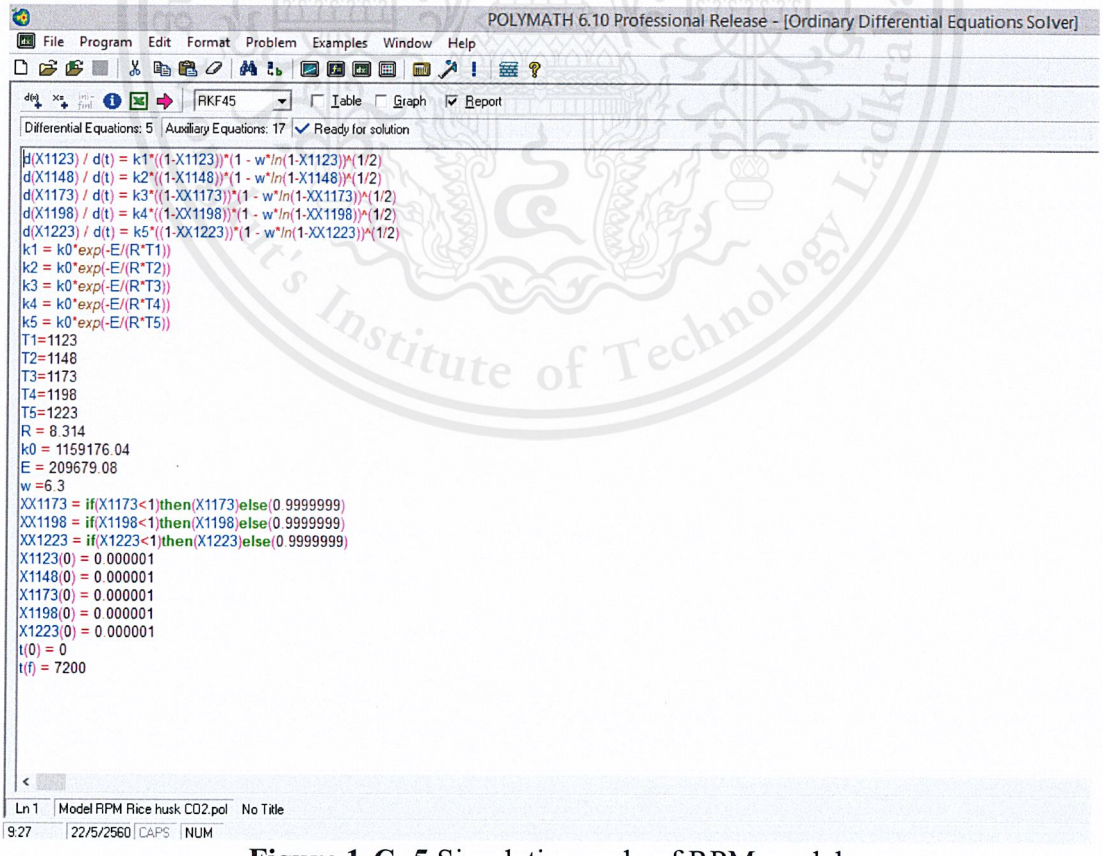


Figure 1-C- 5 Simulation code of RPM model

This material is reserved for educational use only, not allowed for commercial use.
Forbidden to modify the content, and cite the document when use

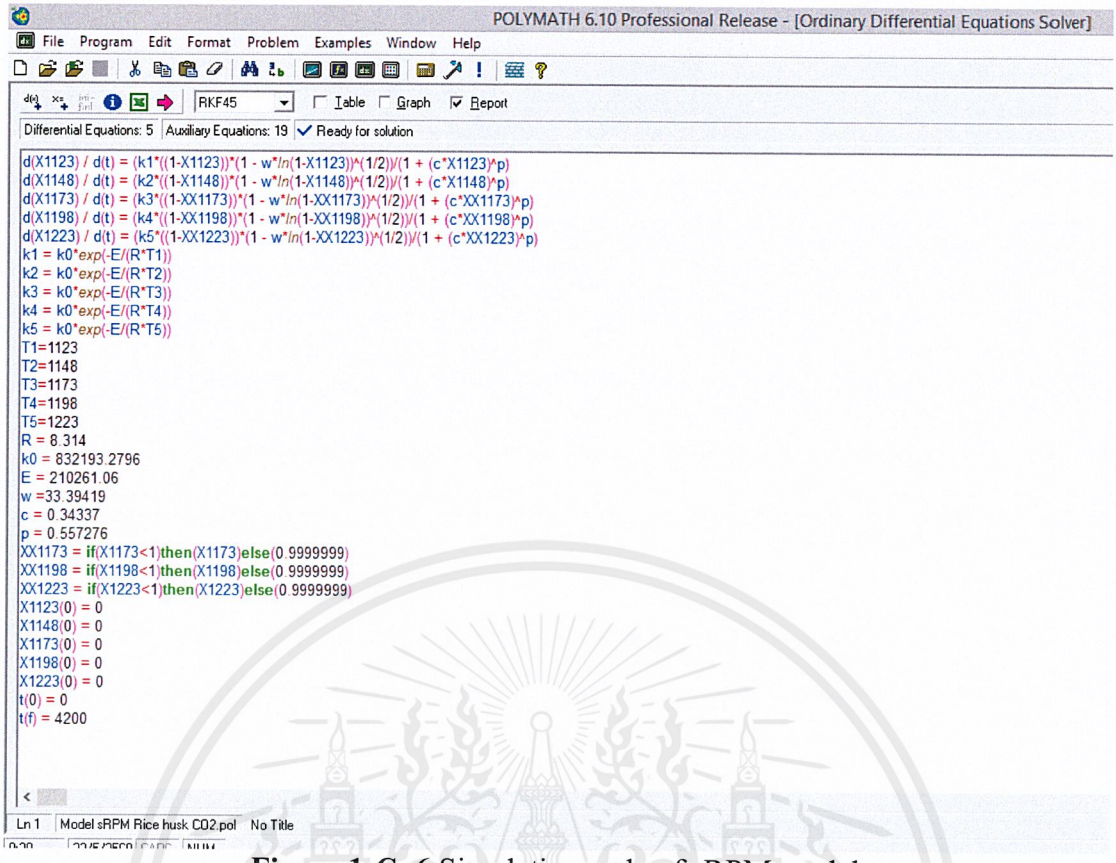


Figure 1-C- 6 Simulation code of sRPM model

This material is reserved for educational use only, not allowed for commercial use.
Forbidden to modify the content, and cite the document when use

CHARPTER 2
KINETIC MODELING OF ETHANOL FERMENTATION IN A TWO-TANK SYSTEM WITH CELL RECYCLING BY USING SUCROSE AS SUBSTRATE

2.1 INTRODUCTION

2.1.1 Background

The ethanol fermentation processes such as batch, fed-batch and continuous fermentation are proposed for production of ethanol [1],[2]. For batch fermentation, it is a commonly process that use in ethanol production. But there is a disadvantage of batch reactor, due to effect of substrate and product concentrations to ethanol production which reduce the ethanol productivity [3]. On the other hand, there is an advantage of the continuous fermentation over batch process which shown in many research [4], because of the reduction of inhibitory effect of substrate and product concentrations which improved the productivity of this process.The cause of continuous fermentation process can reduce and improve inhibition effect of system, due to the continuous will carrier out of product concentration (ethanol) from the fermenter tank. As a result, the less concentration of product (ethanol) in tank. The cell-recycling that use in ethanol fermentation process is a more convenient way to maintain a high cell concentration and increase the ethanol-producing microorganism in fermenters.

To improve the ethanol fermentation process, it very necessary to study the reaction of ethanol production in the system. The mathematic modeling is one of procedure that improve the process. The mathematics that accuracy in phenomenal and physical prediction is essential for science and engineering field. Because of they provide the basic of design, control and optimization of the system [5]–[7]. The objective of mathematic model is to obtain an expression of quantitively describe the behavior of the system under consideration. The preciseness of model depends on the several factors that compose in model, which include complexity and information available concerning the process. For this work, the mathematic models are used describe the fermentation reaction of sucrose. With the introduction of mathematical modelling to the cell growth kinetics, the behavior of the fermentation system under all possible conditions are investigated and the effects of changes of concentration or rate are also predicted. Several scientists attempt to apply the mathematical and modelling techniques for describing batch as well as continuous processes of ethanol

This material is reserved for educational use only, not allowed for commercial use.
Forbidden to modify the content, and cite the document when use

fermentation [7]. In most cases the use and the ability of their models are restricted by several restrictions including the behavior of the system and number of experimental data that use in modeling. So, it very necessary to choose the mathematic model to describe the fermentation system. The most mathematic model that use for describing of the reaction of ethanol fermentation is Monod model, it is the mathematic model for the growth of microorganism. The Monod model consider the major factor that effect to system including the growth rate of cell and the inhibition effect of substrate and product. Due to its assumption involve the system of ethanol fermentation, it is used as the model for describe the reaction of bio-chemistry reaction. For example, Wen-Hung Huang [8] use Monod model to describe the ethanol production from mix-sugar as a substrate. Kompala, D. S use Monod model to describe microbial growth by using multi-substrate [9]. In some case, the mathematic models are improved and modified to describe the fermentation system due to the restriction of the system. Ariyajaroenwong, P modified Monod model to predict continuous ethanol fermentation from sweet sorghum juice.

In this study, three kinetic models are used to predict the experimental data of Feng-Sheng Wang [2] to find the suitable kinetic model for ethanol fermentation. Three model including Monod model, modified Monod model and Extended-modified Monod model. Monod model is the basic model for development of Modified Monod model and Extended-modified Monod model by add some of parameter in the equation to more extensive of equation and accuracy prediction of model. As a result, a developed equation emerged. The prediction values are compared with the experimental data, which the accuracy prediction is indicated by correlation coefficient (R^2).

2.1.2 Objective(s)

1.) To study the mechanism of ethanol production form fermentation process
2.) To determine the suitable kinetic model that describe the production of ethanol form fermentation process

2.1.3 Scope(s) of Work

1.) Kinetics model that used for this study including Monod model, Modified Monod model and Extended-modified Monod model
2.) The production of ethanol for this study use sucrose as the substrate

This material is reserved for educational use only, not allowed for commercial use.
Forbidden to modify the content, and cite the document when use

3.) The system of fermentation process is operated at certain condition

2.1.4 Expected Outputs

1.) The suitable kinetic model that can used to predict reaction of ethanol production.

This material is reserved for educational use only, not allowed for commercial use.
Forbidden to modify the content, and cite the document when use

2.2 LITERATURE REVIEW AND THEORY

2.2.1 Literature review

Bioethanol technology represents an important economic in this age of dynamic development. Bioethanol can be produced from any raw material which has sugar in it, and which the producing microorganism (bacteria, yeasts) can metabolize or which has polysaccharides (starch or cellulose) that can be broken down to monosaccharides, and then metabolized to bioethanol. Although ethanol production processes by different techniques and from different resources. The ethanol production from sucrose is investigated in many literature [9]–[11]. Because of it is very common of substrate that easy to supply.

For the ethanol production, the types of reactor are effect to the efficiency and quantity of production of ethanol. Batch fermentation is one of reactor that use in process, it easy to control the condition of the system but not high conversion of ethanol [12]. The continuous reactor is investigated for ethanol production. For many research, they report that continues ethanol production can give a high conversion of ethanol [1] ,[13] . So, the continuous ethanol fermentation is interested in ethanol production process. With increasing interest in the industrial application of continuous alcoholic fermentation. So, they are efforts to develop the process of ethanol production. Kinetic modelling is regarded as an important step in developing a fermentation process. Various kinetic models have been examined for microbial growth, product formation and substrate consumption. Models help in process control, reducing process costs and increasing product quality[14] . Once the models are defined, Recently, the global model that use to describe the ethanol production from fermentation process is Monod model [9] . enable us to understand, design and control the fermentation process.

2.2.2 Theory

1. Ethanol fermentation

For this study, Feng-Sheng Wang [1] 's experimental data are used as data for ethanol fermentation modeling. There are the two-tank fermentation that consists of two 5 L jet fermenters as show in Figure 2.2.1. For each fermenter consist of gas filter, temperature controller and a settler for recycling yeast. When stabilized sucrose is fed to the fermenter tank as the substrate for ethanol production. The solution will

This material is reserved for educational use only, not allowed for commercial use.
Forbidden to modify the content, and cite the document when use

be draw from the fermenter to settler to separate yeast from solution. The yeast cell will be agglomerated quickly after leaving the fermenter and settle to bottom of settle before recycling to fermenter. The solution will be supplied to the second fermenter. After that, the same procedure is employed for the second fermenter

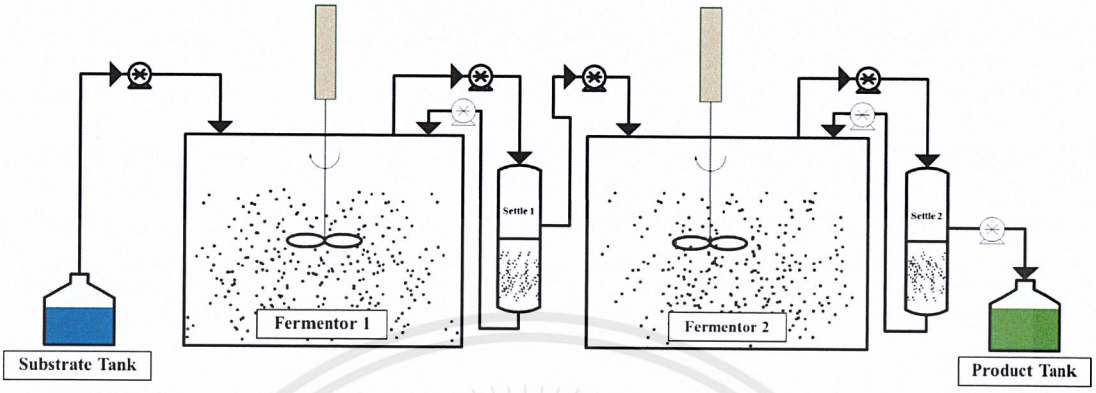


Figure 2.2.1 Illustration of a two-tank continuous fermentation system with cell recycles.

2. Monod model

The concepts in microbial growth kinetics have been dominated by the relatively simple semi-empirical model proposed by Monod [15]. The Monod model differs from the other models in the way that it introduces the concept of a growth controlling substrate show in Figure 2.2.2. This substrate is called limiting substrate to indicate that the microbial growth rate is dictated by the actual concentration of a metabolite. In the 1930s and 1940s, Jacques Monod performed experiments on bacteria feeding on a single limiting nutrient in order to see if the logistic equation accurately described bacterial growth. He found that it did not and therefore he developed a new model to describe his results.

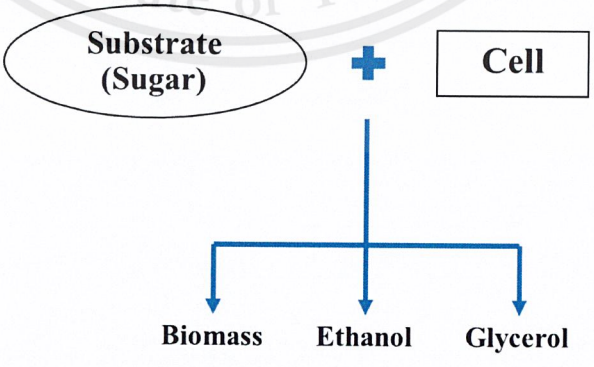


Figure 2.2.2 A simplified scheme of this approach for the ethanol fermentation process by yeasts and bacteria.

This material is reserved for educational use only, not allowed for commercial use.
Forbidden to modify the content, and cite the document when use

After that, Monod model is wildly used in describe the fermentation process of by using bacteria and yeast. The simple scheme of fermentation reaction can represent by Figure 2.2.3.

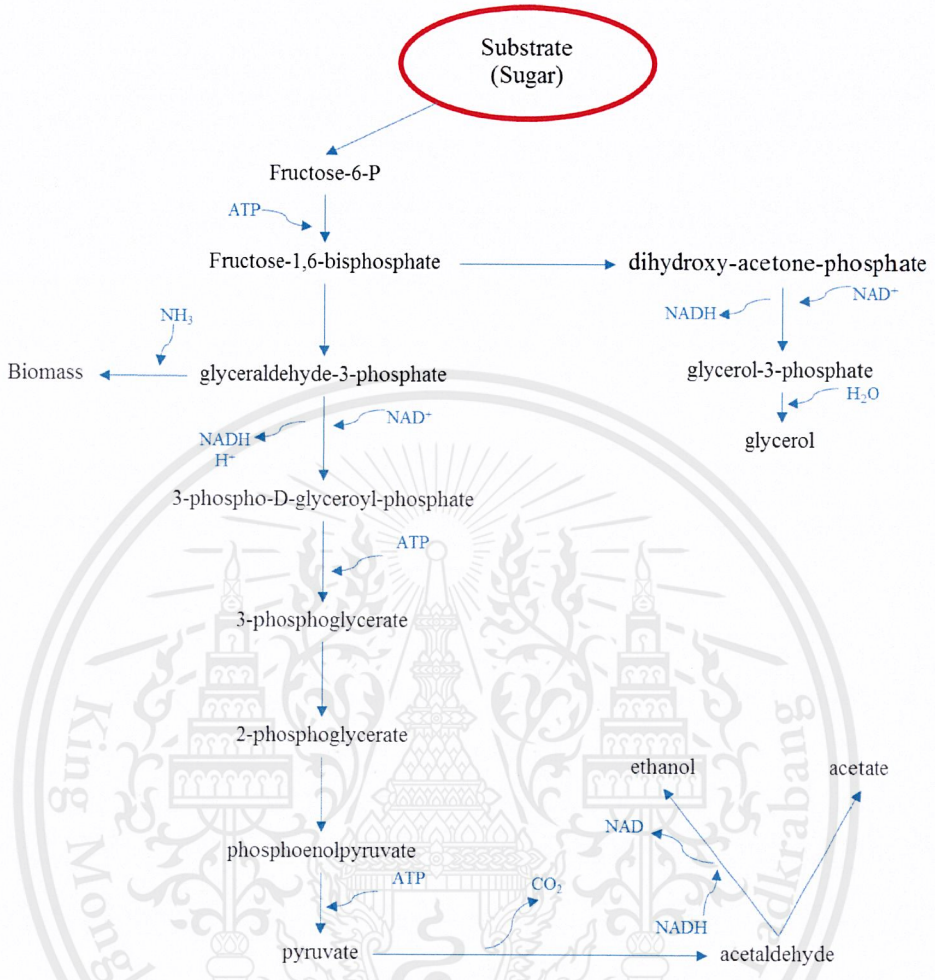


Figure 2.2.3 Schematic representation of sugar metabolism in Saccharomyces yeast

For this model, it is assumed that kind of sugar in media in fermentor as total sugar. The when the reaction proceed, the inhibition of sugar utilized depend on the concentration of total sugar and the priority for in utilization of sugar by cell are negligible. The advantage for this assumption is in simple the find the kinetic parameter and can used as the rough method to find the kinetic for process. However, it not accuracy to predict and describe the reaction in system.

From assumption and Monod equation for ethanol fermentation, the kinetics of growth and ethanol production are generally the following:

$$\mu = \frac{\mu_{max} S}{K_S + S} \qquad (1)$$

This material is reserved for educational use only, not allowed for commercial use.
Forbidden to modify the content, and cite the document when use

A comment on the biological meaning of the parameters K_S and μ_{max}, which are used to characterize microbial growth for given growth conditions, is necessary. The maximum specific growth rate μ_{max} related to their ability to reproduce themselves in nutritional conditions. It is defined as the increase of biomass per unit time under feeding conditions, in which there are not limiting nutrients. Monod constant for growth (K_S) is the substrate concentration which organisms are substrate limited to a growth rate of half the prevailing maximum value. This constant is closely related to the mechanism of transport of the substrate over the cell membrane, so it depends on cell membrane properties and intracellular conditions, on the type of transporter proteins in the cell and on the substrate properties. For this reason, the value of K_S can be defined as a reflection of the affinity of the cell towards the substrate *S*.

The link between growth and substrate utilization was made by Monod, who linearly related the specific rate of biomass growth and the specific rate of substrate consumption through the yield coefficient (Y_{XS}) , a measure for the conversion efficiency of a growth substrate into cell material. The relation between cell growth and substrate consumption is given by

$$Y_{XS} = \frac{dX}{dS} \tag{2}$$

And the relation between cell growth and another substrates consumption and product formation are given by

Ethanol

$$Y_{PS} = \frac{dP}{dS} \tag{3}$$

To describe the dynamics of fermentation, the rate of reaction for each substrates and components are show as follows.

Biomass

$$\frac{dX}{dt} = \mu_{max} \frac{S}{K_S + S} X \tag{4}$$

Sucrose

$$\frac{dS_T}{dt} = -\frac{\mu_{max}}{Y_{XS}} \frac{S}{K_S + S} X \tag{5}$$

Ethanol

$$\frac{dP}{dt} = \frac{\mu_{max}}{Y_{XS}} \frac{S}{K_S + S} X \frac{1}{Y_{SP}} \tag{6}$$

This material is reserved for educational use only, not allowed for commercial use.
Forbidden to modify the content, and cite the document when use

3. Modified Monod model

For this study, the metabolism of fermentation process is approached in Figure 2.2.4. It defers from Monod model in initial of reaction. This model we assume that kind of sugars are effect to ethanol and biomass formation in the process. Sucrose is a disaccharide compound of glucose and fructose joined by an α (1,2) glycosidic linkage. The flocculent yeast *Saccharomyces diastaticus* LORRE-316 can use sucrose as a carbon source. Sucrose can be transported into the cell and hydrolyzed as shown in Figure 2.2.4. After sucrose is hydrolyzed by the flocculent yeast, it will be converted to glucose and fructose. Glucose and fructose is the one more substrate that used to produce ethanol, both will be converted to fructose-6-P before they convert to pyruvate and produced the product. Biomass and glycerol are by-product for this process, they are produced from glyceraldehyde-3-phosphate and glycerol-3-phosphate. Pyruvate is semi-finally converted to ethanol and carbon dioxide.



Figure 2.2.4 Schematic representation of pathway of sucrose hydrolyed to glucose and fructose by Saccharomyces yeast

From assumption above, the specific growth rate of cell can be expressed by equation (1) . And the relation between cell growth and another substrates consumption and product formation are given by

Glucose $$Y_{XG} = \frac{dX}{dG} \quad (7)$$

Fructose $$Y_{XF} = \frac{dX}{dF} \quad (8)$$

Ethanol $$Y_{PS} = \frac{dP}{dS} \quad (9)$$

This material is reserved for educational use only, not allowed for commercial use.
Forbidden to modify the content, and cite the document when use

Ethanol $$Y_{PG} = \frac{dP}{dG} \quad (10)$$

Ethanol $$Y_{PF} = \frac{dP}{dF} \quad (11)$$

To describe the dynamics of fermentation, the rate of reaction for each substrates and components are show as follows. (Biomass is show in equation (4))

Sucrose $$\frac{dS_T}{dt} = -\frac{\mu_{max}}{Y_{XS}} \frac{S}{K_S + S} X\left(1 - \frac{S_T}{S_{T0}}\right) \quad (12)$$

Glucose $$\frac{dG}{dt} = \frac{\mu_{max}}{Y_{XG}} \frac{S}{K_S + S} X \quad (13)$$

Fructose $$\frac{dF}{dt} = \frac{\mu_{max}}{Y_{XF}} \frac{S}{K_S + S} X \quad (14)$$

Ethanol $$\frac{dP}{dt} = -\frac{1}{Y_{PS}} \frac{dS}{dt} - \frac{1}{Y_{PG}} \frac{dG}{dt} - \frac{1}{Y_{PF}} \frac{dF}{dt} \quad (15)$$

4. Extended-modified Monod model

Starting from the Monod model, different growth rate expressions have been proposed in the literature to model more complex reaction. In this section, we analyze the most common Monod model. The general mathematic model that describe the cell kinetic is Monod equation [6] that show in equation (1). It is used to describe the relationship between growth rate and substrate concentration. However, this model does not describe for inhibition that cause by high substrate and product concentrations in ethanol fermentation. During the ethanol fermentation, we found that inhibitor for cell growth including high concentration of sugar (sucrose, glucose and fructose) and ethanol, they affect to cell growth rate. From Figure 2.2.5, we assume that reaction of glucose, fructose and sucrose are inhibition reaction and the reaction part way can abbreviate to mechanism on right hand. From the experimental data of Feng-Sheng Wang [1], we found that priority in utilization of glucose more than fructose and sucrose, respectively. It also reports that ethanol concentration is a significant effect on the cell growth. So, specific growth rate in equation (1) is extended by adding term of substrate inhibition constant for ethanol formation (K_P) and ethanol concentration (P). So, the model is modified to describe for this assumption which include term for substrates (sucrose, glucose and fructose) and product (ethanol). The specific of cell growth is model shows in equation (16).

This material is reserved for educational use only, not allowed for commercial use.
Forbidden to modify the content, and cite the document when use

$$\mu = \frac{\mu_{max} S_T K_S}{1 + K_{IS} S_T + K_{IP} P} \tag{16}$$

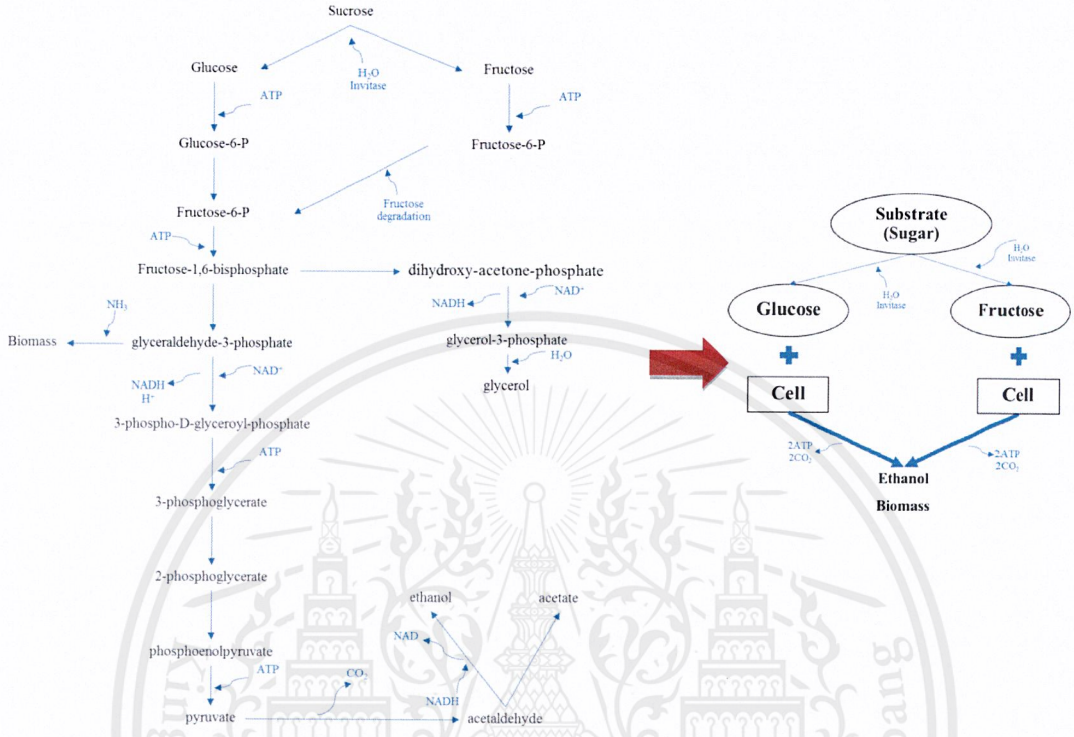


Figure 2.2.5 Schematic represent pathway of sucrose fermentation to ethanol by Saccharomyces yeast

Sucrose is the main substrate for this process. During process, the concentration of glucose and fructose are competitive inhibitory manner for decomposition rate of sucrose. So, when the concentration of high, the rate of sucrose decomposed can be expressed by equation (16). On the other hand, sucrose can be rapid decomposed by cell in low concentration of glucose and fructose environment. So, when low fructose and glucose concentration, the decomposition rate of sucrose can be given by equation (17).

$$r_S = \frac{r_X}{Y_{XS}} \tag{17}$$

$$r_S = \frac{r_X}{Y_{XS}} \left(1 - \frac{S_T}{S_{T0}} \right) \tag{18}$$

This material is reserved for educational use only, not allowed for commercial use.
Forbidden to modify the content, and cite the document when use

Ethanol is a product of decomposition of sugar by cell in metabolism process, this process operates under anaerobic condition. The formation of ethanol is related with the decomposition rate of sugar (sucrose, glucose and fructose). The ethanol formation model is opposed as given in equation (18).

$$r_P = \frac{r_G}{Y_{GP}} + \frac{r_F}{Y_{FP}} + \frac{r_S}{Y_{SP}} \tag{19}$$

For glucose and fructose, rates of decomposition are depended on concentration of cell or biomass and rate of sucrose utilized. When sucrose utilized, the main product this process consists of ethanol, glycerol and two monosaccharide. The two monosaccharide from this reaction are glucose and fructose. So, rate of glucose and fructose are utilized by cell can be expressed by equation (20) and (21), respectively.

$$r_G = \frac{r_X}{Y_{XG}} - \frac{r_S}{Y_{SG}} \tag{20}$$

$$r_F = \left(\frac{r_X}{Y_{XF}} - \frac{r_S}{Y_{SF}} \right) \left(1 - \frac{G}{G_0} \right) \tag{21}$$

To describe the dynamics of fermentation, the rate of reaction for each substrates and components are show as follows.

Biomass
$$\frac{dX}{dt} = \frac{\mu_{max} S_T K_S}{1 + K_{IS} S_T + K_{IP} P} X \tag{22}$$

Sucrose
$$\frac{dS}{dt} = r_S \tag{23}$$

Glucose
$$\frac{dG}{dt} = \frac{\mu_{max} S_T K_S}{(1 + K_{IS} S_T + K_{IP} P) Y_{XG}} X - \frac{r_S}{Y_{SG}} \tag{24}$$

Fructose
$$\frac{dF}{dt} = \left(\frac{\mu_{max} S_T K_S}{(1 + K_{IS} S_T + K_{IP} P) Y_{XF}} X - \frac{r_S}{Y_{SF}} \right) \left(1 - \frac{G}{G_0} \right) \tag{25}$$

Ethanol
$$\frac{dP}{dt} = -\frac{r_S}{Y_{PS}} - \frac{r_G}{Y_{PG}} - \frac{r_F}{Y_{PF}} \tag{26}$$

This material is reserved for educational use only, not allowed for commercial use.
Forbidden to modify the content, and cite the document when use

5. Continuous model

For the continuous ethanol fermentation equation, they will have one more parameter that added in the equation. It is dilution rate (D), the dilution rate is defined as the volumetric flow rate in to tank divided by volume of tank. Base on mass balance in equation (26), the rate of change of biomass, substrate and product are shown in equation (27)-(31).

$$rate\ of\ accumulation = rate\ of\ flow in - rate\ of\ flow out + rate\ of\ generation \quad (27)$$

Biomass
$$\frac{dX}{dt} = (X_{in} - X_{out})D + r_X \quad (28)$$

For this system, there are consist of settling unit. So, D for cell equal to 0

Sucrose
$$\frac{dS}{dt} = (S_{in} - S_{out})D + r_S \quad (29)$$

Glucose
$$\frac{dG}{dt} = (G_{in} - G_{out})D + \frac{r_s}{Y_{SG}} \quad (30)$$

Fructose
$$\frac{dF}{dt} = (F_{in} - F_{out})D + \frac{r_s}{Y_{SF}} \quad (31)$$

Ethanol
$$\frac{dP}{dt} = (P_{in} - P_{out})D + \frac{r_s}{Y_{XP}} \quad (32)$$

This material is reserved for educational use only, not allowed for commercial use.
Forbidden to modify the content, and cite the document when use

2.3 RESEARCH METHODOLOGY

2.3.1 Researching Procedure

1. Study the theory of ethanol fermentation, reaction in the system of fermentation as well as behavior of cell or yeast in fermentation process.
2. Study the mathematic model that can describe the fermentation reaction of sugar by yeast as well as kinetic of ethanol fermentation reaction.
3. Determine the operating system, condition, substrate and yeast that use in this study.
4. Calculate result and model by using Polymath software
5. Analysis result from model and conclude result

2.3.2 Calculation Tool

3. Polymath Fogler 6.10 Professional
4. Microsoft Excel 2016

2.3.3 Calculation

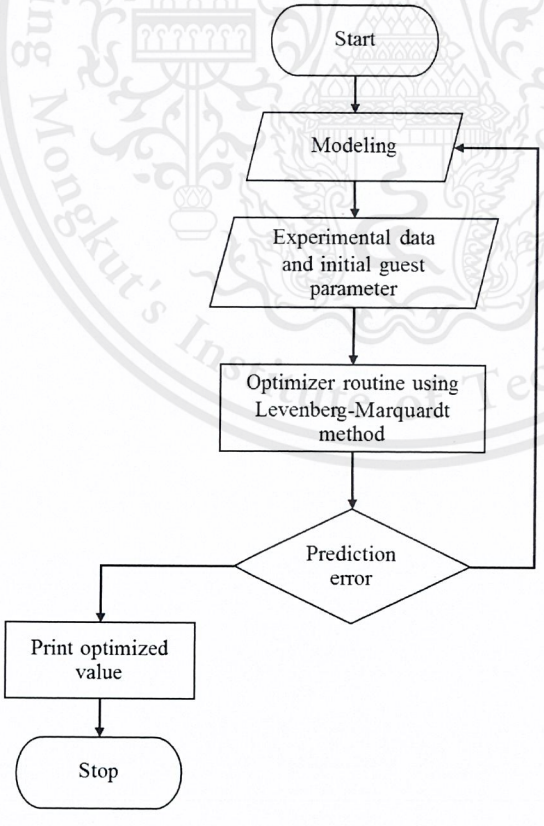


Figure 2.3.1 Calculation flow chart

This material is reserved for educational use only, not allowed for commercial use.
Forbidden to modify the content, and cite the document when use

From Figure 2.3.1, the calculation is described for more understand in methodology for calculation step.

1. The mathematic model is selected for describe the reaction of ethanol fermentation. For this study, Monod equation is the first model for calculation.
2. Experimental data and initial guest parameter are used calculate.
3. The model and experimental data are optimized to find the optimum parameter by using Levenberg-Marquardt method.
4. The model and optimized parameter from previous step is calculated to obtained result for each model. The prediction error is indicated in term of correlation coefficient. If model accuracy prediction, step of calculation is stop.
5. If model not accuracy prediction, model is developed to describe the process.

For Maximum specific growth rate (μ_{MAX}) and Monod constant for growth (K_S). The experimental data of Feng-Sheng Wang [1] are used to find parameter values for this study. From the ethanol fermentation by using sucrose as the substrate, the concentration profile of cell is used to find the parameter value. Samples were collected every 1 h intervals. The cell concentrations both in the carriers and the broth is determined and used for μ determination using Equation (32)-(33). The μ values were used to evaluate μ_{MAX} and K_S by Lineweaver–Burk plots.

$$\mu = \frac{ln X_L - ln X_B}{t_L - t_B} \tag{33}$$

$$\frac{1}{\mu} = \frac{K_S}{\mu_{MAX} S} + \frac{1}{\mu_{MAX}} \tag{34}$$

This material is reserved for educational use only, not allowed for commercial use.
Forbidden to modify the content, and cite the document when use

2.3 RESULTS AND DISCUSSION

2.4.1 Monod model and Modified Monod model

For this study, two kinetic models are used to describe the reaction and mechanism of ethanol fermentation in a two-tank system with cell recycling. The first step, Monod model is used as a simple model to predict concentration profile of ethanol fermentation. It assumes that the concentration of sugars in reactor is not inhibition of utilization them. So, the concentration of sugar is considered as total concentration. The kinetic parameter for Monod are determined by Lineweaver–Burk plots. From Lineweaver–Burk plots, the maximum specific growth rate of cell (μ_{MAX}) and Monod constant for growth (K_S) are determined by relationship between invert of specific growth rate ($1/\mu$) and substrate ($1/S$). To plot relationship between invert of specific growth rate ($1/\mu$) and substrate ($1/S$), it necessary to determine the suitable interval.

The specific growth rate is plot relationship with substrate concentration, the relationship is expressed in the form of linear equation ($y = mx + c$). From this equation, it can be used to find the parameter by compare the linear equation with equation (18). The maximum specific growth rate of cell (μ_{MAX}) and Monod constant for growth (K_S) are 0.32h^{-1} and 19.60 g/L.

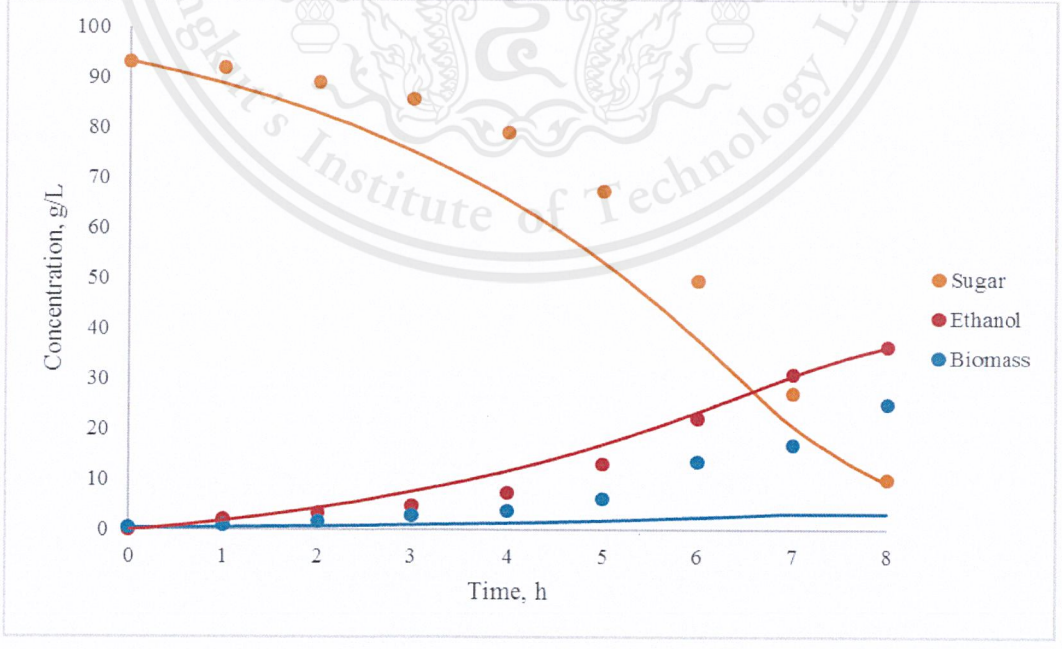


Figure 2.4.1 Experimental data and Monod model results of ethanol production (Total sugar, Solid line: Model)

This material is reserved for educational use only, not allowed for commercial use.
Forbidden to modify the content, and cite the document when use

From Figure 2.4.1, we found that the experimental data is not agree with the predicted value. When we observe the concentration of biomass, we found that it cannot predict biomass concentration after 4-hour pass. The large error in prediction may be the result from the inhibition of sugar and product to substrate utilized and cell growth are not considered.

However, after we know that concentration of sugars and biomass concentration are effect to the substrate utilization and product formation. So, the model is modified. The concentration of glucose (G), fructose (F) and Sucrose (S) are consider and applied to the models.

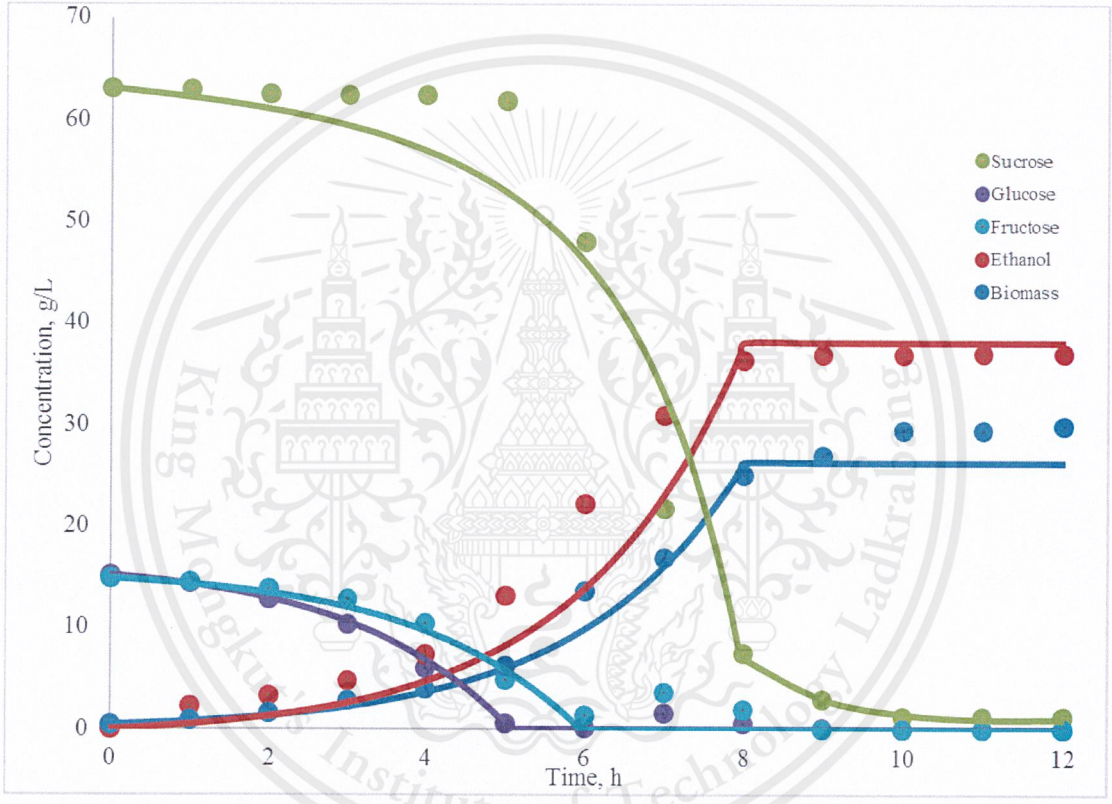


Figure 2.4.2 Experimental data and Modified Monod model results of ethanol production (Solid line: Model)

Figure 2.4.2 show the comparison between the experimental data and model result, we found that the experimental data agree with experimental data which indicate that the assumption is correct. From the result, the most prediction are well, but some predictions are not good enough. Model well fit with glucose and fructose data. At earliest stage, model cannot predict sucrose and ethanol data. the main case, due to the priority of utilization of glucose and fructose by cell more than sucrose. So,

This material is reserved for educational use only, not allowed for commercial use.
Forbidden to modify the content, and cite the document when use

when the concentration of glucose and fructose are high, sucrose is not consumed by cell. From

2.4.2 Extended-Modified Monod model

From Monod model, we found that the prediction values are not accurate enough. So, Modified Monod model is modified for more precision. For this model, the priority of sugar utilization is consider. We found that glucose is more priority in sugar utilization than fructose and sucrose, respectively. The inhibition term of fructose utilization by glucose are represented in term of concentration of glucose ($1 - G/G_0$). This term is introduced into rate of glucose utilization as show in equation (25). The kinetic parameters for each model are show in Table

Table 2.4.1 Kinetic parameters

Parameter	Model (This study)				Other study	
	Monod	Modified Monod	Extended-modified Monod	unit	Value	Reference
μ_{max}	0.32	0.54	0.25	h^{-1}	0.2174	Z. Liu
K_S	19.60	5.50		g/L	9.037	P. Thangprompan
Y_{XP}	0.15	0.65			0.51	P. Thangprompan
Y_{XS}	0.06	0.30	0.12		0.235	P. Thangprompan
K_{IP}			26.70	L/g	16.7864	Z. Liu
K_{IS}			19.00	L/g	19.6015	Z. Liu
Y_{XG}			0.13			
Y_{GP}			1.50			
Y_{SG}			5.00			
Y_{SF}			5.00			
Y_{FP}			1.60			
Y_{SP}			3.10			
Y_{XF}			0.28			
D	0.36	0.36	0.36	h^{-1}		
V	5	5	5	L		

Table 2.4.1 show the parameter value for this study that determine for the experimental data of Feng-Sheng Wang [1]. The maximum specific growth rate of cell (μ_{MAX}) and Monod constant for growth (K_S) are determined by Lineweaver–Burk plots. The other parameters are determined from curve fitting, Yield values for each component are determined based on experimental data.

This material is reserved for educational use only, not allowed for commercial use.
Forbidden to modify the content, and cite the document when use

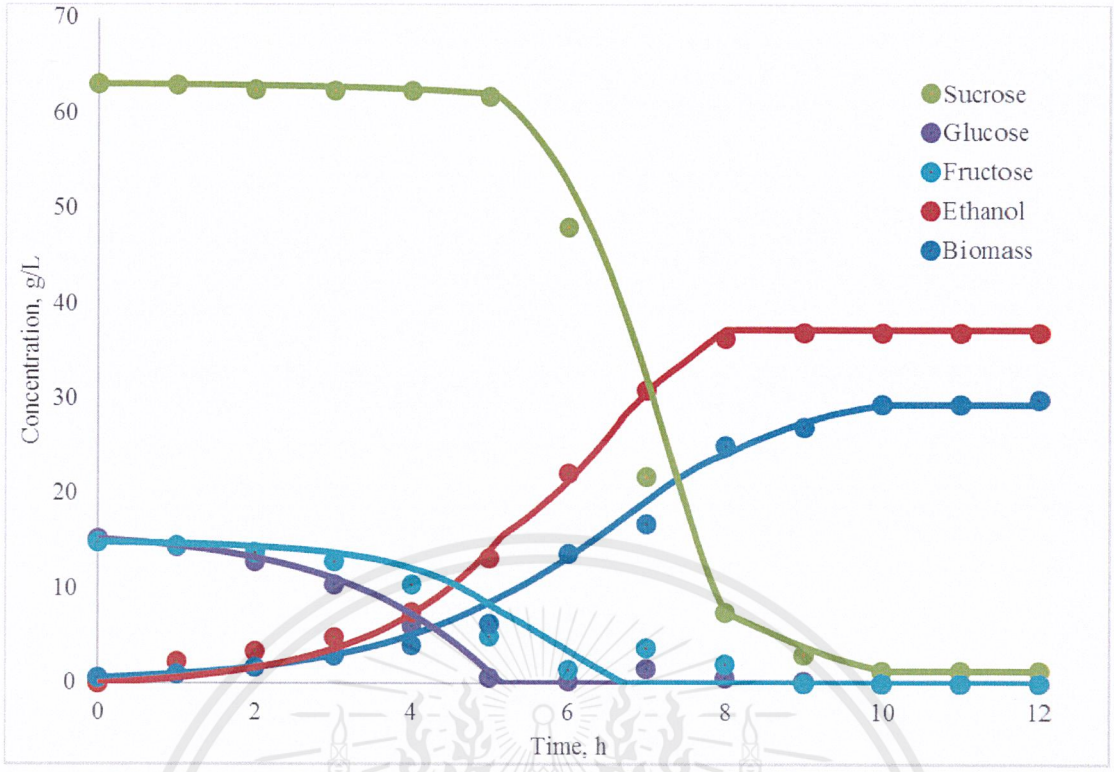


Figure 2.4.3 Experimental data and Modified model results of ethanol production (Solid line: Model)

From Figure 2.4.3, there are concentration profile of substrate and product in ethanol fermentation. It is simulated by using Polymath software. From the result, it shows that at the initial stage, the concentration of glucose and fructose continuous decreasing with time. In the meantime, the concentration of sucrose is hardly decreasing with time. It indicates that reaction of utilization of glucose and fructose are competitive reaction of sucrose utilization. Which it shown that the priority utilization of glucose and fructose by cell more than sucrose. After the concentration of glucose and fructose are utilized almost zero. The concentration of sucrose is rapidly decreasing with time, which confirm that the concentration of glucose and fructose affect to sucrose utilization. For ethanol, graph show that concentration of ethanol increases with time and utilization of substrate by cell (sucrose, glucose and fructose). Which after concentration of glucose almost zero, concentration of ethanol still increases with time and rapidly increase when concentration of sucrose rapidly decreases.

This material is reserved for educational use only, not allowed for commercial use.
Forbidden to modify the content, and cite the document when use

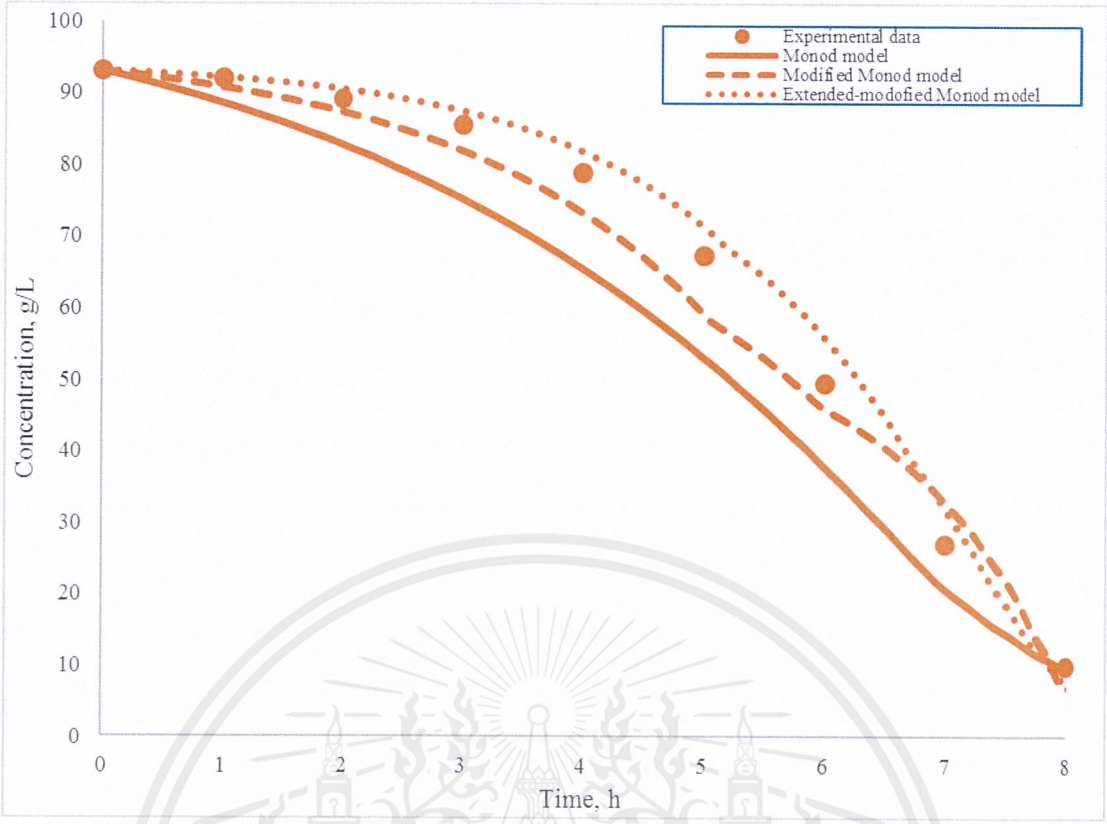


Figure 2.4.4 Comparison of total sugar prediction for each model

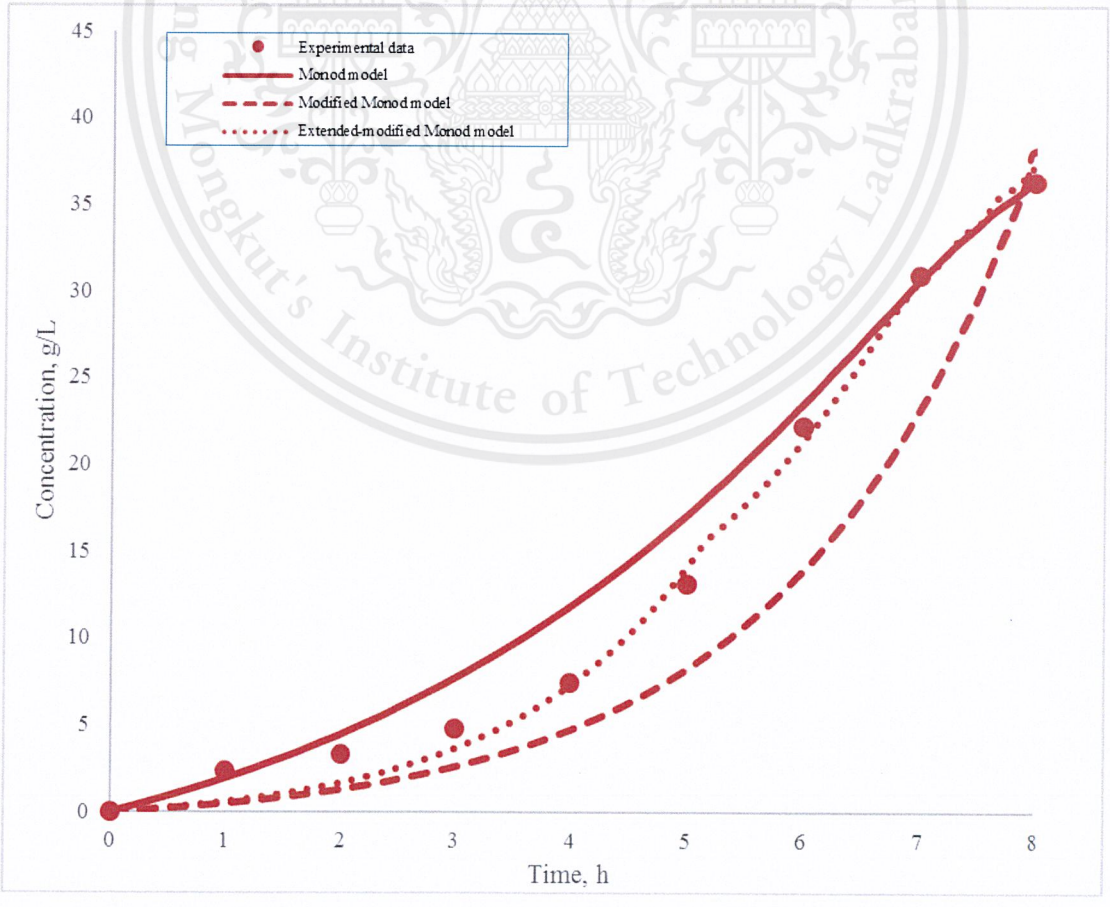


Figure 2.4.5 Comparison of ethanol prediction for each model

This material is reserved for educational use only, not allowed for commercial use.
Forbidden to modify the content, and cite the document when use

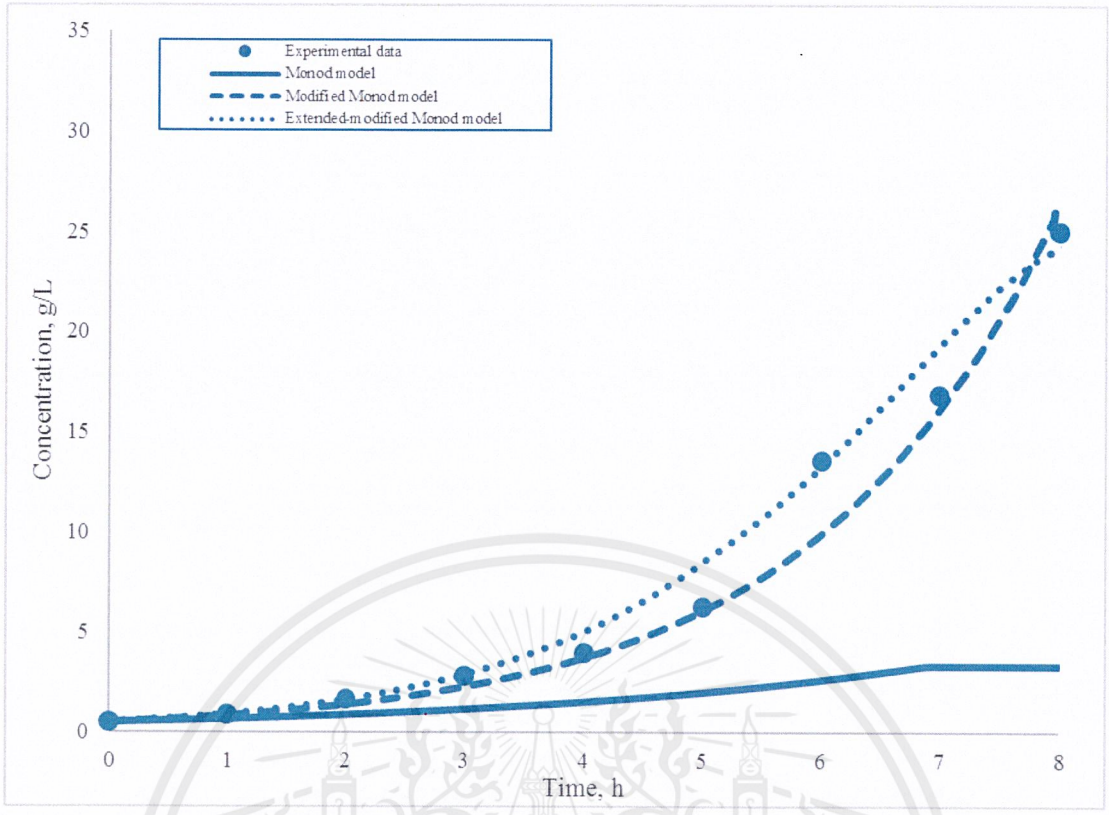


Figure 2.4.6 Comparison of biomass prediction for each model

The prediction of experimental data is show in Figure 2.4.4 - 2.4.6, the predict data are simulate by using polymath software (Runge-Kutta-Fehlberg algorithm) and plot compare with experimental data. From Figure 2.4.4, Extended-modified Monod model more accurate than other two models. When we consider at first period (0-4 h), we found that concentration of total sugar that predict by Monod model is rapidly decrease than Modified Monod model and Extended-modified Monod model, respectively. Because of the effect of substrate (glucose and fructose) inhibition and product inhibition are not taken into account to model. Figure 2.4.5-2.4.6 also show the comparison between experimental data and predicted value of biomass and ethanol, the result show that Extended-modified Monod model better prediction than other two models. The accuracy prediction for each model are indicated by the correlation coefficient (R^2) which show in Table 2.4.2.

This material is reserved for educational use only, not allowed for commercial use.
Forbidden to modify the content, and cite the document when use

Table 2.4.2 The correlation coefficient (R^2) for each model

Model	Total sugar	ethanol	biomass
Monod model	0.90	0.97	-0.35
Modified Monod model	0.98	0.88	0.97
Extended-modified Monod model	0.99	0.99	0.98

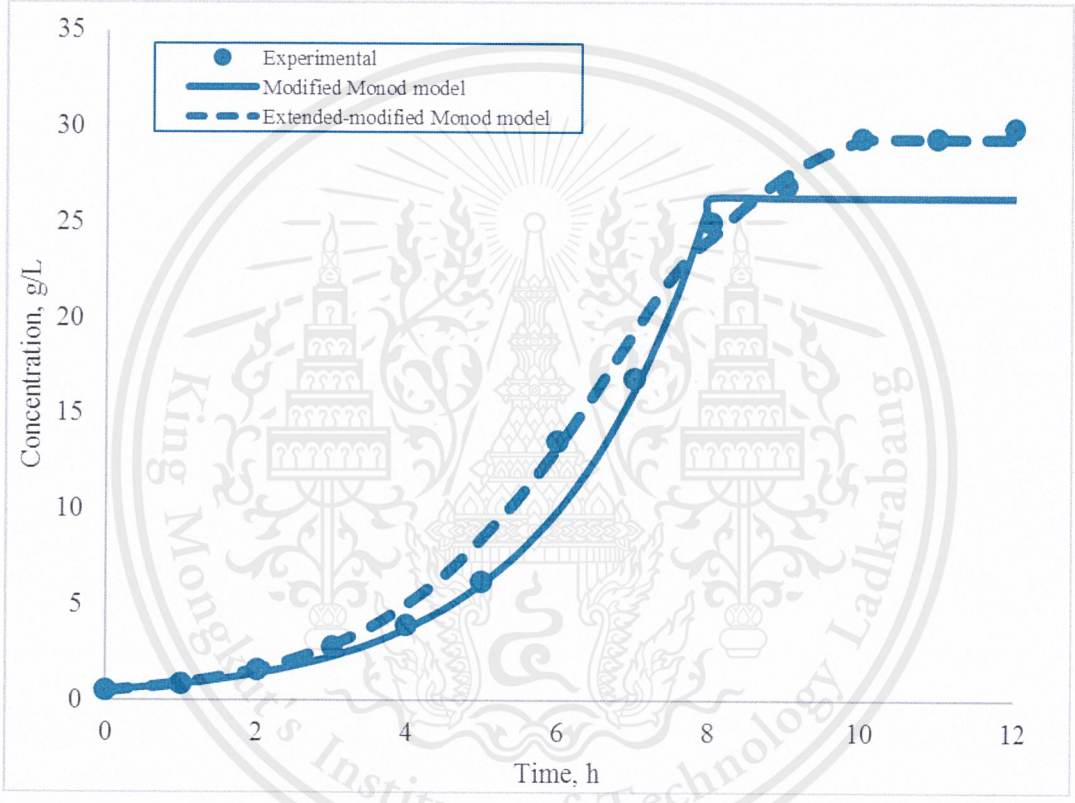


Figure 2.4.71 Comparison of biomass prediction for each model (with continuous phase)

This material is reserved for educational use only, not allowed for commercial use.
Forbidden to modify the content, and cite the document when use

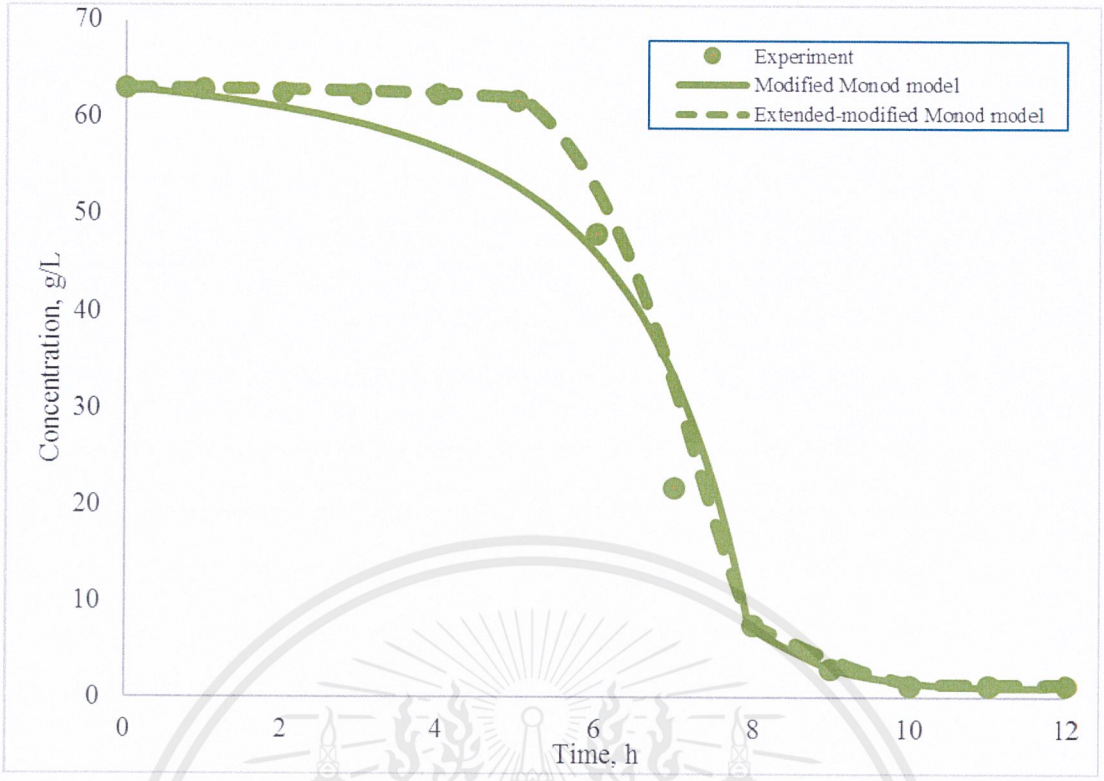


Figure 2.4.8 Comparison of sucrose prediction for each model (with continuous phase)

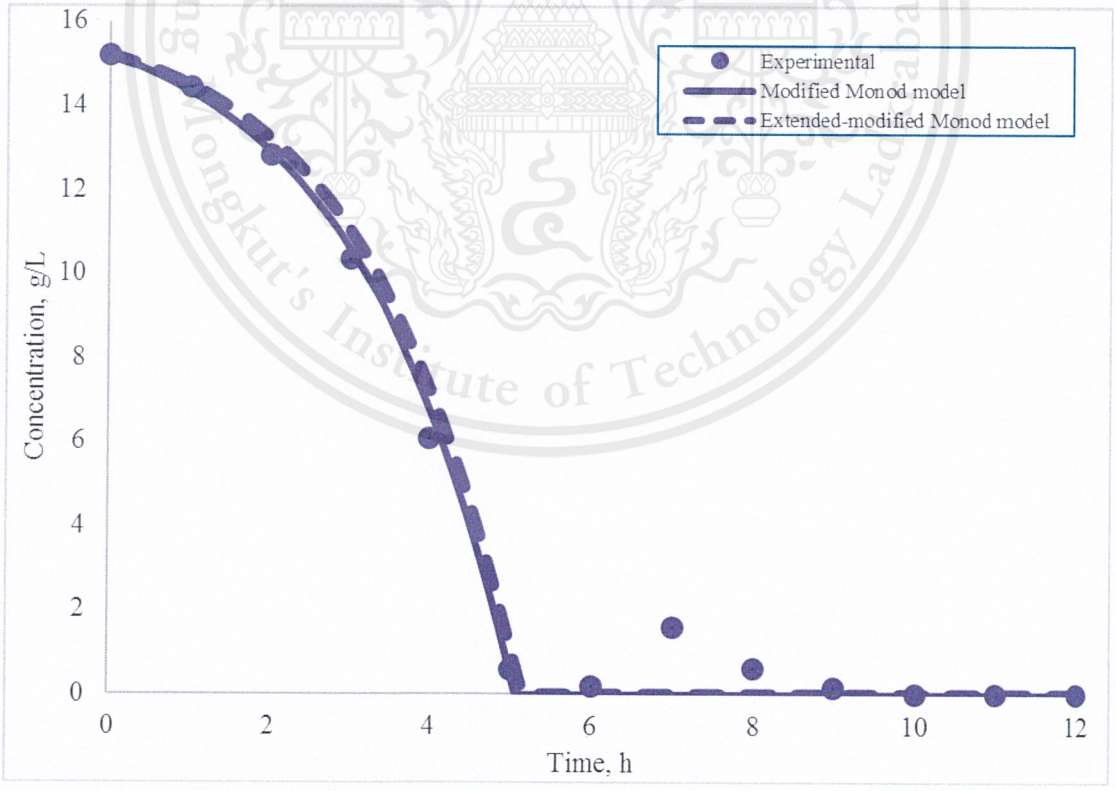


Figure 2.4.9 Comparison of glucose prediction for each model (with continuous phase)

This material is reserved for educational use only, not allowed for commercial use.
Forbidden to modify the content, and cite the document when use

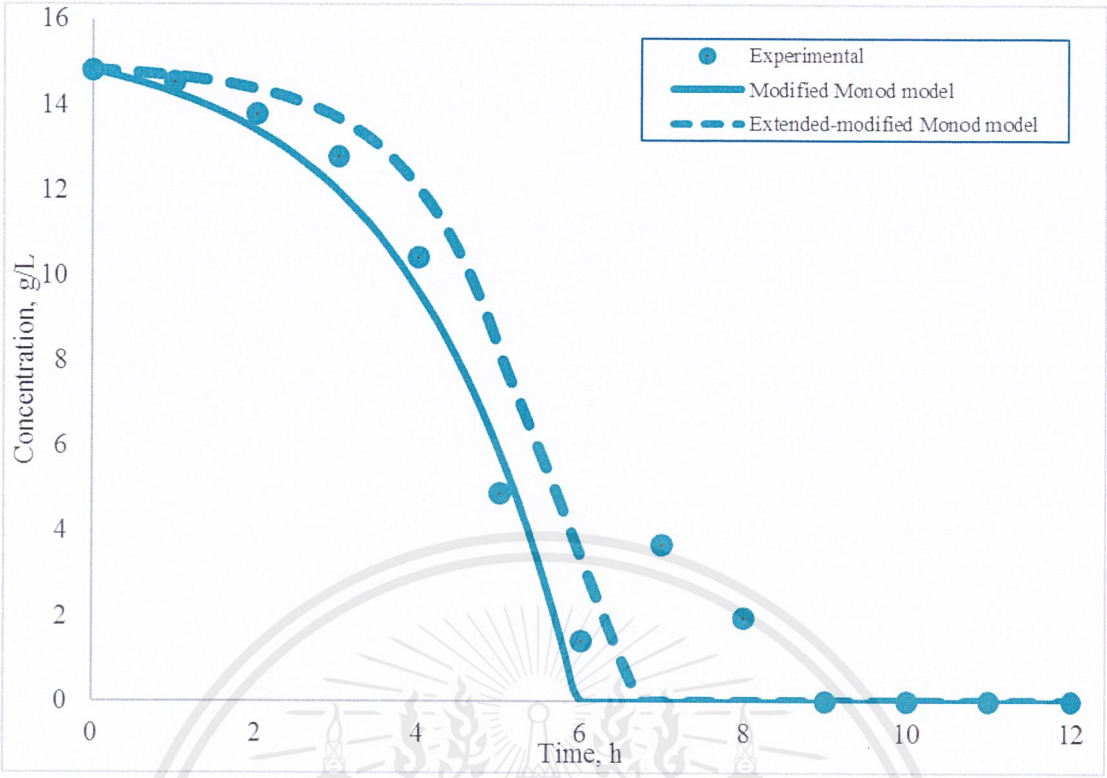


Figure 2.4.10 Comparison of fructose prediction for each model (with continuous phase)

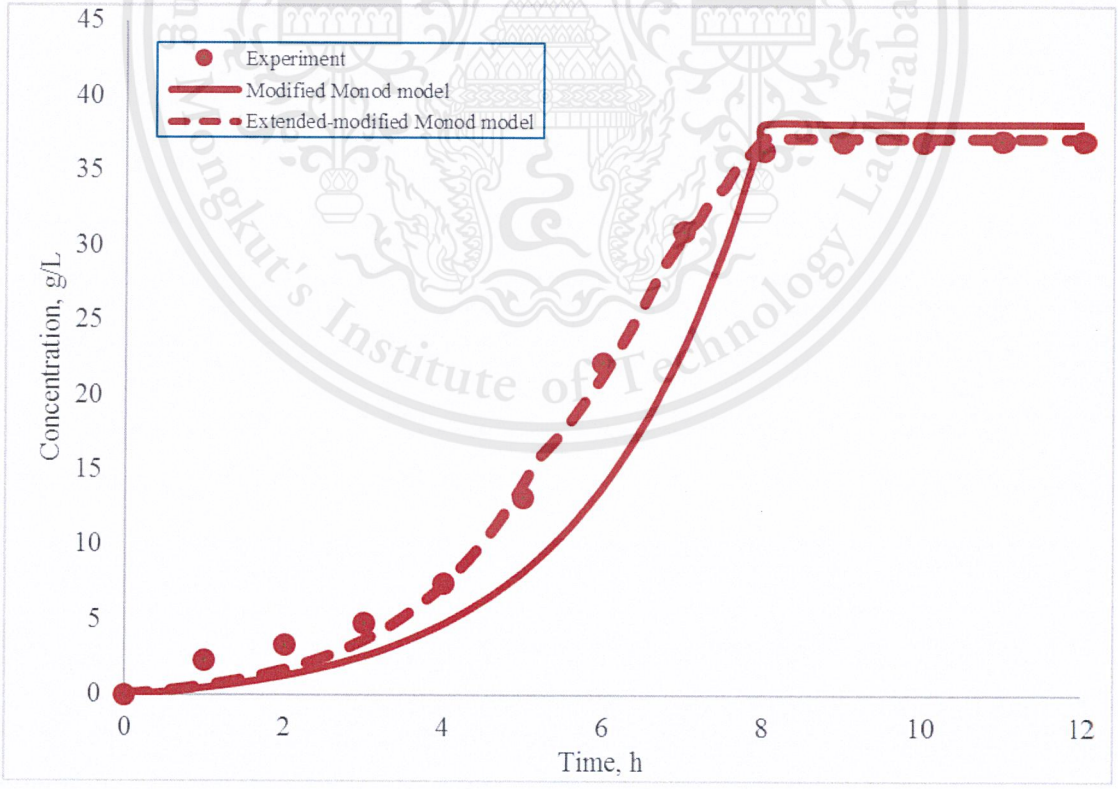


Figure 2.4.11 Comparison of ethanol prediction for each model (with continuous phase)

This material is reserved for educational use only, not allowed for commercial use.
Forbidden to modify the content, and cite the document when use

When we compare the result for each model, Figure 2. 4. 7-2. 4. 11 show that the prediction of Modified model more accuracy than Monod model except data of fructose. Monod model can predict the data of fructose accurate than Modified model. The main case may be from the assumption of Modified model, they are assumed that the priority of utilization of glucose more than fructose. Due to the mechanism of ethanol production show that glucose is transform to pyruvate pass through glucose-6-P, fructose-6-P, glyceraldehyld-3-phosphate and phosphoenolpyruvate. Fructose will be decomposed to fructose-6-P which combine with fructose-6-P from glucose decomposed. So, if the concentration of glucose high, concentration of fructose-6-P also high and rate of fructose decomposed are low. So, the concentration of glucose is inhibitor for fructose utilization by cell. The accuracy for each model are show in Table 2.4.3 in term of correction coefficient (R^2).

Table 2.4.3 The correlation coefficient (R^2) for Modified Monod model and Extended-modified Monod model (With continuous mode)

Model	Sucrose	glucose	fructose	ethanol	biomass
Modified Monod model	0.97	0.99	0.95	0.94	0.97
Extended-modified Monod model	0.99	0.99	0.93	1.00	0.99

This material is reserved for educational use only, not allowed for commercial use.
Forbidden to modify the content, and cite the document when use

2.5 CONCLUSION

From the result, based on a mechanism analysis, Monod model has been developed for ethanol production from fermentation by using the flocculent yeast *Saccharomyces diastaticus* LORRE-316 as the fermentation yeast and glucose, fructose and sucrose as the substrate. Extended-modified Monod model can describe the behavior of *Saccharomyces diastaticus* LORRE-316 on batch and continuous mode. When the concentration of sucrose, fructose and glucose are present in the medium, this model can describe the substrate inhibition on the specific growth rate. The formation of biomass and ethanol, as well as the uptake of sucrose, for the fermentation of *Saccharomyces diastaticus* in mixtures of glucose, fructose and sucrose are predictable with this model. The predictions with this model agreed well with the experimental results. For this study, we obtain the model structure and important parameter that involve the ethanol production from fermentation process including maximum specific growth rate of cell (μ_{MAX}), adsorption equilibrium constant of substrate (K_{IS}) and adsorption equilibrium constant of ethanol (K_{IP}). These model structure and parameters can be used as basic for design, control and optimization of system. However, this study we used only one experimental data to find the kinetic parameter and validate, which may be not robust enough for a global model. To obtain more robust kinetic parameter and model, we should study by using several experiments.

This material is reserved for educational use only, not allowed for commercial use.
Forbidden to modify the content, and cite the document when use

2.6 NOMENCLATURE

D	dilute rate, h^{-1}
K_{IP}	adsorption equilibrium constant of ethanol, L/g
K_{IS}	adsorption equilibrium constant of substrate, L/g
K_S	Monod constant for growth, g/L
P	ethanol concentration, g/L
G	glucose concentration, g/L
S	sucrose concentration, g/L
F	fructose concentration, g/L
X	biomass concentration, g/L
P_i	inlet ethanol concentration, g/L
G_i	inlet glucose concentration, g/L
S_i	inlet sucrose concentration, g/L
X_i	inlet biomass concentration, g/L
F_i	inlet fructose concentration, g/L
t	time, h
S_T	total sugar concentration, g/L
S_{T0}	initial total sugar concentration, g/L
μ_{MAX}	maximum specific growth rate, h^{-1}
X_L	biomass concentration at the end of the log phase, g/L
X_B	biomass concentration at the commencement of the log phase, g/L
Y_{XS}	biomass yield from sucrose
Y_{XG}	biomass yield from glucose
Y_{XF}	biomass yield from fructose
Y_{XF}	biomass yield from fructose
Y_{SF}	fructose yield from sucrose
Y_{SG}	glucose yield from sucrose
Y_{GP}	ethanol yield from glucose
Y_{FP}	ethanol yield from fructose
Y_{SP}	ethanol yield from sucrose

This material is reserved for educational use only, not allowed for commercial use.
Forbidden to modify the content, and cite the document when use

REFERENCES

[1] Nishiwaki, A.; Dunn, I. J. Analysis of a Two-Stage Fermentor With Recycle for Continuous Ethanol Production. *Chem. Eng. Commun.* **1998**, *168* (September), 207–227.

[2] Wang, F. S.; Li, C. C.; Lin, Y. S.; Lee, W. C. Enhanced Ethanol Production by Continuous Fermentation in a Two-Tank System with Cell Recycling. *Process Biochem.* **2013**, *48* (9), 1425–1428.

[3] Veeramallu, U.; Agrawal, P. A Structured Kinetic Model for Zymomonas Mobilis ATCC10988. *Biotechnol. Bioeng.* **1990**, *36* (7), 694–704.

[4] Nishiwaki, a; Dunn, I. J. Analysis of the Performance of a Two-Stage Fermenter with Cell Recycle for Continuous Ethanol Production Using Different Kinetic Models. *Biochem Eng J* **1999**, *4* (1), 37–44.

[5] Ait-Abdelkader, N.; Baratti, J. C. Estimation of Kinetic and Yield Parameters: Ethanol Fermentation of a Glucose and Fructose Mixture Using Zymomonas Mobilis. *Biotechnol. Tech.* **1993**, *7* (5), 329–334.

[6] Ariyajaroenwong, P.; Laopaiboon, P.; Salakkam, A.; Srinophakun, P.; Laopaiboon, L. Kinetic Models for Batch and Continuous Ethanol Fermentation from Sweet Sorghum Juice by Yeast Immobilized on Sweet Sorghum Stalks. *J. Taiwan Inst. Chem. Eng.* **2016**, *66*, 210–216.

[7] Birol, G.; Doruker, P.; Kirdar, B.; Önsan, Z. I.; Ülgen, K. Mathematical Description of Ethanol Fermentation by Immobilised Saccharomyces Cerevisiae. *Process Biochem.* **1998**, *33* (7), 763–771.

[8] Huang, W. H.; Wang, F. S. Kinetic Modeling of Batch Fermentation for Mixed-Sugar to Ethanol Production. *J. Taiwan Inst. Chem. Eng.* **2010**, *41* (4), 434–439.

[9] Kompala, D. S. " Microbial Growth on Multiple Substrates ." *Bioprocess Eng. Fundam. Appl.* **2011**, 750.

[10] Jarz??bski, A. B.; Malinowski, J. J.; Goma, G. Modeling of Ethanol Fermentation at High Yeast Concentrations. *Biotechnol. Bioeng.* **1989**, *34* (9), 1225–1230.

[11] Lee, W. C.; Huang, C. T. Modeling of Ethanol Fermentation Using Zymomonas Mobilis ATCC 10988 Grown on the Media Containing Glucose and Fructose. *Biochem. Eng. J.* **2000**, *4* (3), 217–227.

[12] Ngoh, G. C.; Hasan, M. The Prediction of the Cell and Substrate in a Fed-

This material is reserved for educational use only, not allowed for commercial use.

Forbidden to modify the content, and cite the document when use

Batch Fermentation System by Modification of Models. *Inst. Eng. Malaysia* **2008**, *69* (4), 9–14.

[13] Monod, J. THE GROWTH OF BACTERIAL CULTURES. *Annu. Rev. M* **1949**, *3* (Xl), 371–394.

[14] Thangprompan, P.; Thanapimmetha, A.; Saisriyoot, M.; Laopaiboon, L.; Srinophakun, P. Production of Ethanol from Sweet Sorghum Juice Using VHG Technology: A Simulation Case Study. *Appl. Biochem. Biotechnol.* **2013**, *171* (2), 294–314.

This material is reserved for educational use only, not allowed for commercial use.
Forbidden to modify the content, and cite the document when use

APPENDIX 2

Appendix 2-A Raw data of Ethanol Fermentation

Table 2-A-1 Raw data of ethanol fermetation at any time

Time(h)	Sucrose	Glucose	Fructose	Ethanol	Glycerol	Biomass
0	63.11	15.22	14.84	0.00	0.00	0.53
1	62.97	14.46	14.55	2.31	0.64	0.91
2	62.49	12.82	13.80	3.33	0.88	1.64
3	62.42	10.36	12.80	4.78	1.14	2.82
4	62.42	6.07	10.45	7.45	1.26	3.95
5	61.82	0.59	4.92	13.15	1.69	6.26
6	48.00	0.19	1.44	22.18	2.60	13.63
7	21.79	1.59	3.69	30.96	3.50	16.89
8	7.47	0.61	1.98	36.35	4.26	25.04
9	3.01	0.17	0.00	36.96	4.35	27.00
10	1.28	0.00	0.00	36.97	4.35	29.44
11	1.27	0.00	0.00	37.03	4.36	29.48
12	1.27	0.00	0.00	37.04	4.36	29.98

Table 2-A-2 Concentration of total sugar in tank 1 and 2

Time(h)	Tank1	Tank2
8	40.6184	10.0499
9	40.6182	3.1792
10	43.9993	1.2839
11	43.787	1.2704
12	43.7875	1.2703

This material is reserved for educational use only, not allowed for commercial use.
Forbidden to modify the content, and cite the document when use

Appendix 2-B Example of calculation

Calculation of Specific growth of cell

Specific growth rate of can find from equation B-1

$$u = r_X / X \tag{B-1}$$

And

$$\frac{1}{\mu} = \frac{K_S}{\mu_{MAX} S} + \frac{1}{\mu_{MAX}} \tag{B-2}$$

r_X can find from least-square methanol by fit curve with polynomial equation.

Table 2-B-1 Calculation of rate of cell growth by polymath soft ware

POLYMATH Report — No Title
Polynomial Regression — 19-พ.ค.-2560

Analytical polynomial derivative
X = 0.6708758 + 0.0491003*t + 0.0747553*t^2 + 0.0375141*t^3
d(X)/d(t) = 0.0491003 + 0.1495106*t + 0.1125424*t^2

Statistics

R^2	0.990114
R^2adj	0.9841824
Rmsd	0.2692628
Variance	1.17454

From Table 2-B-1, we will get

X = 0.6708758 + 0.0491003*t + 0.0747553*t^2 + 0.0375141*t^3

And

d(X)/d(t) = 0.0491003 + 0.1495106*t + 0.1125424*t^2

So, we can find r_X form dX/dt

This material is reserved for educational use only, not allowed for commercial use.
Forbidden to modify the content, and cite the document when use

Table 2-B-2 Table show relation ship between 1/μ and 1/S

t	*dX/dt*	*μ*	*1/μ*	*1/S*
0	0.0491	0.0933	10.7128	0.0107
1	0.3112	0.3410	2.9323	0.0109
2	0.7983	0.4875	1.7139	0.0112
3	1.5105	0.5348	1.6576	0.0117
4	2.4478	0.6203	1.8238	0.0127
5	3.6102	0.5765	2.0704	0.0149
6	4.9977	0.3666	2.3530	0.0202
7	6.6103	0.3914	2.6542	0.0369
8	8.4479	0.3373	2.9646	0.0995

We used data at 2 to 7 h to find the parameter, after that use the Lineweaver–Burk plots to find u_{max} and K_S

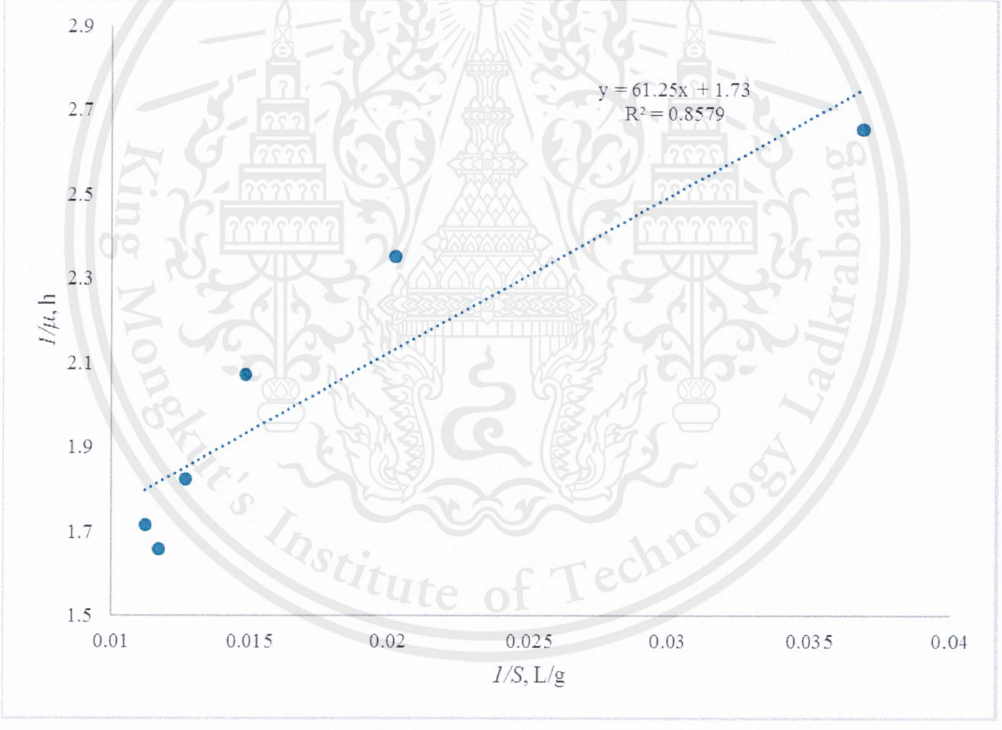


Figure 2-B-1 Lineweaver–Burk plots

$$\frac{K_S}{\mu_{MAX}} = 61.25 \text{ and } \frac{1}{\mu_{MAX}} = 1.37$$

The maximum specific growth rate (μ_{MAX}) and Monod constant (K_S) are 0.32 $h^{-1}$and 19.60

This material is reserved for educational use only, not allowed for commercial use.
Forbidden to modify the content, and cite the document when use

Appendix 2-C simulation code

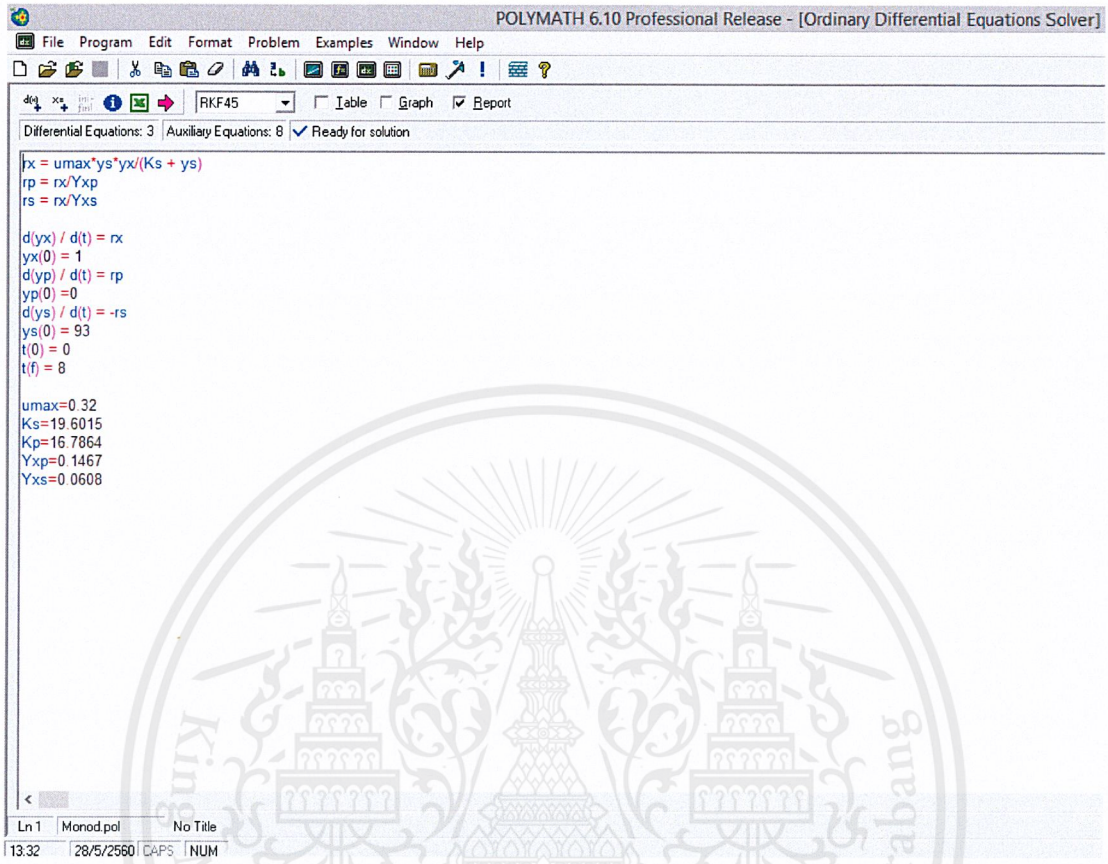


Figure 1-C-1 Simulation code of Monod model for ethanol fermentation

This material is reserved for educational use only, not allowed for commercial use.
Forbidden to modify the content, and cite the document when use

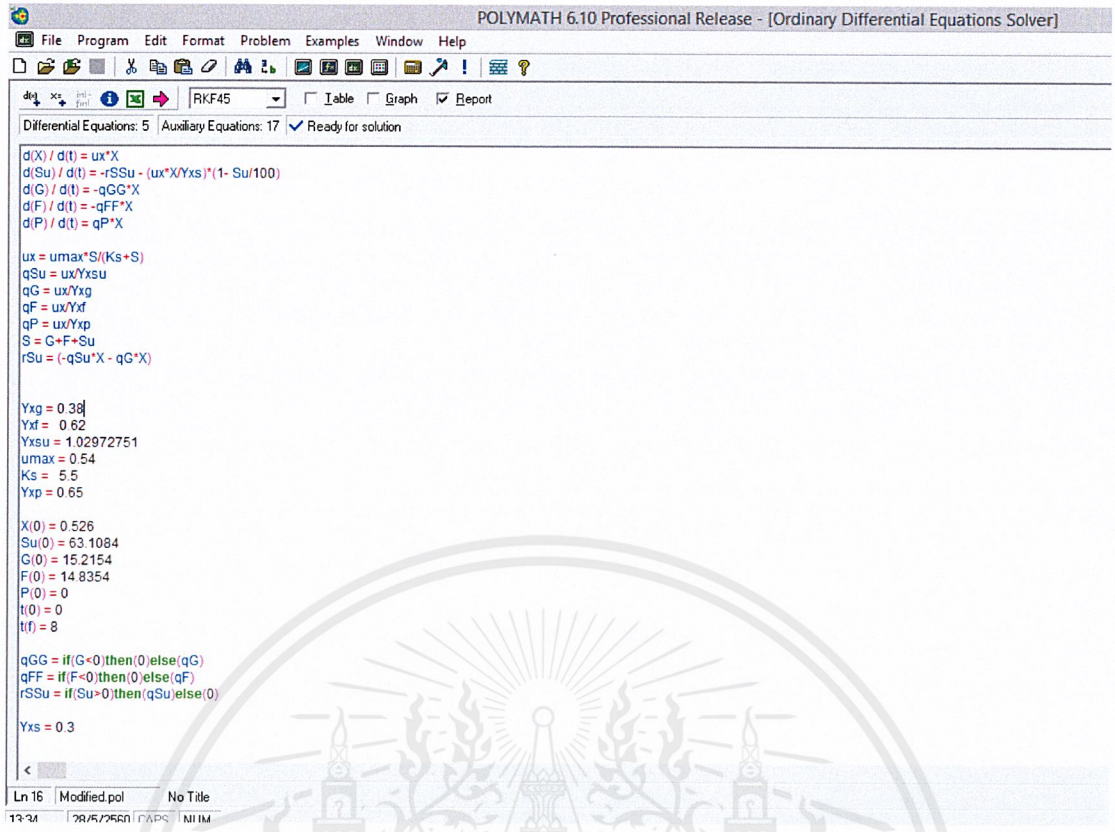


Figure 1-C-2 Simulation code of Modified Monod model for ethanol fermentation

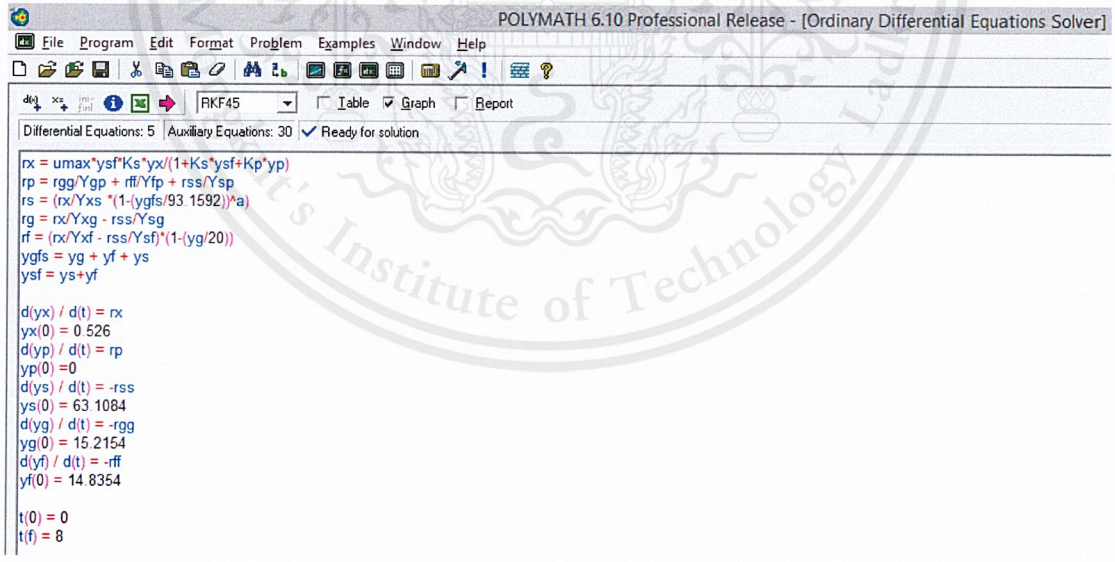


Figure 2-C-3 Simulation code of Extended-modified Monod model for ethanol fermentation

This material is reserved for educational use only, not allowed for commercial use.
Forbidden to modify the content, and cite the document when use

BIBLIOGRAHPY

Name: Phanuphong Nonwiangkae

Date of Birth (DD/MM/YY): 01/04/1994

Address: 24/11 Aummao sub-district, Yangtalad district, Kalasin province, 46120

E-mail: Phanuphong.N@hotmail.com

Academic Background:

2013-2016	Bachelor degree of Petrochemical Engineering at King's Mongkut Institute of Technology Ladkrabang
2010-2013	Kalasin Pittayasn School
2007-2009	Kalasin Pittayasn School

This material is reserved for educational use only, not allowed for commercial use.
Forbidden to modify the content, and cite the document when use